ULTRACENTRIFUGE STUDIES ON DEOXYRIBONUCLEIC ACID AND TOBACCO MOSAIC VIRUS

I The Effect of Angular Velocity on the Sedimentation Velocity Behavior of DNA and TMV

II The Three Component Theory of Sedimentation Equilibrium in a Density Gradient and the Hydration of DNA

III The Effects of Pressure on the Buoyant Behavior of DNA and TMV in a Density Gradient at Equilibrium

Thesis by
John Eugene Hearst

In Partial Fulfillment of the Requirements
For the Degree of
Doctor of Philosophy

California Institute of Technology
Pasadena, California

1961

to my parents

whose love and courage have
contributed greatly to this thesis

Acknowledgments

Under the direction of Jerry Vinograd, the past four years have been both enlightening and enjoyable. I sincerely thank him for the aid he gave me and the independence he allowed me.

I wish to thank Jim Ifft for the experiences shared in the laboratory and in the High Sierra.

Thanks are extended to my wife, Jean. Her patience, aid and love have been so important.

I am indebted to the National Science Foundation for the fellowships that have been awarded to me.

Abstract

Part 1 - A dependence of sedimentation coefficient and sedimentation boundary shape upon the angular velocity of the ultracentrifuge has been observed for T-4 bacteriophage deoxyribonucleic acid (DNA), E. coli DNA, and tobacco mosaic virus. The effects resulting from extrapolation of high-speed data are discussed along with possible causes of the phenomenon.

Part 2 - T-4 bacteriophage DNA is renatured by slow dialysis of a sodium citrate buffer solution into a solution of DNA in formamide. The first step in the renaturation appears to require the formation of approximately fifty percent of the possible hydrogen bonds.

Part 3 - The dependence of the buoyant density of DNA on the presence of a second cation is studied and a theory presented. The system enables one to evaluate a relative binding constant of the two cations to DNA.

Part 4 - The theory of density gradient sedimentation equilibrium including the effects of solvation is presented. The correction terms necessary for the evaluation of an anhydrous molecular weight are shown to be experimentally available. DNA is observed to have a large hydration parameter which is strongly dependent on water activity.

Part 5 - The theory for the effect of pressure on the density gradient in a concentrated salt solution is presented. The effect of pressure on the buoyant density of DNA and tobacco mosaic virus is measured and found to be a linear function of pressure.

Part 6 - The apparent molecular weight of T-4 bacteriophage DNA is evaluated using the density gradient sedimentation equilibrium theory presented in Parts 4 and 5. The DNA appears to have density heterogeneity.

Table of Contents

Part 1

The Effect of Angular Velocity on the Sedimentation Behavior of Deoxyribonucleic Acid and Tobacco Mosaic Virus in the Ultracentrifuge

ARCHIVES OF BIOCHEMISTRY AND BIOPHYSICS 92, 206–215 (1961)

The Effect of Angular Velocity on the Sedimentation Behavior of Deoxyribonucleic Acid and Tobacco Mosaic Virus in the Ultracentrifuge[1]

JOHN E. HEARST AND JEROME VINOGRAD

From the Gates and Crellin Laboratories of Chemistry, California Institute of Technology, Pasadena, California

Received June 17, 1960

A dependence of sedimentation coefficient and sedimentation boundary shape upon the angular velocity of the ultracentrifuge has been observed for T-4 bacteriophage deoxyribonucleic acid (DNA), *E. coli* DNA, and tobacco mosaic virus. The effect is shown to be concentration and molecular-weight dependent. The errors resulting from extrapolation of high-speed data are discussed along with possible causes of the phenomenon.

INTRODUCTION

The sedimentation behavior of deoxyribonucleic acid (DNA) has been studied by many workers (1). Early work with the schlieren optical system yielded low results for the sedimentation coefficient even on extrapolation to zero concentration (2–5); more recent studies employing the ultraviolet optical system have been carried out at much lower concentrations. Attempts to correlate extrapolated sedimentation coefficients, viscosities, and light-scattering results have been unsuccessful (6, 7), although the correlations of Doty *et al.* (8, 9) appear promising. Surely the majority of the inconsistencies in the literature today are the result of differing methods of preparation and handling.

As early as 1953, Koenig and Perrings (5) looked for an effect of angular velocity on the sedimentation coefficient of DNA. Their results were negative. A dependence of sedimentation coefficient on centrifuge speed has now been observed with higher molecular weight DNA's. Although an earlier attempt to observe such effects with tobacco mosaic virus (TMV) using schlieren optics failed (10), a speed dependence has also been observed in the ultraviolet concentration region for TMV. The appearance of the sedimentation boundary is also shown to be dependent on the centrifuge speed.

The extent to which previous work is affected by these results is unclear since the phenomenon is concentration and molecular-weight dependent.

EXPERIMENTAL

PREPARATION OF T-4r$_{240}$ BACTERIOPHAGE DNA

The phage coats were dissolved by saturating a 10^{13}-titer phage stock solution with recrystallized guanidinium chloride. After 12 hr. in the refrigerator, this solution was diluted tenfold with 0.15 *M* NaCl and 0.02 *M* Tris buffer, pH 9.0, and stored in the refrigerator for 3 days. Mechanical stirring was avoided at this step and in all subsequent handling of the material. The solution was then dialyzed against the above buffer, and the insoluble protein was removed by centrifugation in a clinical centrifuge; the undissolved DNA was also removed by decantation in this step. The dissolved DNA was precipitated with an equal volume of cold isopropyl alcohol; it was removed by slowly wrapping the fibers around a glass rod and redissolved in the pH 9.0 buffer. This precipitation and dissolution was repeated, and the product was dialyzed to equilibrium against the pH 9.0 buffer. Dilutions of this stock solution with the same

[1] Contribution No. 2596.

buffer were used for the ultracentrifuge studies. The ultraviolet spectrum of the product had a ratio of a maximum at 258 mμ to a minimum at 230 mμ of 2.2.

The *Escherichia coli* K 12 DNA was supplied by Dr. R. Rolfe, who prepared the material by the isolation technique of J. Marmur (private communication). The intrinsic viscosity of this material at zero rate of shear was 0.44/O.D.$_{260}$ or approximately 97 dl.g. The pH 9.0 buffer was used for all work on *E. coli* DNA.

The tobacco mosaic virus was supplied by Professor R. L. Sinsheimer and prepared by the procedure of N. Simmons (private communication). All of the TMV sedimentation studies were carried out in 0.02 *M* potassium phosphate and 0.0001 *M* Versene at pH 7.1.

The Spinco model E analytical ultracentrifuge equipped with temperature control and a photoelectric speed-measuring device was used. The ultraviolet optical system was employed exclusively, and films were analyzed on a Joyce-Loebl double-beam recording microdensitometer, model E 12 MK III. Optical densities were determined with a Beckman model DU spectrophotometer and were recorded for a 1-cm. liquid column for all solutions.

For the DNA work, syringe needles were not used; instead, the cells, while partially assembled, were filled with an eye dropper to avoid breakage of the DNA. The cell and rotor were equilibrated at 20°C. in the centrifuge chamber for 30 min. before all runs.

A 12-mm. Kel-F 2°-sector centerpiece was used for solutions of O.D.$_{260}$ 0–1. The 2° centerpiece, instead of the more common 4° sector, was used to conserve material. For solutions of O.D.$_{260}$ greater than 1, an Epon 3-mm. 4° centerpiece was used.

Speed fluctuations of the centrifuge were measured in several runs. The maximum fluctuations observed in any run are listed below, together with the maximum deviations of the average centrifuge velocity calculated from the odometer readings.

R.p.m.	Maximum fluctuation observed	Maximum deviation of average from rated r.p.m.
	%	%
4,908	1.5	0.05
9,945	0.7	0.1
13,410	0.6	0.2
20,410	—	0.1
35,600	0.2	0.1

Previous workers (11, 12) have considered boundary stability problems at low concentrations and speeds and have come to favorable conclusions. As a check on the stability of our system, the diffusion coefficient of deoxyadenylic acid in 0.15 *M* NaCl, 0.02 Tris pH 9.0, was measured at a weight concentration of approximately 27 μg./ml. A DNA solution of this weight concentration has an O.D.$_{260}$ of 0.6. This experiment was performed in a double-sector epon synthetic boundary cell at 9945 r.p.m. The buffer side of the cell was blocked off so that no light would pass through it. The diffusion coefficients were evaluated by the absorption method similar to the method discussed by Alexander and Johnson (13). Using their nomenclature, the diffusion boundary may be described by the equation

$$C/C_0 = \frac{1}{2} - \frac{1}{\pi}\int_0^y e^{-y^2}\,dy,$$

where

$$y = \frac{x}{2\sqrt{Dt}}$$

and x is measured from the midpoint of the boundary. This equation neglects the effect of radial walls in the centrifuge and assumes an infinitely long cell. The diffusion coefficient is also assumed to be concentration independent. For this calculation the absolute value of the two abscissas at equal but opposite relative concentration increments again measured from the midpoint were averaged; The square of the average value was plotted against time; the slope of the best straight line through these points was $4y^2D$; and y was obtained from a table in Alexander and Johnson (13) for a given C/C_0.

The 65% confidence intervals calculated for the sedimentation coefficients at 4908 r.p.m. indicate that the limit of stability is approached at this speed. Attempts to obtain a sedimentation coefficient at this centrifuge speed but at 0.08 O.D.$_{260}$ gave erratic results.

Linear response of the film to incident light was verified by a rotor aperture as described by Robkin, Meselson, and Vinograd (14).

In order to check cell alignment as a possible cause of the speed effect, a 2°-sector cell was misaligned in a rotor so that its sides were about 2° out of alignment. For this extreme case, the sedimentation coefficient was found to be 10% greater than that measured when the cell was properly aligned. Boundary spreading also occurred. On the other hand, alignment with use of the scribe lines provided for this purpose is accurate to better than 15′, so the effect would be reduced to about 1% if cells were carefully aligned and the scribe lines were in the correct position on the cell housing and rotor. Conventional runs are not believed (15) to be affected by small cell misalignments, which of course are unavoidable. As a final check

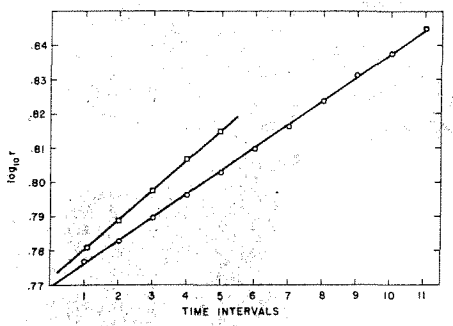

FIG. 1. Log_{10} r vs. time for the sedimentation coefficient determination of T-4 phage DNA. ○ O.D.$_{260}$ = 0.458, 9945 r.p.m. Time intervals = 64 min. □ O.D.$_{260}$ = 0.458, 20,410 r.p.m. Time intervals = 16 min.

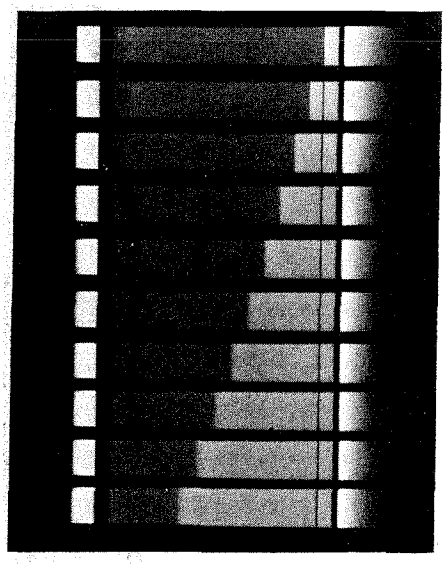

FIG. 2. Centrifuge pictures of sedimenting T-4 phage DNA, O.D.$_{260}$ = 0.458, 9945 r.p.m.

on the system, a 4°-sector cell was aligned in a rotor independent of the scribe lines, using the center line between rotor holes as a reference radius. A Kodak Contour Projector, model 2A, was used for this purpose. In addition, the position of the rotor holes with respect to the extremities of the rotor was checked. The estimated error in alignment of the sector walls using the contour projector is 5′. The positions of the scribe lines were correct for the cell housing and rotor as indicated by their relative positions after the cell-aligning process. The same cell housing and rotor were used for all runs in this paper. The boundary spreading and increase in sedimentation coefficient at high speeds were observed in these carefully aligned 4°-sector cells; on the basis of this evidence, we conclude that the effect observed is not an artifact dependent on cell alignment.

Various workers (16, 17) have considered the effect of scratches in the cell wall. Although these scratches have been shown to cause convection in the plateau region, no effect on the bulk sedimentation velocity has been observed.

In all cases the sedimentation coefficients were determined from the slope of the log r vs. time, where r is the distance from the center of rotation to the point in the cell at which the polymer concentration is half that in the plateau region. The concentrations referred to in the data are the concentrations of the solutions before sedimentation. Figure 1 shows the log r vs. time plot for two runs at the same concentration but different speeds. Figures 2 and 3 are the centrifuge pictures for these same runs and show the spreading of the boundary at the higher speed. The concentration dependence of the sedimentation coefficient, Fig. 4, for these conditions is so small that no curvature in the log r vs. time plot is observable. The curvature in all runs was, in general, insignificant except for the T-4 DNA runs at 4908 r.p.m. This curvature was ignored in view of the stability problems at this speed as mentioned previously.

With severe boundary spreading, the plateau region was immediately lost; the boundary positions were taken to be at the concentration levels of one-half the initial concentrations, multiplied by the radial dilution factor $(r_m/r)^2$. Since the spreading of the boundary is always such that the gradient in the concentration curve is skewed to

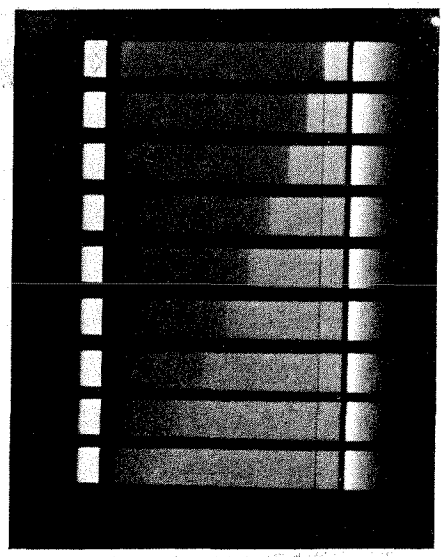

FIG. 3. Centrifuge pictures of sedimenting T-4 phage DNA, O.D.$_{260}$ = 0.458, 20,410 r.p.m.

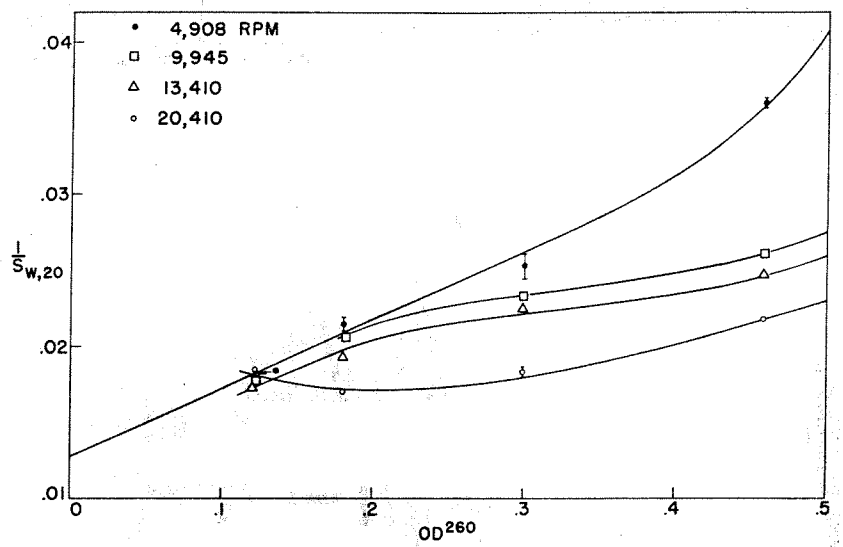

FIG. 4. The reciprocal of the sedimentation coefficient of T-4 phage DNA as a function of concentration at different centrifuge speeds.

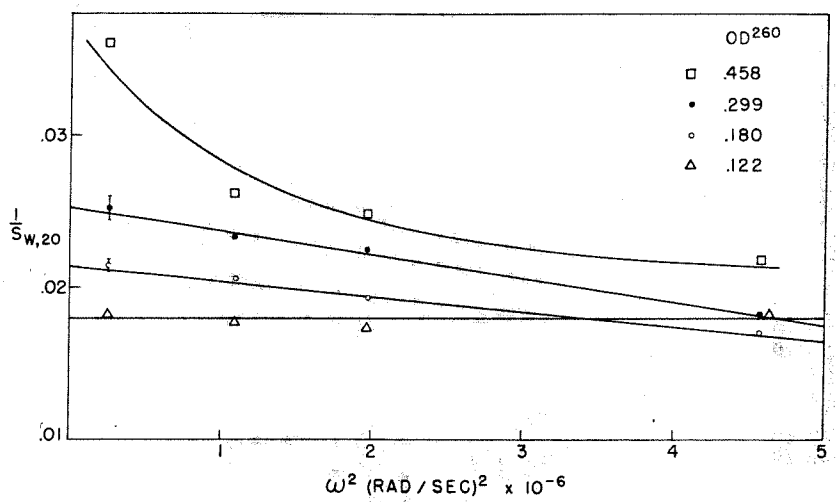

FIG. 5. The reciprocal of the sedimentation coefficient of T-4 phage DNA as a function of the square of angular velocity at different concentrations.

the fast side, this method will underestimate the weight-average sedimentation coefficient of the solution when spreading occurs.

In the case of the T-4 DNA, a least-squares determination of all slopes was made, and the 65% confidence intervals of the slope were determined. Those intervals which exceed the size of the data symbols are shown in Figs. 4 and 5.

Sedimentation coefficients were corrected to $S_{w,20}$ in the usual manner for the effect of buffer viscosity and density. Correction for temperature was unnecessary since all runs were made at 20°C.

The sedimentation distributions were calculated by the method described by Schachman (18*a*). This method involves differentiating the concentration distribution obtained from the densitometer by taking slopes. Its accuracy is limited at very low concentrations by film noise.

RESULTS

1/S vs. Concentration

For both T-4 DNA and *E. coli* DNA, Figs. 4 and 6, the plot of $1/S$ vs. concentration

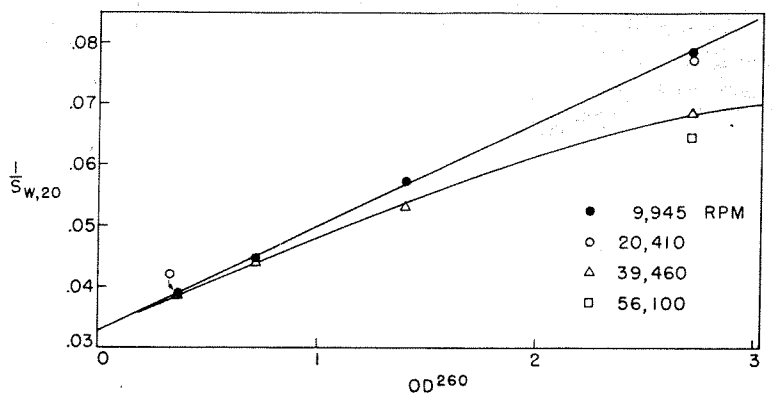

FIG. 6. The reciprocal of the sedimentation coefficient of *E. coli* DNA as a function of concentration at different centrifuge speeds.

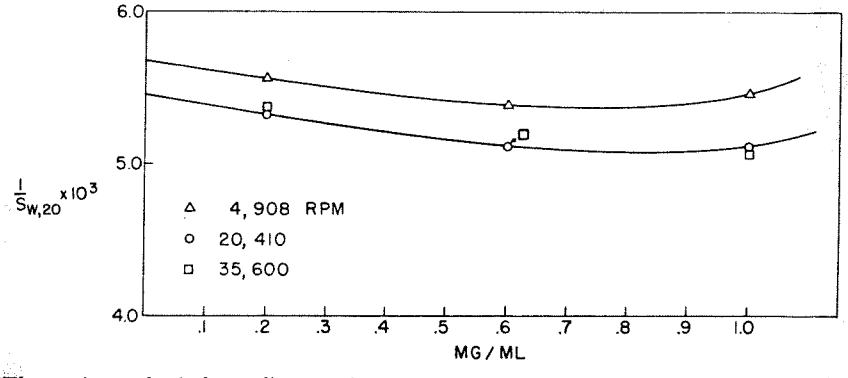

FIG. 7. The reciprocal of the sedimentation coefficient of TMV as a function of concentration at different centrifuge speeds.

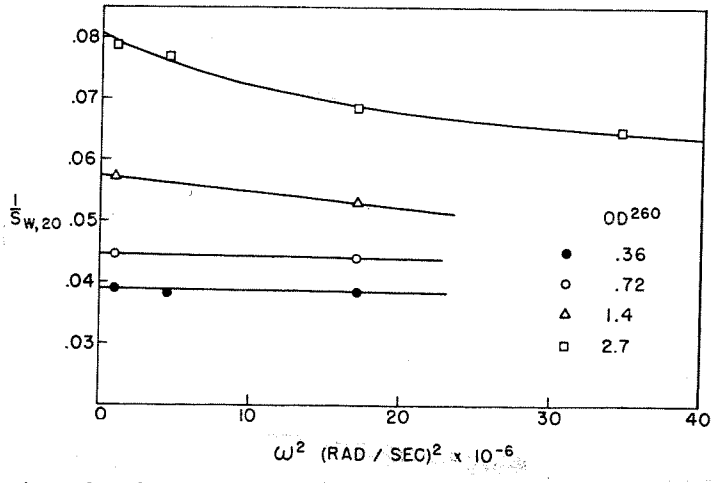

FIG. 8. The reciprocal of the sedimentation coefficient of *E. coli* DNA as a function of the square of angular velocity at different concentrations.

shows the linear behavior at low speeds that is predicted from the expansion of the frictional coefficient as a function of polymer concentration. At higher speeds a downward deviation in $1/S$ or an increase in S is observed. At intermediate speeds the plot of $1/S$ approaches the low-speed $1/S$ curve asymptotically with decreasing concentration. This behavior is not observed at a higher speed (20,410 r.p.m.) with T-4 DNA.

The TMV curves, Fig. 7, behave qualitatively like the high-speed T-4 DNA data. The extent to which these curves approach a common curve at low concentrations needs further study. The sedimentation coefficient of the TMV increases with increased concentration in the region studied, and the conditions of pH and ionic strength are such that dimerization should not occur. Therefore the effect of increased concentration on the speed effect is believed to be greater than its effect on solution viscosity.

$1/S$ vs. w^2

These graphs illustrate the speed dependence of $1/S$ at constant concentration. For T-4 DNA and *E. coli* DNA, Figs. 5 and 8, the speed dependence becomes more acute as the polymer concentration is increased.

Sedimentation Boundaries

The correlation between increased sedimentation coefficients at higher centrifuge speeds and the broadening of the sedimentation boundaries is impressive. The sedimentation boundaries, Figs. 9–13, are diagrammed for approximately equal positions in the cell. The small vertical line at the extreme left of each boundary indicates the position of the meniscus. Since plateau heights are affected by film and developer condition, only the boundary shapes are significant, not their relative heights.

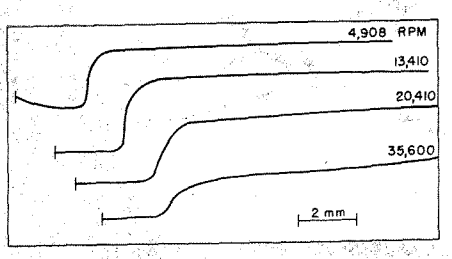

Fig. 9. Sedimentation boundaries for T-4 phage DNA, O.D.$_{260}$ 0.180.

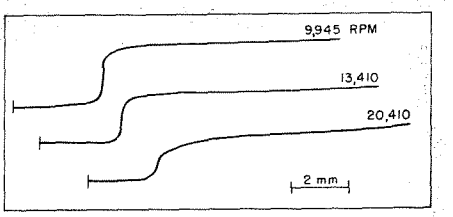

Fig. 10. Sedimentation boundaries for T-4 phage DNA, O.D.$_{260}$ 0.299.

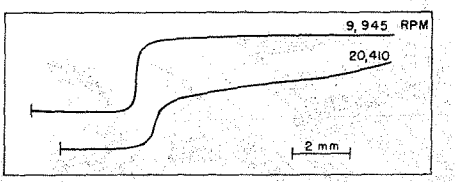

Fig. 11. Sedimentation boundaries for T-4 phage DNA, O.D.$_{260}$ 0.458.

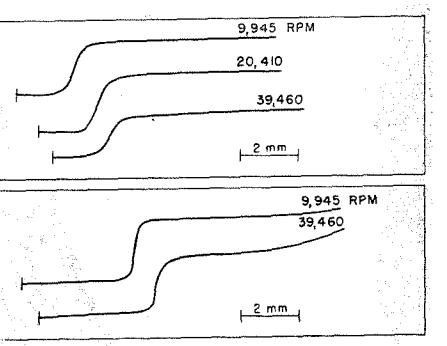

Fig. 12. Sedimentation boundaries for *E. coli* DNA, O.D.$_{260}$ 0.36.

Fig. 13. Sedimentation boundaries for *E. coli* DNA, O.D.$_{260}$ 1.4, 3-mm. cell.

The spreading is shown to increase with increased speed and increased concentration. At low speeds the boundaries are sharp. The extent of sharpening caused by the concentration dependence of the sedimentation coefficient (S on c self-sharpening) has not been considered.

The boundaries shown for TMV at 0.2 mg./ml., Fig. 14, sharpen for higher speeds instead of broadening. This is expected in a concentration region where there is an appreciable amount of diffusion at low speeds. The 1.0 mg./ml. boundaries for TMV are sharper than the 0.6 mg./ml. boundaries, Figs. 15 and 16. This is caused by the S on c sharpening overcoming the spreading effect.

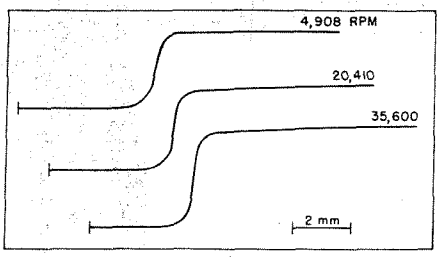

FIG. 14. Sedimentation boundaries for TMV 0.2 mg./ml.

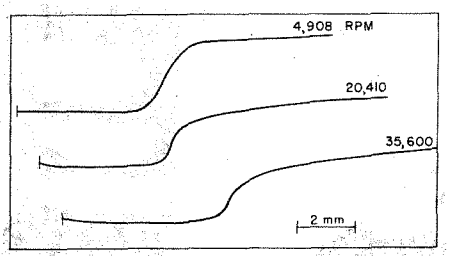

FIG. 15. Sedimentation boundaries for TMV 0.6 mg./ml., 3-mm. cell.

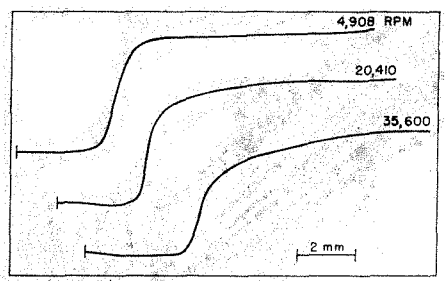

FIG. 16. Sedimentation boundaries for TMV 1.0 mg./ml., 3-mm. cell.

SEDIMENTATION DISTRIBUTIONS

Distributions, Fig. 17, are shown for T-4 DNA at a high concentration (0.025 mg./ml.) at two different speeds to illustrate the marked effect of speed on the distribution. A distribution is also shown for T-4 DNA in low concentration (0.006 mg./ml.) at a moderate speed; this result may be compared with that of other workers (19, 20) who have recently published sedimentation data on T-4 DNA.

At the present time we do not regard the actual magnitude of the high sedimentation velocity of the T-4 DNA studied here as the value characteristic of the purified, non-aggregated and unbroken material. Subsequent preparations involving only small changes in preparative procedures have yielded lower results.

DIFFUSION COEFFICIENT

The diffusion coefficient of deoxyadenylic acid was measured at three combined concentration levels. The results are listed in the following table:

C/C_0	D	*sq. cm./sec.*
.10	.90	40×10^{-7}
.25	.75	36×10^{-7}
.40	.60	34×10^{-7}

Figures 18 and 19 are an example of the diffusion boundary and one of the x^2 vs. t plots.

DISCUSSION

A theoretical explanation for the results of this paper has not been obtained; however, a discussion of various aspects of the problem is presented below.

There is sound evidence for the fact that the dependence of sedimentation coefficient on angular velocity is not caused by convection. First, the diffusion coefficient obtained for deoxyadenylic acid is reasonable in magnitude. There is also no indication of convective disturbances from the shapes of the diffusion boundaries that appear normal even in the regions least stabilized by density, Fig. 18. If the phenomenon were caused by convection, a limiting speed, above which no additional boundary spreading or speed dependence occurs, would be observed. This was not the case with either DNA sample, although it was true for the TMV. Finally, the greatest effects of convection would be expected at low polymer concentrations. The greatest effect of angular velocity is found at high polymer concentration, and the effect extrapolates out at low concentration (Figs. 4 and 6). An argument that the sharpness of the T-4 DNA sedimentation boundaries at low speeds might be caused by convection is contradicted by the sharpness of the boundaries in a CsCl density gradient during the formation of a band, Fig. 20. Convection parallel to the field in such a density gradient is not possible. Boundaries as sharp as these are uncommon in density-gradient studies as well as in DNA sedimentation studies.

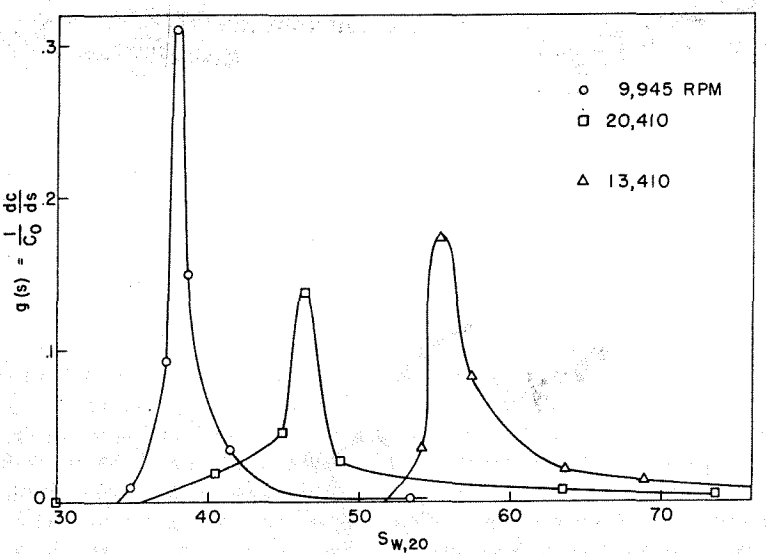

FIG. 17. Apparent distribution of sedimentation coefficients of T-4 phage DNA. ○ O.D.$_{260}$ 0.458, □ O D.$_{260}$ 0.458, △ O.D.$_{260}$ 0.120.

For a given polymer concentration, an increase in the angular velocity of the centrifuge is felt by the polymer molecule in two ways: (*a*) an increase in pressure and (*b*) an increase in the centrifugal force on the polymer, which increases its sedimenting velocity relative to its surroundings.

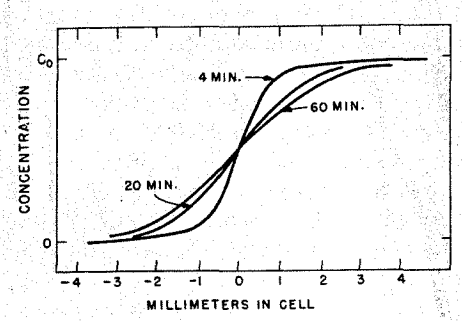

FIG. 18. Diffusion boundaries of deoxyadenylic acid at times after cell filling.

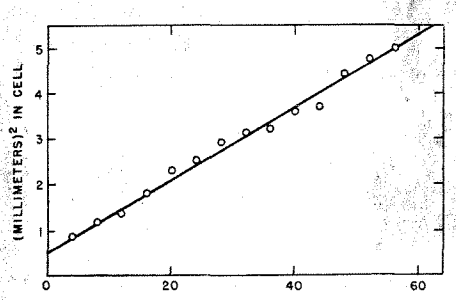

FIG. 19. x^2 vs. time for diffusion coefficient determination of deoxyadenylic acid, C/C_0 = .1 and .9.

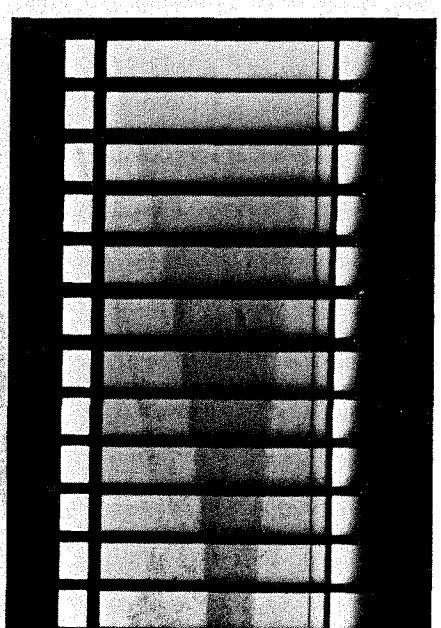

FIG. 20. Band formation of T-4 phage DNA in a CsCl density gradient. Original DNA, O.D.$_{260}$ = 0.038. Centrifuge speed = 25,980. Time intervals between pictures = 128 min.

Fujita (21) has calculated the effect of pressure on the sedimentation of a polymer;

this problem is also discussed by Schachman (18*b*). The net effect of pressure results from the compressibilities of both polymer and solvent including a viscosity increase of the solvent, a density increase of the solvent, and a volume decrease of polymer. If the compressibility of the polymer is smaller than that of the solvent, as is certainly the case with DNA, the sedimentation coefficient would decrease with increased pressure. In most cases, these effects are negligible; if they were not, they would produce the opposite result from our experiments. An increase in S with pressure might be expected if a pressure-dependent aggregation were occurring. Comparison of sedimentation coefficients at different speeds but at estimated equal pressures eliminates this as an explanation. In addition, a large dependence of S on position in the cell would be expected if this were the case; this was not observed as indicated by the confidence intervals of the least-squares slopes.

The suggestion that such results could be obtained if a slow equilibrium reaction were taking place between single molecules and aggregates has been considered. This is convincingly ruled out by two factors. If $nA \rightleftharpoons A_n$, and A_n has a larger sedimentation coefficient than A, the weight-average sedimentation coefficient must increase as the polymer concentration is increased; this was not observed with either DNA sample. Secondly, the sedimentation coefficient as measured by the second moment of the gradient in concentration is a measure of the weight-average sedimentation coefficient in the plateau region where relative concentrations are unchanged during a run except for the small effect of radial dilution. Considering the half-concentration point a good approximation to the second moment, a reacting system should in no way have its average sedimentation coefficient dependent on the speed at which it is sedimenting.

Johnson and Rowe (22) have recently published a paper on the sedimentation anomalies of myosin. They accounted for an increase in sedimentation coefficient at low speeds by a transformation reaction whose rate is comparable to the time of sedimentation. In addition to the fact that the effect is opposite in direction to the one reported in this paper, DNA is known to have a stable configuration at 20°C.

It is recognized that these data have neither been corrected for the concentration dependence of S during a single run nor have the second moments been used to evaluate the sedimentation coefficients. The measured effects, however, are much too large to be contingent upon either of these two simplifications in handling the data.

Another alternative is a hydrodynamic alignment of the nonspherical molecules. Singer (23) has considered this problem for a flexible chain, and his results predict that the centrifugal fields are far too small to decrease the friction factor appreciably. If one considers the case of a rigid rod it can be shown that as the ratio of the length-to-diameter approaches infinity, the ratio of the friction factor parallel to that perpendicular to its length approaches ½ for laminar flow (24). The magnitude of the observed effect is within this range so that orientation could explain the data. A rigid rod in a radial field has a slightly lower energy when oriented parallel to the direction of the field than when oriented perpendicular to the direction of the field. The magnitude of this energy difference has been calculated for a radial field corresponding to 10,000 r.p.m. in the ultracentrifuge and for a rigid rod of length equal to the contour length of a DNA molecule of molecular weight 5×10^7. Even for this extreme case, which is certainly a poor model for DNA, the value of this energy difference is $1/1000\ kT$ and is thus insignificant.

If alignment does occur in addition to a decrease in friction factor, there would be a decrease in the effective viscosity of the solution, which would in turn further increase the sedimentation velocity.

The fact that the effect is strongly concentration dependent indicates that if caused by alignment, the alignment is brought about by the interaction of polymer molecules during sedimentation. The nonrandom collisions resulting from the interaction of sedimenting molecules, which are in different orientations with respect to the field, also involve very small energies. The effect of hydrodynamic interactions between mole-

cules is not clear but appears to be a possible explanation. An unusual entropy effect similar to the formation of tactoids but dependent on the intermolecular stresses resulting from sedimentation is also conceivable.

Since sedimentation coefficients at infinite dilution are important as molecular parameters, we now examine the effect of the angular velocity on these extrapolations, Figs. 4, 6, and 7. In general, for DNA we conclude that extrapolated S values will be lower at high speeds than at low speeds. This is especially true for the T-4 DNA data if the points at 0.12 O.D.$_{260}$ are disregarded since experimenters rarely go to this low region in concentration. The extrapolated values range between 58 and 79 S, depending on the curve chosen.

For *E. coli* DNA the extrapolated sedimentation coefficient, $S^{\circ}_{w,20}$, changes from 30 to 31 S between 39,460 and 9945 r.p.m. using data below 1.5 O.D.$_{260}$. For DNA's of lower molecular weight than this material, the effect is expected to be negligible in this concentration region, but an effect is to be expected at higher concentrations for such materials.

It is to be noted that the concentration dependence of the sedimentation coefficient of TMV even at the lowest speed, 4908 r.p.m., is opposite to that usually encountered with schlieren optics at higher concentrations. This may be taken to indicate that the concentration dependence of the speed effect is greater than the concentration dependence of the friction factor. The high-speed extrapolation of the TMV data yields an $S_{w,20}$ of 183 S. The value of 188 S obtained by Boedtker and Simmons (25) by extrapolation of schlieren data (with one point obtained at about 0.2 mg./ml. with ultraviolet optics) for TMV is in fair agreement with our value. At low speed the extrapolated value of $S_{w,20}$ is 176 S.

REFERENCES

1. Shooter, K. V., *Progr. in Biophys.* **8,** 310 (1957).
2. Kahler, H., *J. Phys. Chem.* **52,** 676 (1948).
3. Cecil, R., and Ogston, A. G., *J. Chem. Soc.* **1948,** 1382.
4. Conway, B. E., Gilbert, L., and Butler, J. A. V., *J. Chem. Soc.* **1950,** 3421.
5. Koenig, V. L., and Perrings, J. D., *J. Colloid Sci.* **8,** 452 (1953).
6. Butler, J. A. V., Laurence, F. R. S., Robins, A. B., and Shooter, K. V., *Proc. Roy. Soc.* (London) **A250,** 1 (1959).
7. Hermans, J., Jr., and Hermans, J. J., *J. Phys. Chem.* **63,** 170 (1959).
8. Doty, P., McGill, B. Bunce, and Rice, S., *Proc. Natl. Acad. Sci. U. S.* **44,** 432 (1958).
9. Doty, P., Marmur, J., Eigner, J., and Schildkraut, C., *Proc. Natl. Acad. Sci. U. S.* **46,** 461 (1960).
10. Schachman, H. K., *J. Am. Chem. Soc.* **73,** 4808 (1951).
11. Shooter, K. V., and Butler, J. A. V., *Trans. Faraday Soc.* **52,** 734 (1956).
12. Schumaker, V. N., and Schachman, H. K., *Biochim. et Biophys. Acta* **23,** 628 (1957).
13. Alexander, A. E., and Johnson, P., "Colloid Science," Vol. I, p. 233–245. Clarendon Press, Oxford, 1949.
14. Robkin, E., Meselson, M., and Vinograd, J., *J. Am. Chem. Soc.* **81,** 1305 (1959).
15. Hersh, R. T., and Schachman, H. K., *J. Phys. Chem.* **62,** 170 (1958).
16. Pickels, E. G., *Rev. Sci. Instr.* **13,** 426 (1942).
17. Moore, D. H., *Rev. Sci. Instr.* **14,** 295 (1943).
18. (*a*) Schachman, H. K., "Ultracentrifugation in Biochemistry," p. 133. Academic Press, New York, 1959; (*b*) *ibid.* p. 174.
19. Davison, P. F., *Proc. Natl. Acad. Sci. U. S.* **45,** 1560 (1959).
20. Thomas, C. A., and Knight, J. H., *Proc. Natl. Acad. Sci. U. S.* **45,** 332 (1959).
21. Fujita, H. J., *J. Am. Chem. Soc.* **78,** 3598 (1956).
22. Johnson, P., and Rowe, A. J., *Biochem. J.* **74,** 432 (1960).
23. Singer, S. J., *J. Polymer Sci.* **2,** 290 (1947).
24. Barr, G., "A Monograph of Viscometry." Oxford Univ. Press, London, 1931.
25. Boedtker, H., and Simmons, N., *J. Am. Chem. Soc.* **80,** 2550 (1958).

Addendum - Part 1

It has been pointed out by colleagues that an error was made in estimating the difference in potential energy of a rigid rod aligned parallel to a centrifugal field compared with one perpendicular to this position. In point of fact, there is no difference between the potential energy in these two positions if the center of mass of the rod remains fixed. The conclusion resulting from the calculation remains unchanged.

Part 2

The Renaturation of Deoxyribonucleic Acid in Formamide Solutions

Introduction

Marmur and Lane (1) and Doty et al. (2) have recently presented evidence for what they call the renaturation of DNA. The data presented indicates a bimolecular reaction, dependent on ionic strength and polymer concentration. The process of renaturation involved the slow cooling of a heat denatured sample. The methods of detection involved the recovery of transforming activity, a small recovery of optical hyperchromicity, a shift in buoyant density in a density gradient from the position of denatured DNA toward that of native, and recovery of the characteristic rod structure as observed by electron microscopy. The strong disadvantage to the slow cooling system used was that the phosphate ester linkages in the DNA strands were continually breaking at a slow rate.

Helmkamp and T'so (3) have recently studied the denaturation of DNA in formamide and found that a sharp transition in specific rotation of DNA occurs at 70% by volume formamide. This system apparently is not accompanied by chain degradation and is therefore an interesting candidate for renaturation studies on DNA.

The following experiments combine the ideas of renaturation and formamide denaturation. The methods used for determining the extent of renaturation were buoyant density and hyperchromicity. The original purpose of

these experiments was the determination of the number of biological subunits in the T-4 DNA molecule. If the renaturation process were perfected so that the physical properties of the native and renatured DNA were the same, the number of subunits could be determined by the renaturation of mixtures of normal and isotopically labelled heavy DNA. The experiments, however, were not completed.

Procedures and Results

One milliliter samples of a T-4 Bacteriophage DNA solution prepared by the procedure described in Part I were dialyzed against 100 ml of 99% formamide to equilibrium at 35°C. The volume of solution inside the dialysis sack decreased by about a factor of two during this dialysis. All DNA concentrations listed in the data below are concentrations in the DNA solution before dialysis.

The renaturation step involved the addition of a sodium citrate solution, pH 7.0, to the 100 ml of formamide at a rate of 10-20 ml/hr until the dialysate was less than 40% by volume formamide. During this step the solution was constantly stirred with a magnetic stirrer and controlled at 35°C. The DNA solutions were then dialyzed to equilibrium with one dialysate change against 100 ml of a pH 7, .06 M sodium citrate solution in the refrigerator.

Two series of experiments were done. The first involved renaturing solutions of different DNA concentrations with 0.1 M sodium citrate buffer, Appendix, page 100, figure 13. The second series involved renaturing a 0.8 OD^{260} DNA solution with buffers of different concentration, Appendix, page 101, figure 14. The extent of renaturation was measured in a CsCl gradient in the analytical ultracentrifuge (Part I). B. Bronchi DNA

supplied by Dr. R. Rolfe was used as a density marker. The light bands to the left in figures 13 and 14 are the marker DNA. Two of the runs were made before the marker was obtained. These were positioned in the series by knowledge of the initial solution density, the isoconcentration position (4), and the density gradient.

Figure 1 shows the optical density of both native and renatured T-4 DNA as a function of temperature. Both curves were normalized by their optical density at 94°C. The points plotted represent the optical density at the maximum near 260 mμ in the spectrum. The Beckman Model DK 2 Recording Spectrophotometer, equipped with a heating unit, was used for this experiment. The instrument had a thermometer immersed in the reference cell as well as in the heating block. When these two thermometers indicated the cell and block were at the same temperature, the spectrum in the region of the maximum was recorded. The DNA was renatured at a DNA concentration of 0.80D and with a .06 M sodium citrate buffer. The two upper curves in figure 1 are the cooling curves after heat denaturation.

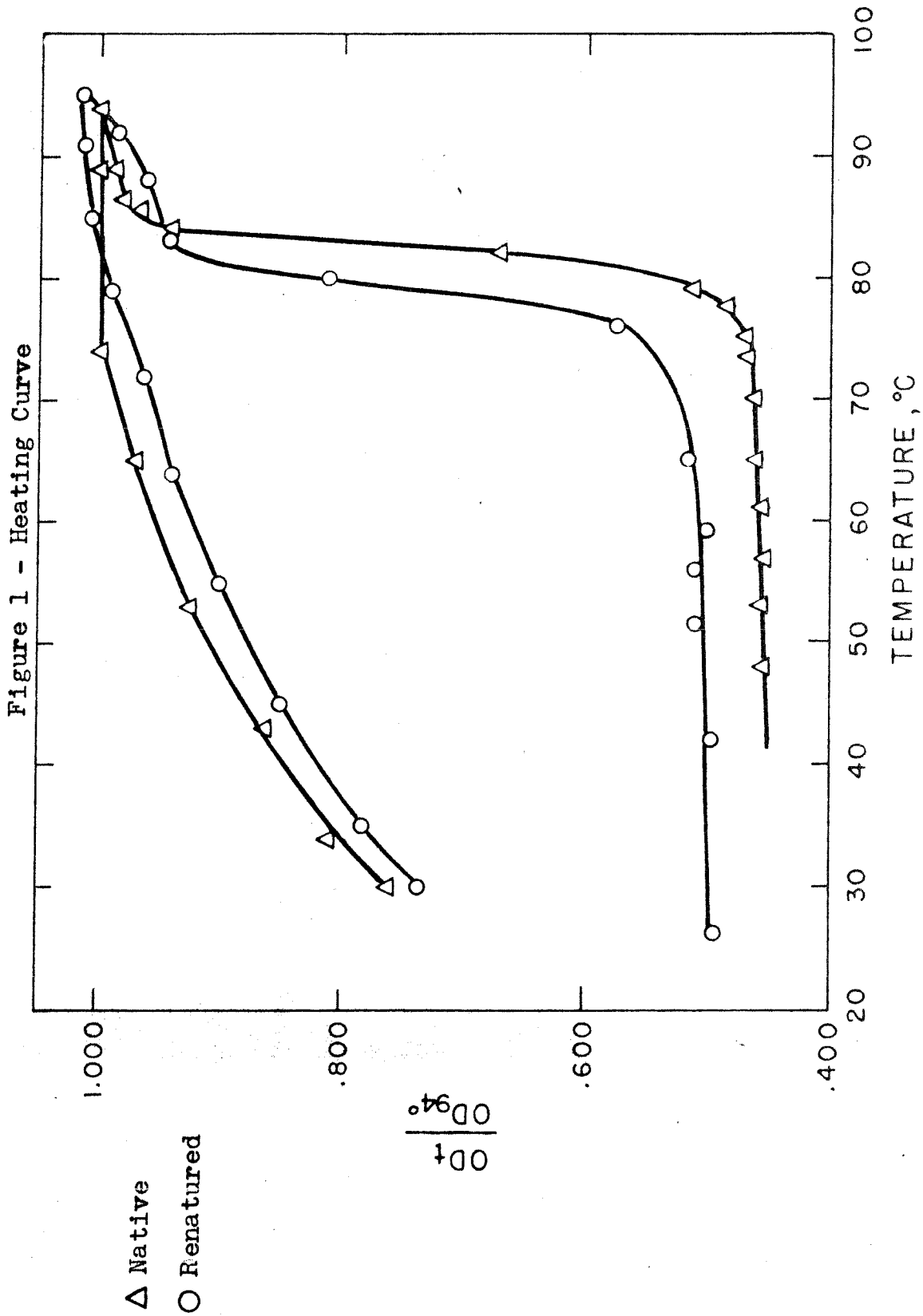
Figure 1 - Heating Curve
Δ Native
O Renatured
$\frac{OD_t}{OD_{94°}}$
1.000
.800
.600
.400
20
30
40
50
60
70
80
90
100
TEMPERATURE, °C

Discussion

The ionic strength series and the DNA concentration series show the same behavior. At low ionic strength or DNA concentration no renaturation occurs. As either of these experimental variables are increased, a transition from denatured to approximately half renatured occurs. This manner of speech assumes that buoyant density is a linear function of native DNA content. As the parameters are increased still farther, the half renatured material perfects itself, continuously moving toward the native DNA density, and finally aggregating. These results are in qualitative agreement with the results of references 1 and 2. The ultracentrifuge pictures, Appendix, page 100, figures 13 and 14, and the heating curves, figure 1, indicate the renaturation process never perfects a DNA molecule to better than 90% native under these conditions.

The interesting new piece of information demonstrated by these experiments is that the initial bimolecular reaction is an all or none reaction. The strands must mate about 50% their hydrogen bonds before the double stranded structure is stable.

The discussion above tacitly assumes the interpretation of renaturation as stated in references 1 and 2 is correct: that the strands of the Watson-Crick struc-

ture do separate on denaturation, and that the observed concentration dependence and ionic strength dependence of the renaturation process is that expected from the recoiling of two single strands into a helix. The evidence for this is good although not conclusive.

Experiments were designed to renature deuterium and nitrogen 15 labelled T-4 DNA with light T-4 DNA. Considerable problems were encountered in the growth of deuterium labelled T-4 phage, although a low yield system was finally developed. The work, however, was left incomplete because of interest in the solvation studies described in Part 4.

Part 3

The Buoyant Density of Deoxyribonucleic Acid in Solutions Containing Two Cations

Introduction

This section concerns itself with factors governing the effectiveness of the density gradient sedimentation equilibrium method as an analytical tool. The factors governing the buoyant density of DNA in a density gradient have up to this time been ignored, even though such puzzling problems as the large difference in the buoyant density of DNA and RNA despite their chemical similarity and the density shift of DNA on denaturation have not been explained. In an effort to get deeper insight into these problems, various mixed cation salt systems have been studied.

Theory

The following treatment assumes that the specific volume of the solvated DNA ion does not change in the region it is being studied. The validity of this assumption will be considered after the data is presented. The DNA is in a solution containing two salts, AX and BX. It is assumed all ionic sites on the DNA are bound with either A^+ or B^+. The buoyant density may then be written:

$$\frac{1}{\rho_o} = \nu_{DNA} w_{DNA} + \nu_A w_A + \nu_B w_B \qquad (1)$$

where w equals the weight fraction of total DNA molecule, and v equals the specific volume of each species. The subscript DNA refers to the DNA ion.

Defining m_A as the ratio of the molecular weight of A^+ to the average nucleotide residue molecular weight and n_A as the fraction of sites binding A^+, the following equations may be written: $n_A + n_B = 1$

$$w_{DNA} = \frac{1}{1 + n_A(m_A - m_B) + m_B}$$

$$w_A = \frac{n_A m_A}{1 + n_A(m_A - m_B) + m_B} \qquad (2)$$

$$w_B = \frac{(1 - n_A) m_B}{1 + n_A(m_A - m_B) + m_B}$$

Substituting equations 2 into equation 1, equation 3 is obtained.

$$\rho_o = \left[\frac{1 + m_B}{v_{DNA} + m_B v_B}\right] \frac{\left[1 + \left(\frac{m_A - m_B}{1 + m_B}\right) n_A\right]}{\left[1 + \left(\frac{m_A v_A - m_B v_B}{v_{DNA} + m_B v_B}\right) n_A\right]} \qquad (3)$$

The magnitude of $\frac{m_A v_A - m_B v_B}{v_{DNA} + m_B v_B}$ will in general be less than 0.1, so the denominator of equation 3 can be expanded keeping only first order terms. The resulting equation is;

$$\rho_o = \left[\frac{1 + m_B}{v_{DNA} + m_B v_B}\right]\left[1 + \left(\frac{m_A - m_B}{1 + m_B} - \frac{m_A v_A - m_B v_B}{v_{DNA} + m_B v_B}\right) n_A\right] \quad (4)$$

which can be rewritten as $\rho_o = a(1 + b n_A)$

where $a = \rho_{BDNA}$ and $a(1+b) = \rho_{ADNA}$.

A relative binding constant K is defined by equation 5

$$f \equiv \frac{[B^+]}{[A^+]} = \frac{1}{K}\frac{[BDNA]}{[ADNA]} \quad (5)$$

where $[ADNA]$ refers to the concentration of sites in the DNA binding A^+. The following equations are then self evident.

$$n_A = \frac{[ADNA]}{[ADNA] + [BDNA]} = \frac{1}{1 + Kf}$$

$$\rho_o - a = ab\left(\frac{1}{1 + Kf}\right) \quad (6)$$

$$f = \left(\frac{ab}{K}\right)\left(\frac{1}{\rho_o - a}\right) - \frac{1}{K}$$

It is therefore expected from equation 6 that a plot of ρ_o versus f would be hyperbolic under the limitations of the derivation.

Materials and Procedures

Part 4 contains most of the pertinent facts relating to the materials and procedures of this section. The guanidinium bromide and guanidinium chloride were prepared by Donald H. Voet by the following procedure which he has written:

> "Dissolve guanidinium carbonate in a minimum of water, clarify with washed Norite and filter through a paper filter and then a millipore filter. To the guanidinium carbonate solution add four volumes 95% ethanol and filter off the guanidinium carbonate. Dry in vacuum over night without heating. To the dry guanidinium carbonate carefully add a stoichimetric amount of HCl and HBr. The vessel in which the addition takes place should be kept in an ice bath. The solution of guanidinium halide should then be boiled under vacuum, the pH adjusted to 7 with either guanidinium carbonate, HCl or HBr. The solution should then be boiled under vacuum until the guanidinium halide crystallizes out. These crystals can be recrystallized from water."

Results

Figure 2 shows ρ_o versus f for $A^+ = Cs^+$ and B^+ = guanidinium ion. The anion for the one curve was chloride* ion, for the other bromide ion. The constant, a, in equation 6 was obtained for both of these curves by plotting the same data in the form of ρ_o versus 1/f and extrapolating to 1/f = 0. The result of this operation in the chloride solution was 1.462, and in the bromide was 1.453.

Figure 3 shows f versus $1/(\rho_o - a)$ for these same systems. The linearity of these plots indicates that the assumptions of the previous derivation are valid. As would be expected, both curves have the same intercept. The value for K is 5.5. The fact that the two curves are not superimposed indicates that the ν_{DNA} and/or the ν of the cations are different in the two solutions, although the relative binding constant is not. This fact suggests a difference in the solvation of the DNA in the two systems. It will be seen in the next section that it was somewhat fortuitous that the results fit the model so well. The changes in water activity in these mixtures were evidently small, making solvation changes insignificant.

---

* Two of the points on this curve were obtained by Donald H. Voet.

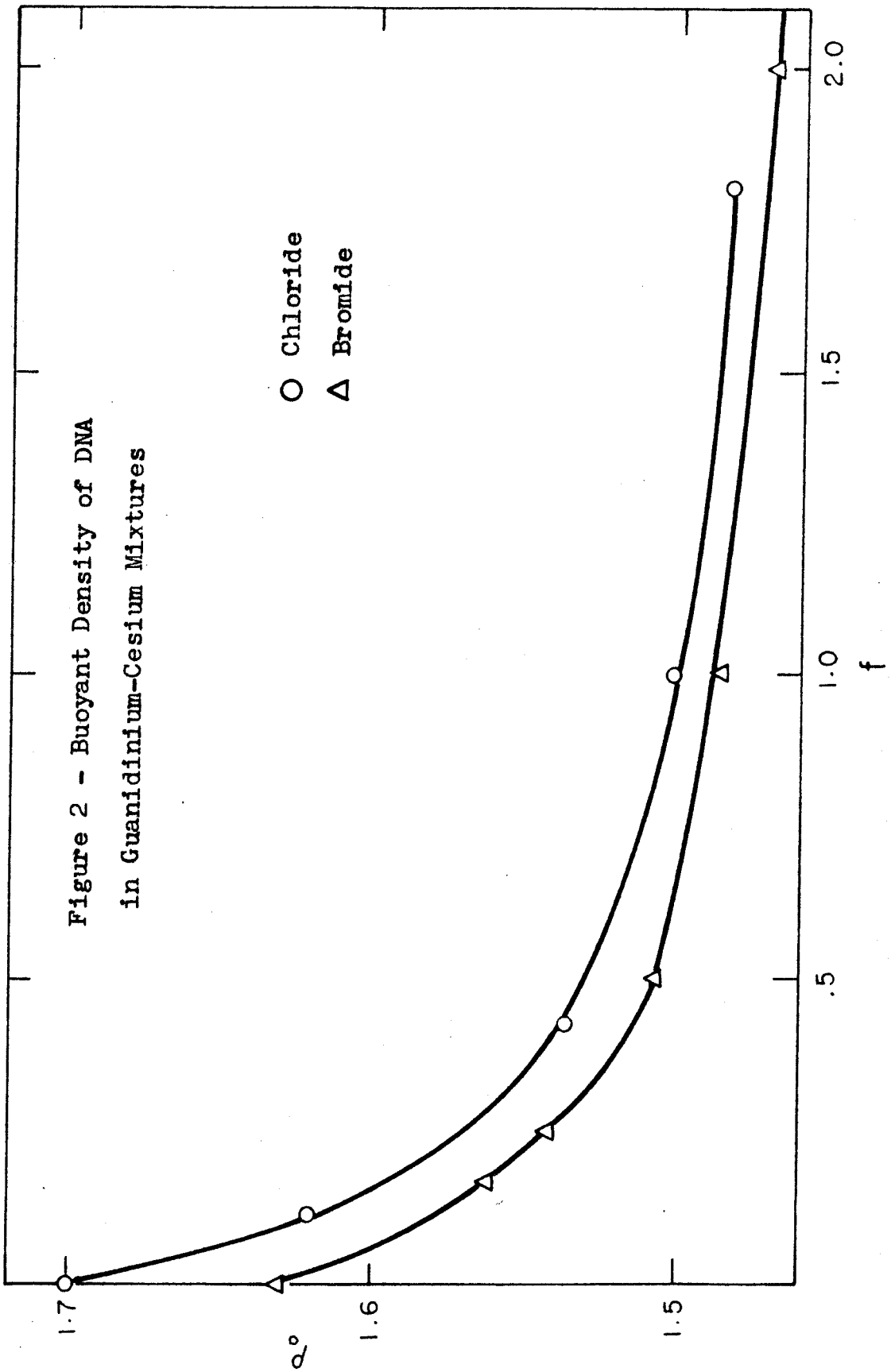

Figure 2 - Buoyant Density of DNA in Guanidinium-Cesium Mixtures

Figure 3

Guanidinium-Cesium Mixtures

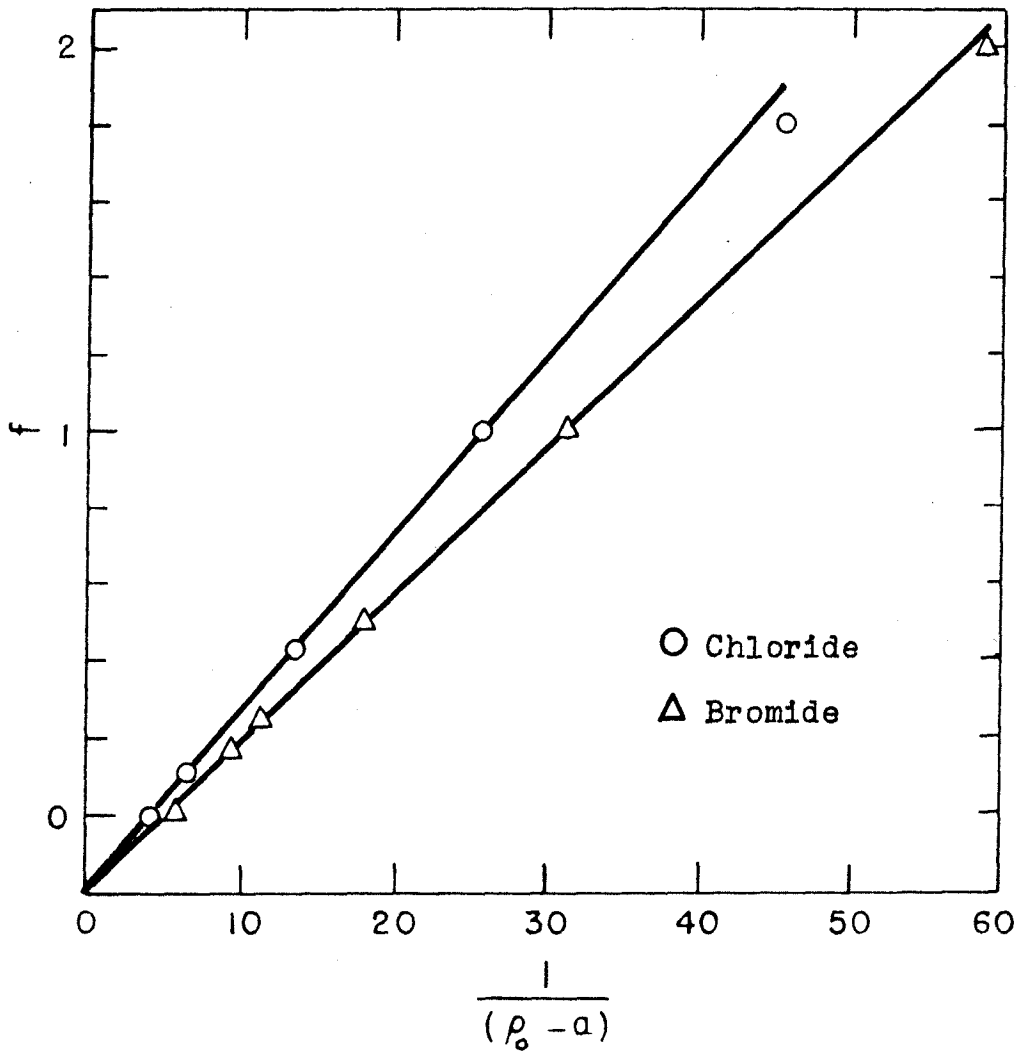

Part 4

The Three Component Theory of Sedimentation Equilibrium in a Density Gradient and the Hydration of DNA

Introduction

The theory of three component sedimentation equilibrium has been in such form that experiments with these systems are difficult to interpret. Although the equations describing the state of equilibrium have been presented many times (5,6,7), the proper physical insight into the problem has been lacking. It is now believed that at least in the case of the density gradient system, the problems have been successfully solved.

In 1954, Jacobson, Anderson and Arnold (8) presented evidence for the extensive hydration of DNA from studies of the proton magnetic resonance in aqueous solutions of sodium DNA. The following year Wang (9) concluded that DNA was hydrated to the extent of only 0.35 gm water/gm dry deoxynucleate from self diffusion measurements of water in NaDNA solutions. This section presents evidence for hydration of almost 2 gm water/gm CsDNA.

Theory

In a three component system the equations for equilibrium in a centrifugal field may be written as follows (10):

$$M_1\left(1-\bar{v}_1\rho\right)\omega^2 r\,dr = \left(\frac{\partial \mu_1}{\partial m_1}\right)_{m_3} dm_1 + \left(\frac{\partial \mu_1}{\partial m_3}\right)_{m_1} dm_3$$

$$= \left(\frac{\partial \mu_1}{\partial m_1}\right)_{m_3} dm_1 - \Gamma\left(\frac{\partial \mu_1}{\partial m_1}\right)_{m_3} dm_3 \qquad (7)$$

$$M_3\left(1-\bar{v}_3\rho\right)\omega^2 r\,dr = \left(\frac{\partial \mu_3}{\partial m_1}\right)_{m_3} dm_1 + \left(\frac{\partial \mu_3}{\partial m_3}\right)_{m_1} dm_3$$

$$= -\Gamma\left(\frac{\partial \mu_1}{\partial m_1}\right)_{m_3} dm_1 + \left(\frac{\partial \mu_3}{\partial m_3}\right)_{m_1} dm_3 \qquad (8)$$

These equations are all at constant temperature and pressure. Because the differential equation applies for a given radial distance the constant pressure restriction is valid. Γ is defined as $-\left(\frac{\partial \mu_1}{\partial m_3}\right)_{m_1} \Big/ \left(\frac{\partial \mu_1}{\partial m_1}\right)_{m_3}$ which equals $\left(\frac{\partial m_1}{\partial m_3}\right)_{\mu_1}$ by the triple product rule. Γ represents the net solvation of the polymer in moles solute per mole polymer. The fact that it has the proper properties for a solvation parameter is apparent from the properties of $\left(\frac{\partial m_1}{\partial m_3}\right)_{\mu_1}$. In addition the relation $\left(\frac{\partial \mu_1}{\partial m_3}\right)_{m_1} = \left(\frac{\partial \mu_3}{\partial m_1}\right)_{m_3}$ has been used. This relation is valid if concentrations are expressed in molalities,

and is the consequence of the fact that the order of partial differentiation of a state function does not affect the result.

Focusing attention on the polymer first, if dm_1 is eliminated from equations 7 and 8, equation 9 is obtained.

$$\left[(M_3+\Gamma M_1)-(M_3\bar{v}_3+\Gamma M_1\bar{v}_1)\rho\right]\omega^2 r\,dr = \left[\left(\frac{\partial \mu_3}{\partial m_3}\right)_{m_1}-\Gamma^2\left(\frac{\partial \mu_1}{\partial m_1}\right)_{m_3}\right]dm_3 \qquad (9)$$

Defining a solvation parameter on a weight basis, $\Gamma' = \Gamma\left(\frac{M_1}{M_3}\right)$ equation 9 becomes:

$$M_3(1+\Gamma')\left[1-\left(\frac{\bar{v}_3+\Gamma'\bar{v}_1}{1+\Gamma'}\right)\rho\right]\omega^2 r\,dr = \left(\frac{\partial \mu_3}{\partial m_3}\right)_{m_1}\left[1-\frac{\left(\frac{\partial \mu_1}{\partial m_3}\right)^2_{m_1}}{\left(\frac{\partial \mu_1}{\partial m_1}\right)_{m_3}\left(\frac{\partial \mu_3}{\partial m_3}\right)_{m_1}}\right]dm_3 \qquad (10)$$

Defining the position of the band by the point of maximum polymer concentration, $\left(\frac{dm_3}{dr}\right) = 0$, the buoyancy condition from equation 10 is $\frac{1}{\rho_o} = \frac{\bar{v}_3+\Gamma'\bar{v}_1}{1+\Gamma'}$ (7).

Clearly the experimentally determined buoyant density is that of the solvated species. The ρ_o refers to the buoyant density of the polymer. It should be emphasized that up to this point no assumptions have been made. The density gradient provides a method of determing Γ' if $\bar{v}_1$ and $\bar{v}_3$ are known.

If one is interested in the polymer distribution, the right side of equation 10 must be evaluated. The term, $\left(\frac{\partial \mu_1}{\partial m_3}\right)^2_{m_1} \Big/ \left(\frac{\partial \mu_1}{\partial m_1}\right)_{m_3} \left(\frac{\partial \mu_3}{\partial m_3}\right)_{m_1}$, which shall be referred to as ϵ, is interesting. It is a general condition of stability with respect to the formation of a new phase that ϵ be less than 1. To estimate an order of magnitude of ϵ all the terms are assumed to be ideal. $w \equiv M m$

$$\epsilon_i = \Gamma'^2 \left(\frac{M_3}{M_1}\right)^2 \frac{\frac{RT}{m_1}}{\frac{RT}{m_3}} = \Gamma'^2 \left(\frac{M_3}{M_1}\right)\left(\frac{w_3}{w_1}\right) \tag{11}$$

At common experimental conditions for DNA and proteins in CsCl, ϵ_i takes on values between 0.2 and 8 at band center without the formation of a new phase. Furthermore, because this term is concentration dependent, it would make the distribution very non-Gaussian.

These facts demonstrate that the ideality assumption is certainly not valid for this system, despite the very low DNA concentrations usually used.

Independent particles are suggested by the observed Gaussian distributions. From experimental evidence, the solvation of DNA is a function of solute activity. The solvated molecules, therefore, would be expected to behave independently only at constant solute

chemical potential. It is thus assumed that $\left(\frac{\partial \mu_3}{\partial m_3}\right)_{\mu_1} = \frac{RT}{m_3}$. The following equations result from this assumption.

$$\left(\frac{\partial \mu_3}{\partial m_3}\right)_{\mu_1} = \left(\frac{\partial \mu_3}{\partial m_3}\right)_{m_1} + \left(\frac{\partial \mu_3}{\partial m_1}\right)_{m_3}\left(\frac{\partial m_1}{\partial m_3}\right)_{\mu_1} = \frac{RT}{m_3}$$

$$\left(\frac{\partial m_1}{\partial m_3}\right)_{\mu_1} = \Gamma \quad , \quad \left(\frac{\partial \mu_3}{\partial m_1}\right)_{m_3} = -\Gamma\left(\frac{\partial \mu_1}{\partial m_1}\right)_{m_3} \tag{12}$$

Therefore $\left(\frac{\partial \mu_3}{\partial m_3}\right)_{m_1} - \Gamma^2\left(\frac{\partial \mu_1}{\partial m_1}\right)_{m_3} = \frac{RT}{m_3}$, and

$$RT\left(\frac{\partial \ln \gamma_3}{\partial m_3}\right)_{m_1} = \Gamma^2\left(\frac{\partial \mu_1}{\partial m_1}\right)_{m_3}. \qquad \epsilon = \frac{\Gamma^2\left(\frac{\partial \mu_1}{\partial m_1}\right)_{m_3}}{\frac{RT}{m_3} + \Gamma^2\left(\frac{\partial \mu_1}{\partial m_1}\right)_{m_3}}$$ and is always less than one under the original assumption.

γ_3 is the activity coefficient of the polymer.

With the above assumption equations 9 and 10 become the equation for independent solvated molecules,

$$M_s\left[1 - \bar{v}_s \rho\right] \omega^2 r \, dr = \frac{RT}{m_3} \, dm_3 \tag{13}$$

where $M_s = M_3\left(1 + \Gamma'\right)$ and $\bar{v}_s = \frac{\bar{v}_3 + \Gamma' \bar{v}_1}{1 + \Gamma'}$

Returning to the solvation parameter, it can be shown that the assumption $\left(\frac{\partial \mu_3}{\partial m_3}\right)_{\mu_1} = \frac{RT}{m_3}$ is consistent with the idea that Γ is independent of polymer concentration at constant μ_1. $\left(\frac{\partial \mu_3}{\partial m_1}\right)_{m_3} = -\Gamma \left(\frac{\partial \mu_1}{\partial m_1}\right)_{m_3}$

Partial differentiation at constant μ_1 gives

$$-\frac{\partial}{\partial m_3}\left[\left(\frac{\partial \mu_3}{\partial m_1}\right)_{m_3}\right]_{\mu_1} = \left(\frac{\partial \Gamma}{\partial m_3}\right)_{\mu_1}\left(\frac{\partial \mu_1}{\partial m_1}\right)_{m_3} + \Gamma \frac{\partial}{\partial m_3}\left[\left(\frac{\partial \mu_1}{\partial m_1}\right)_{m_3}\right]_{\mu_1}$$

$$\frac{\partial}{\partial m_3}\left[\left(\frac{\partial \mu_3}{\partial m_1}\right)_{m_3}\right]_{\mu_1} = \frac{\partial}{\partial m_1}\left[\left(\frac{\partial \mu_3}{\partial m_3}\right)_{\mu_1}\right]_{m_3} = \frac{\partial}{\partial m_1}\left(\frac{RT}{m_3}\right)_{m_3} = 0$$

$$\frac{\partial}{\partial m_3}\left[\left(\frac{\partial \mu_1}{\partial m_1}\right)_{m_3}\right]_{\mu_1} = \frac{\partial}{\partial m_1}\left[\left(\frac{\partial \mu_1}{\partial m_3}\right)_{\mu_1}\right]_{m_3} = 0$$

Therefore $\left(\frac{\partial \Gamma}{\partial m_3}\right)_{\mu_1}\left(\frac{\partial \mu_1}{\partial m_1}\right)_{m_3} = 0$. $\left(\frac{\partial \mu_1}{\partial m_1}\right)_{m_3} > 0$ by a stability condition, and so $\left(\frac{\partial \Gamma}{\partial m_3}\right)_{\mu_1} = 0$.

The polymer introduces one more interesting problem. Equation 13 has two solutions. If the solute, 1, is water, Γ' is positive; if the solute is salt, Γ' is negative. One solution yields a value of M_3 less than M_S; the other, greater. This is physically reasonable because the system can not distinguish between dry polymer, and polymer plus just enough solution of polymer density so that when Γ moles of salt are removed per mole of polymer, only water remains in the solvate layer.

To obtain a molecular weight of dry polymer, it is obvious that Γ' must be chosen to be positive. In the following experimental work on DNA all molalities are expressed as moles per 1000 gm of salt. In this case Γ is positive and represents moles water bound per mole polymer. With this definition of molality, M_3 becomes the molecular weight of the dry polymer.

The final question to be answered by the theory is the effect of solvation on the density gradient. If one eliminates dm_3 from equations 7 and 8, equation 14 is obtained,

$$\frac{dm_1}{dr} = \frac{\left[\left(M_1 + \gamma\Gamma M_3\right) - \left(M_1\bar{v}_1 + \gamma\Gamma M_3\bar{v}_3\right)\rho\right]\omega^2 r}{\left(\frac{\partial \mu_1}{\partial m_1}\right)_{m_3}\left[1 - \Gamma^2\gamma\right]} \qquad (14)$$

where $\gamma = \left(\frac{\partial \mu_1}{\partial m_1}\right)_{m_3} \Big/ \left(\frac{\partial \mu_3}{\partial m_3}\right)_{m_1}$. Although hydrated water represents a very small fraction of the total water, it makes a large contribution to the water concentration gradient. Free water alone, however, determines the density gradient, because the hydrated polymer has a density almost identical with that of the solution. Its effect on the density gradient is therefore negligible. The gradient of free water can be expressed by the equation $\left(\frac{dm_1}{dr}\right)_f = \frac{dm_1}{dr} - \Gamma\frac{dm_3}{dr}$.

Substituting equations 9 and 14 into this expression, equation 15 is obtained.

$$\left(\frac{dm_1}{dr}\right)_f = \frac{M_1\left(1-\bar{v}_1\rho\right)\omega^2 r}{\left(\partial\mu_1/\partial m_1\right)_{m_3}} \qquad (15)$$

The expression for the gradient is therefore unaffected by the presence of solvation. Effects of polymer on the activity of the solvent are completely negligible at the polymer concentrations normally used. Equation 15 is the condition for equilibrium in a two component system. It therefore does not matter which definition of molality is used in determining the density gradient.

In order to obtain an expression for the polymer distribution, ρ , $\bar{v}_s$, and M_s are expanded about band center. $\delta = r - r_0$

$$\rho = \rho_0 + \left(\frac{d\rho}{dr}\right)\delta \qquad \bar{v}_s = \bar{v}_{s,0} + \left(\frac{d\bar{v}_s}{dr}\right)\delta \qquad M_s = M_{s,0} + \left(\frac{dM_s}{dr}\right)\delta$$

Substituting these equations into equation 13, using the buoyancy condition $\left(1-\bar{v}_{s,0}\rho_0\right) = 0$ and keeping only first order terms in δ , equation 16 is obtained.

$$-M_{s,0}\left[\bar{v}_{s,0}\left(\frac{d\rho}{dr}\right)+\rho_0\left(\frac{d\bar{v}_s}{dr}\right)\right]\delta\,\omega^2 r_0\,d\delta = RT\,d\ln m_3 \qquad (16)$$

Integrating equation 16, a distribution of the form $m = m_o \exp\left(-\frac{\delta^2}{2\sigma^2}\right)$ where σ^2 is given by equations 17 and 18, is obtained.

$$\sigma^2 = \frac{RT}{M_{s,o}\,\bar{v}_{s,o}\left(\frac{d\rho}{dr}\right)_{eff}\,\omega^2\,r_o} \tag{17}$$

$$\left(\frac{d\rho}{dr}\right)_{eff} = \left(\frac{d\rho}{dr}\right) + \frac{\rho_o}{\bar{v}_{s,o}}\left(\frac{d\bar{v}_s}{dr}\right) \tag{18}$$

From the experimental evidence presented in parts 4 and 5, $\bar{v}_s$ is known to be a function of pressure and solute activity at atmospheric pressure, a_1^o. The following equations allow the separation of these two effects and define an apparent compressibility for the solvated polymer, K_s.

$$\frac{d\bar{v}_s}{dr} = \left(\frac{\partial \bar{v}_s}{\partial P}\right)_{a_1^o}\left(\frac{dP}{dr}\right) + \left(\frac{\partial \bar{v}_s}{\partial a_1^o}\right)_P\left(\frac{da_1^o}{dr}\right) \tag{19}$$

$$K_s = -\frac{1}{\bar{v}_s}\left(\frac{\partial \bar{v}_s}{\partial P}\right)_{a_1^o} \quad ; \quad \frac{1}{\bar{v}_{s,o}}\left(\frac{\partial \bar{v}_s}{\partial a_1^o}\right)_P = -\frac{1}{\rho_o}\left(\frac{\partial \rho_o}{\partial a_1^o}\right)_P$$

$$\left(\frac{d\rho}{dr}\right)_{eff} = \frac{d\rho}{dr} - \rho_o K_s \frac{dP}{dr} - \left(\frac{\partial \rho_o}{\partial a_1^o}\right)_P\left(\frac{da_1^o}{dr}\right) \tag{20}$$

In order to obtain a workable buoyancy condition it is necessary to expand $\bar{v}_s$ about atmospheric pressure, P equal zero. The activity of the solute a_1°, and the density of the solution ρ° at zero pressure are not independent. It is therefore possible to expand in ρ° * instead of a_1°. The expansion is given by equation 21.

$$\bar{v}_{s,o} = \bar{v}_{s,o}^\circ \left[1 - K_s P_o - \frac{1}{\rho_o^\circ} \left(\frac{\partial \rho_o^\circ}{\partial a_1^\circ} \right)_P \left(\frac{da_1^\circ}{d\rho^\circ} \right) \left(\rho_o^\circ - \frac{1}{\bar{v}_{s,o}^\circ} \right) \right] \quad (21)$$

Using the relation $\rho_o = \dfrac{\rho_o^\circ}{1 - K P_o}$ the buoyancy condition, $\bar{v}_{s,o}\, \rho_o = 1$, can now be written as follows.

$$\rho_o^\circ = \frac{1}{\bar{v}_{s,o}^\circ} \left[1 - (K - K_s) P_o + \frac{1}{\rho_o^\circ} \left(\frac{\partial \rho_o^\circ}{\partial a_1^\circ} \right)_P \left(\frac{da_1^\circ}{d\rho^\circ} \right) \left(\rho_o^\circ - \frac{1}{\bar{v}_{s,o}^\circ} \right) \right]$$

$$\rho_o^\circ = \frac{1}{\bar{v}_{s,o}^\circ} \left[1 - \frac{(K - K_s) P_o}{1 - \left(\frac{\partial \rho_o^\circ}{\partial a_1^\circ} \right)_P \left(\frac{da_1^\circ}{d\rho^\circ} \right)} \right] \quad (22)$$

where $\bar{v}_{s,o}^\circ$ is the reciprocal of the buoyant density at atmospheric pressure. Higher order corrections throughout this discussion have been neglected. It is

---

* See Part 5 for explanation of the notation. The superscript $^\circ$ signifies atmospheric pressure, subscript $_o$ signifies band center.

shown in part 5 that the solution density gradient is given by equation 23.

$$\frac{d\rho}{dr} = \left[\frac{1}{\beta^\circ} + K\rho^{\circ 2}\right]\omega^2 r \qquad (23)$$

The complete effective gradient is obtained by substituting equation 23 into equation 20. Higher order corrections are again neglected and the a_1° dependence is expressed in terms of the density at atmospheric pressure concentration scale. The substitution $\frac{dP}{dr} = \rho\omega^2 r$ (10) has also been made.

$$\left(\frac{d\rho}{dr}\right)_{eff} = \left[\frac{1}{\beta^\circ} + \frac{(K-K_s)\rho^{\circ 2}}{1-\left(\frac{\partial\rho_0^\circ}{\partial a_1^\circ}\right)_p\left(\frac{da_1^\circ}{d\rho^\circ}\right)}\right]\left[1-\left(\frac{\partial\rho_0^\circ}{\partial a_1^\circ}\right)_p\left(\frac{da_1^\circ}{d\rho^\circ}\right)\right]\omega^2 r \qquad (24)$$

All the terms of this equation can be experimentally determined. The $(K-K_s)\Big/1-\left(\frac{\partial\rho_0^\circ}{\partial a_1^\circ}\right)_p\left(\frac{da_1^\circ}{d\rho^\circ}\right)$ can be determined by studying the pressure dependence of the buoyant density as can be seen from equation 22. The $\left(\frac{\partial\rho_0^\circ}{\partial a_1^\circ}\right)$ is the slope of the plot of buoyant density versus solute activity at P = 0. The $\left(\frac{da_1^\circ}{d\rho^\circ}\right)$ is the slope of the plot of solute activity versus density for the salt solution at P = 0.

Materials

Cesium Chloride - The CsCl was supplied by Maywood Chemical Co.. It was treated with activated charcoal which had been washed three times with distilled water, and then crystallized three times from a water solution saturated at its boiling point. The optical density at 260 mμ, OD^{260}, of a $\rho = 1.7$ solution of the final material was 0.025.

Cesium Bromide - The CsBr was supplied by A. B. Mackay, Inc.. It was used as supplied by the manufacturer.

Cesium Iodide- The CsI was purchased from the Kawecki Chemical Co.. It was used as supplied except that an insoluble brown material was centrifuged from a 45 weight percent solution of the salt in water. The stock solution had an OD^{260} of infinity and a density of 1.55.

Cesium Sulfate - The Cs_2SO_4 was supplied by the Kawecki Chemical Co.. Insoluble matter was separated from a 50 weight percent solution by centrifugation. Because the solution had a pH of 2.9 it was titrated with Cs_2CO_3 solution to pH 9 after boiling. The salt was then precipitated with 5 volume parts anhydrous methanol. The precipitate was separated from the solution by centrifugation and rinsed five times with

methanol. The methanol was evaporated from the salt in a vacuum desiccator. The stock solution of this material had a density of 1.66, a pH of 7.0 and an OD^{260} of 0.08.

Cesium Acetate - The CsAc was made by titrating a 50% cesium carbonate solution with glacial acetic acid. The Cs_2CO_3 was supplied by the Kawecki Chemical Co.. After boiling, the titrated solution had a pH of 7. Insoluble material was separated by centrifugation. The solution was evaporated until its boiling point at atmospheric pressure reached 190°C. The cooled residue was taken up in two weight parts anhydrous methanol and evaporated again to 190°C. The residue was dissolved in 4 weight parts anhydrous methanol and the solution was evaporated until it was about 50 weight percent CsAc. Eight volume parts of anhydrous ethyl ether were then added to the solution and the CsAc precipitated. The product was filtered on paper and dried in a vacuum desiccator. Insolubles were separated by centrifugation. The stock solution of this salt had a density of 2.020, a pH of 7.6 and an OD^{260} of 0.78.

Cesium Formate - Cesium carbonate was titrated with formic acid. The solution was evaporated until its boiling point reached 160°C. The cooled residue was dissolved in about 2 weight parts methanol and evaporated

to 160°C. This step was repeated and the residue again dissolved in two weight parts anhydrous methanol. To this solution twenty parts ethyl ether were added. A small semi-solid phase formed which was separated from the bulk ether and repeatedly rinsed with ether. The solid was dried in a vacuum desiccator. A stock solution of this cesium formate had a density of 2.105, a pH of 6 to 7 and an OD^{260} of 0.55.

Cesium Selenate - This salt was prepared by heating stoichiometric amounts of selenious acid and cesium carbonate in a porcelain crucible. (11) A 50% solution of the Cs_2SeO_4 had a pH of 11, indicating a small excess of Cs_2CO_3. The solution was titrated to pH 9 with nitric acid. The final stock solution had a density of 1.46, an OD^{260} of 0.43, and a nitrate ion concentration of less than 0.1 M.

Lithium Silicotungstate - Lithium carbonate was added to a 50% silicotungstic acid solution to a pH of 4.5. Carbon dioxide was removed by evacuation of the solution. The stock solution had a density of 1.63 and and OD^{260} of infinity.

All other chemicals not given a specific source were standard reagent grade materials.

The Appendix, Table 2, page 102, contains the emission spectrographic analysis of most of the cesium salts

used in this section of my work. Although in most cases there are cationic impurities present at a concentration of about 1%, the activity trends observed are too large to be explained by these analyses. In addition there is no obvious parallel between the analyses and the buoyant densities in the salt solutions. It cannot be said, however, that there are not small errors in buoyant densities because of these cationic impurities.

Procedures

The method used for determining density was the same for all buoyant densities in this thesis. The polymer was banded in two solutions of different densities arranged so that one solution would be too heavy and the other too light. It was then assumed the gradient and the buoyant density in both solutions were the same. The following equations apply to this situation:

$$\rho_o = \rho_{e,1} + \left(\frac{d\rho}{dr}\right)(r_{o,1} - r_{e,1})$$

$$\rho_o = \rho_{e,2} + \left(\frac{d\rho}{dr}\right)(r_{o,2} - r_{e,2})$$

$$\left(\frac{d\rho}{dr}\right) = \frac{\rho_{e,2} - \rho_{e,1}}{(r_{o,1} - r_{e,1}) - (r_{o,2} - r_{e,2})}$$

where the r_o's are banding positions, the r_e's are the isoconcentration points (4), the ρ_o and ρ_e are the densities at the respective points, the 1 and 2 refer to the different solutions, and $\left(\frac{d\rho}{dr}\right)$ is the density gradient. The r_e's were taken to be at the center of the liquid column of each cell. The ρ_e's were measured with a calibrated 0.3 milliliter micropipette to an accuracy of $\pm$ .0001 gm/cc. This treatment neglects pressure and gradient changes, but corrections to the center of the cell were generally small, so errors were small. Densities are estimated to be accurate to $\pm$ 0.3%.

The T-4 bacteriophage DNA was liberated from a phage stock with guanidinium chloride as described in Part 1 of this thesis. The DNA was not alcohol precipitated for the solvation studies. The stock solutions of DNA were in the pH 9 buffer (Part 1) and all stock salt solutions with the exception of the lithium silicotungstate solution were diluted with the same buffer to the appropriate density. The DNA concentrations employed for the density gradient runs were 2 to 20 x 10^{-6} gm/cc. Except in cesium acetate, all band positions were determined using the schlieren optical system. In cesium acetate the band was too broad to be seen with the schlieren system, so the ultraviolet optics were used. In the Appendix, Table 3, page [103], equations for refractive index versus density of several of the salt solutions are listed. These were experimentally determined for the density ranges listed. They should be considered approximate because the salt solutions were diluted with pH 9 buffer and therefore contain small amounts of sodium chloride. The curves in addition were mostly determined from only four points. They are very useful, however, as approximate guides.

Because the silicotungstate ion is unstable in basic solutions, the lithium silicotungstate solution was diluted with 0.1 M sodium acetate pH 4.7.

Equation 22 shows that if the effect of a_1° on ρ_o is studied, it should be done at P = 0. In practice the effect of water activity on ρ_o is so much larger than the pressure effect under experimental conditions, that the pressure has been ignored during the solvation studies.

Because osmotic coefficient data were not available for several of the salts studied, isopiestic measurements were made to determine water activity. The apparatus used is shown in figures 4 and 5. About 1 ml of solution was placed in the two platinum crucibles, one containing the cesium salt solution, the other a solution of sulfuric acid. The copper block in which the crucibles were set assured thermal equilibrium between the solutions. The block was then placed in the glass desiccator. The system was evacuated with a water aspirator and the entire assembly was rotated in a 25°C water bath for twenty-four hours with the axis of rotation about 5° off the vertical axis.

The rotation at a rate of three revolutions per minute kept the solutions constantly mixed. The weight percent of the equilibrated sulfuric acid solution was determined refractometrically at 15°C on a Zeiss Abbe' Model C-5032 Refractometer, using the data of Veley and Manley (12) for the sodium D line. Water activities

Figure 4 - Apparatus for Isopiestic Measurements

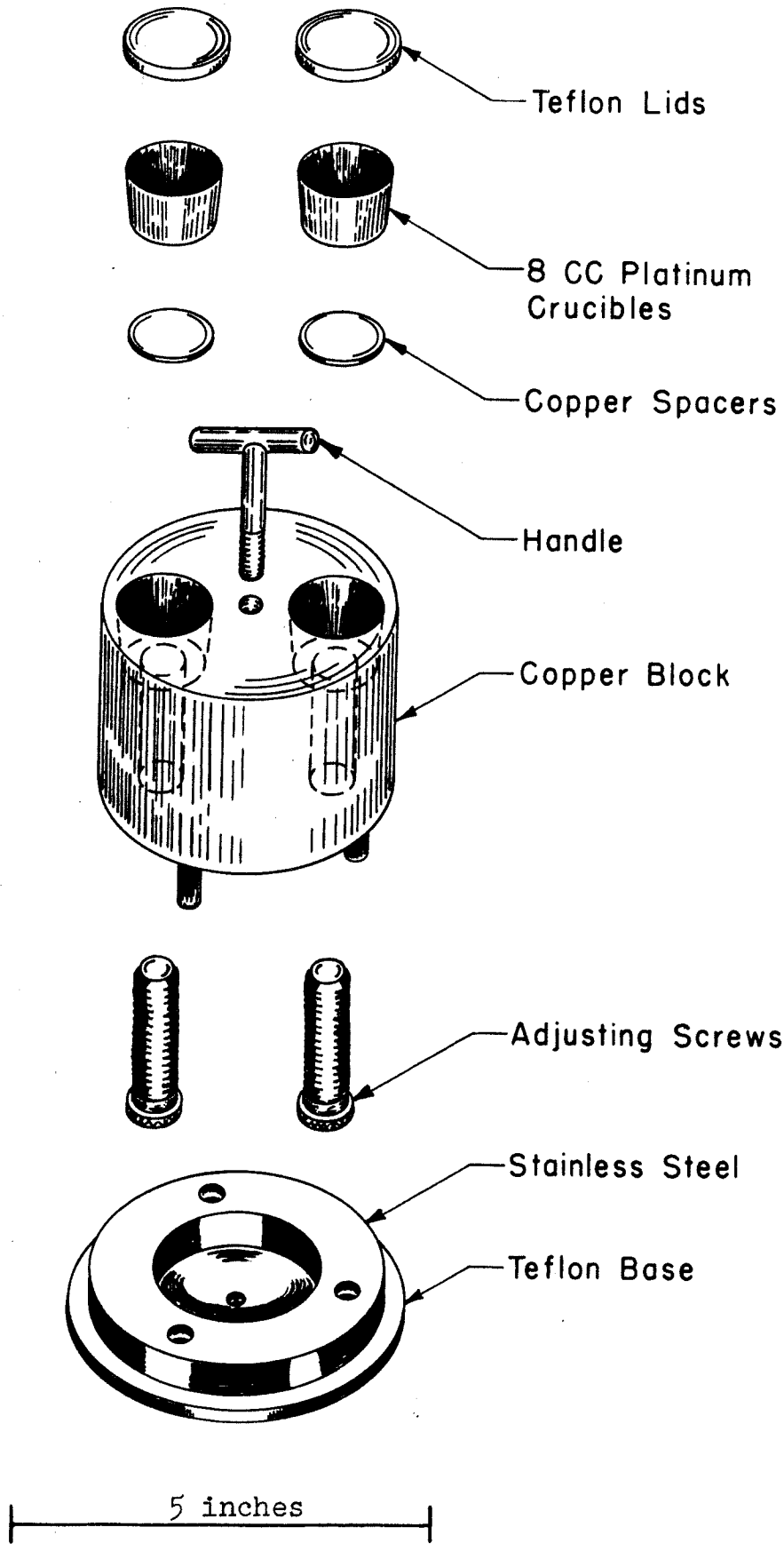

Figure 5 - Apparatus for Isopiestic Measurements

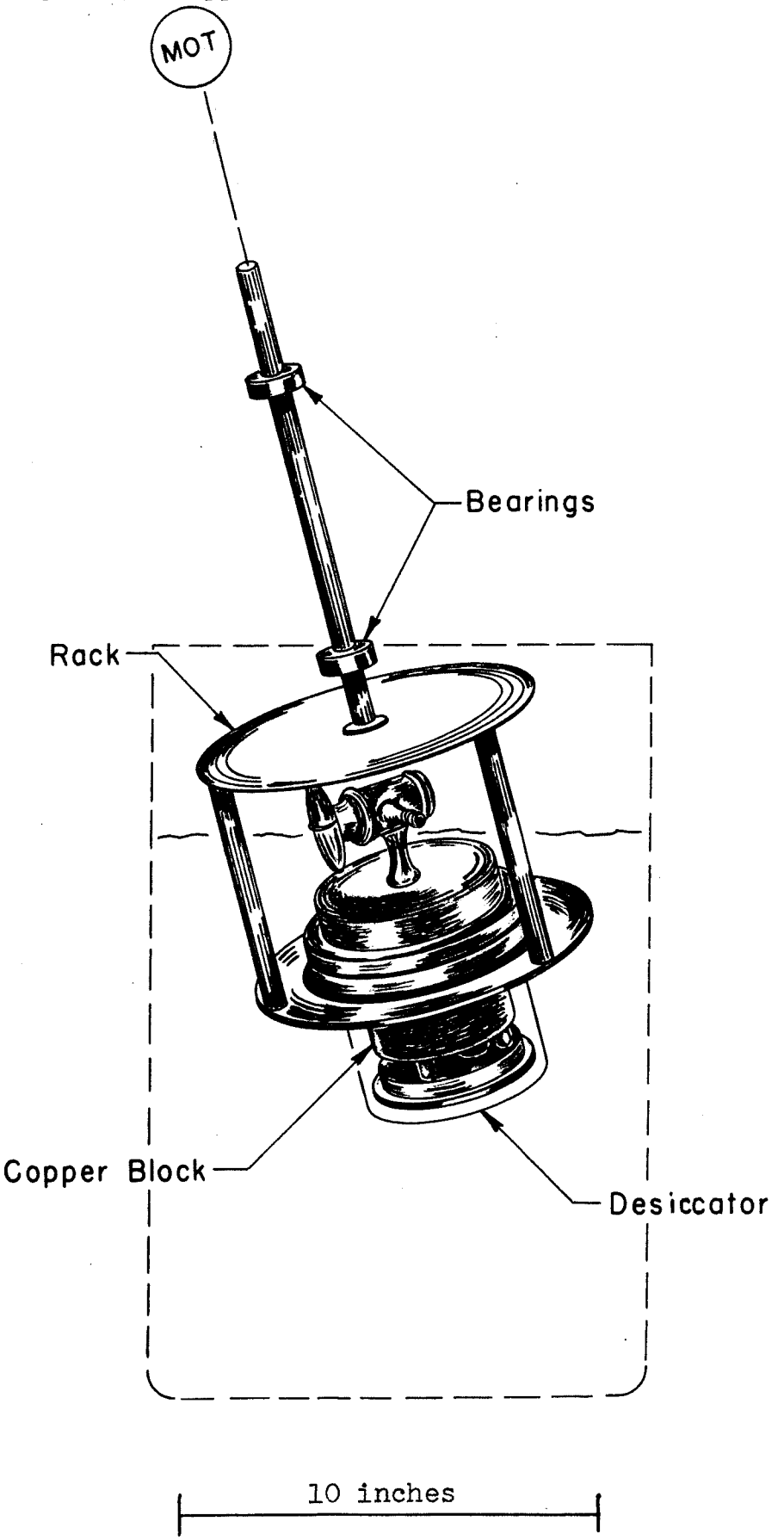

were then determined from a plot of a_w at 25°C against weight percent sulfuric acid drawn from data in Robinson and Stokes (13) and Harned and Owen (14). The densities of the salt solutions were determined as described previously.

Results

The first data were obtained on solution mixtures of CsBr and LiBr. On addition of small amounts of LiBr to a CsBr solution, there is a sudden drop in the buoyant density associated with the replacement of Cs ions on the DNA by Li ions, figure 6. In the event that solvation of the DNA does not change, it has been shown that the plot of ρ_0 against the mole ratio Li/Cs in the solution should be approximately hyperbolic. An analysis of this plot using only the points between $f = 0$ and $f = 1$ yielded a value for the constant q, equation 5, of 1.477. K was found to be 5.2.

Although the curve for LiBr-CsBr mixtures is hyperbolic at low LiBr concentrations, the buoyant density increases at high LiBr concentrations. At these concentrations the DNA is entirely in the lithium form as indicated in figure 6 by the dashed hyperbola. The increase in buoyant density of the solvated LiDNA is then to be expected, as solvation should decrease at the low water activities in concentrated lithium bromide solutions.

The same data with additional points have been plotted against water activity in figure 7. The water activities were calculated with the Guggenheim rule (13) for mixed electrolytes and with data for osmotic coef-

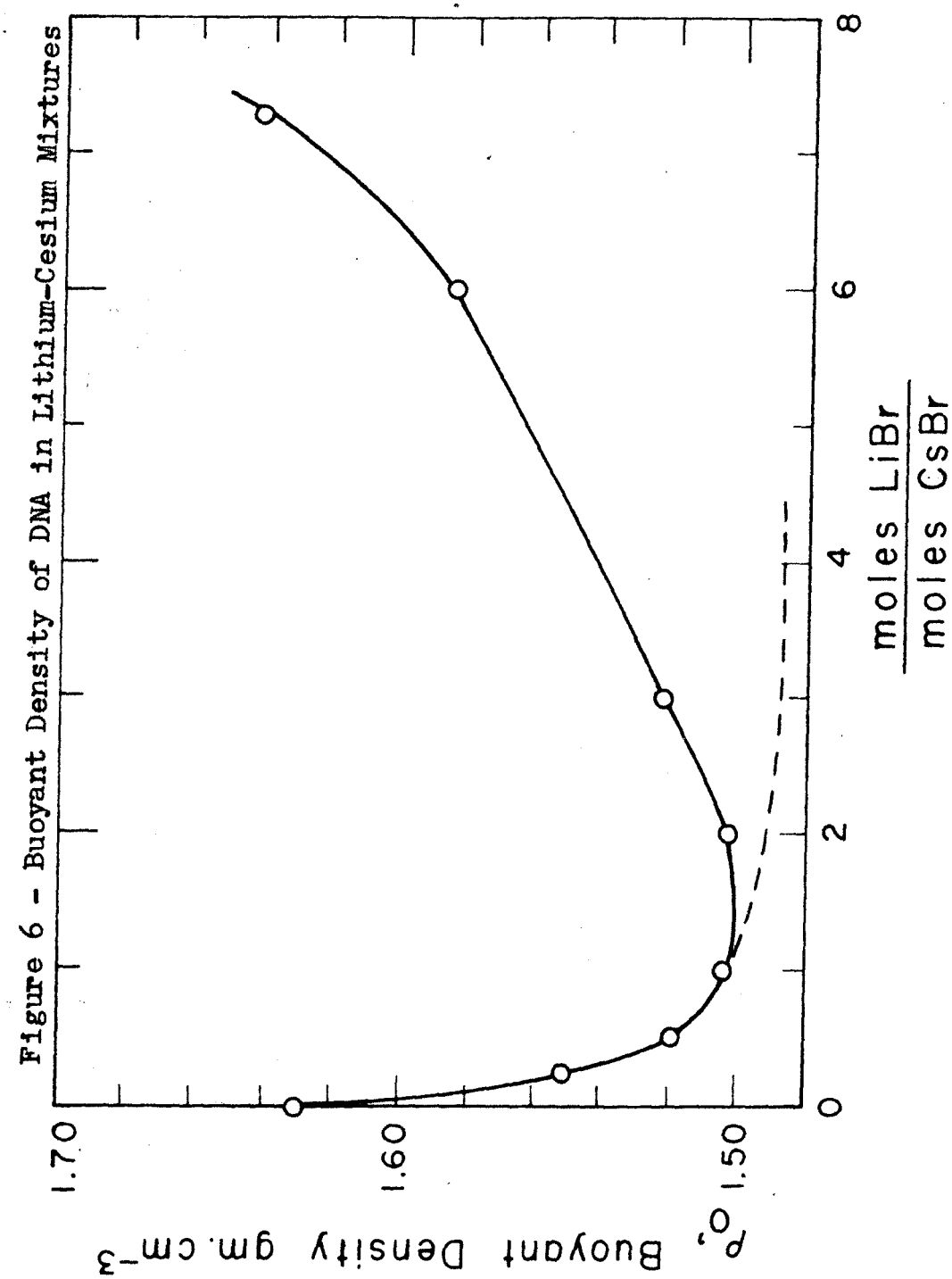
Figure 6 - Buoyant Density of DNA in Lithium-Cesium Mixtures
ρ_o, Buoyant Density gm.cm^{-3}
1.70
1.60
1.50
0
2
4
6
8
moles LiBr / moles CsBr

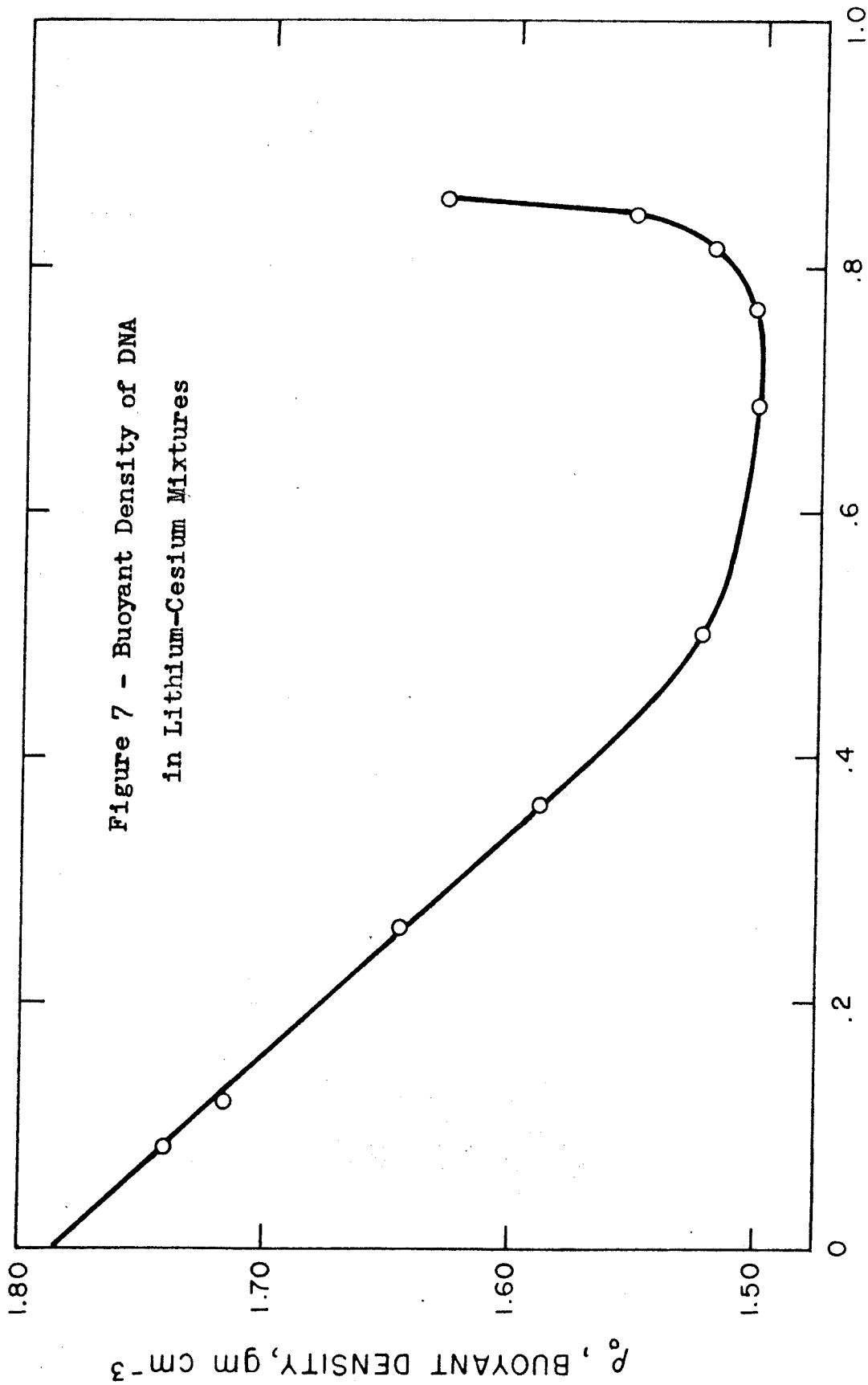

Figure 7 - Buoyant Density of DNA in Lithium-Cesium Mixtures

ficients tabulated in Robinson and Stokes (13). Because osmotic coefficients for CsBr are not available at high salt molalities, the osmotic coefficients of CsCl were used for CsBr for total molalities between 5 and 10. Above molality 10 the osmotic coefficient of CsBr was taken to be 1.02. Errors resulting from this procedure are small as the mole fraction of CsBr is small. The buoyant density in aqueous LiBr was not obtained because the salt is not soluble enough at 25°C.

A second method demonstrating the effects of water activity on buoyant density is shown in figure 8. The buoyant densities* of T-4 DNA in different cesium salt solutions are plotted against water activity, calculated from data in Robinson and Stokes (13) or measured by the isopiestic method.

The point at a_w equal to zero in figure 8 was calculated from the linearly extrapolated LiDNA value, figure 7, using an average nucleotide ion residue weight of 340** The specific volume of the DNA ion was

---

* The CsI point is only approximate because the buoyant density was only slightly less than that of a saturated CsI solution at about 200 atmospheres pressure at 25°C.

** This average nucleotide ion residue weight was calculated from the base compositions for T-4 DNA given in Adams (15), taking into account the glucose on the hydroxymethylcytosine.

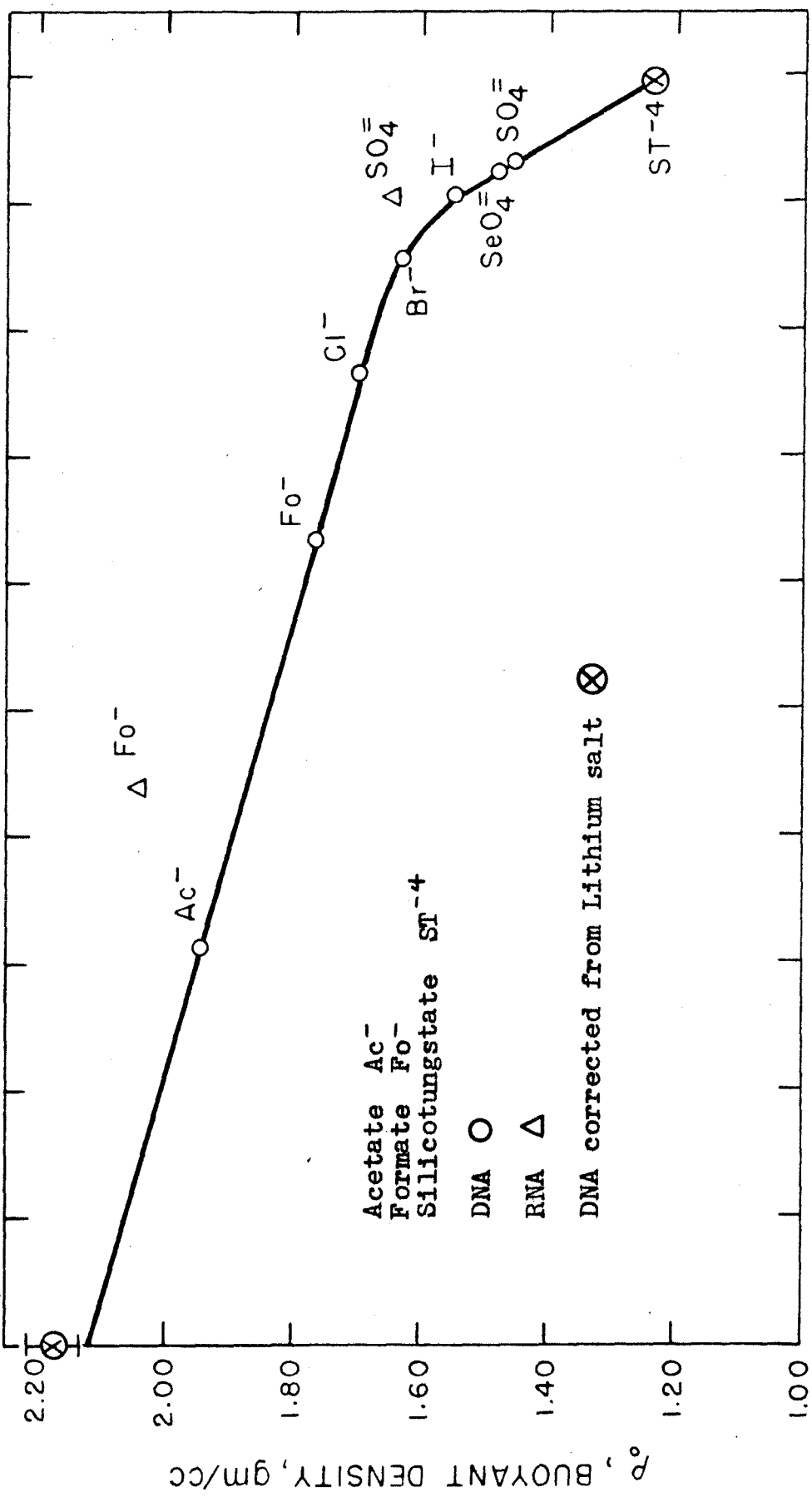
Figure 8 - Buoyant Density of DNA in Various Cesium Salts
ρ, BUOYANT DENSITY, gm/cc
2.20
2.00
1.80
1.60
1.40
1.20
1.00
a_w, WATER ACTIVITY
.1
.2
.3
.4
.5
.6
.7
.8
.9
1.0
Δ Fo⁻
Ac⁻
Fo⁻
Cl⁻
Δ $SO_4^=$
Br⁻
I⁻
$SeO_4^=$
$SO_4^=$
ST-4
Acetate Ac⁻
Formate Fo⁻
Silicotungstate ST⁻⁴
DNA ○
RNA Δ
DNA corrected from Lithium salt ⊗

calculated from the extrapolated LiDNA buoyant density assuming the lithium ion added weight but no volume to the DNA. The maximum error resulting from this assumption is 2% of the specific volume. The buoyant density for CsDNA at $a_w = 0$ was then calculated using the difference in the molar volumes of the Cs ion and the Li ion obtained from the difference in the crystal molar volumes of CsBr and LiBr. In these concentrated salt solutions, partial molar volumes and crystal molar volumes are almost identical; consequently little error is made in this procedure. The value obtained from this calculation was 2.18 ± .04 gm/cc. The intercept, $\rho = 2.12$, of figure 8 is outside of this estimated error margin. This is either caused by the assumptions made to arrive at the 2.18 figure or by the fact that the extrapolation should not be linear. The agreement to 3% does suggest there is no error in concept.

Figure 8 also shows two RNA points. The cesium formate density was taken from C. Davern's thesis (16). The cesium sulfate point was measured at pH 5.5 using ultraviolet optics.*

---

* The RNA was supplied by Dr. P. T'so and prepared as described in his publication. (17) The sample was pea seedling microsomal RNA.

LiDNA has been banded in lithium silicotungstate at pH 4.7. The buoyant density of the DNA in this solution was 1.138 gm/cc. The DNA in this solution is hydrated nearly as much as can be expected in pure water. The amount of water per nucleotide was calculated from the extrapolated LiDNA density at $a_w = 0$ assuming the hydrated water had a density of 1.0. The buoyant density was then corrected to CsDNA, figure 8, assuming that CsDNA and LiDNA are equally solvated.

Figure 9 shows Γ' and Γ_n against a_w. Γ_n is the solvation parameter in moles water per mole average nucleotide. Γ' was calculated using the following equation:

$$\frac{1}{\rho_o} = \frac{v_3 + \Gamma' v_1}{1 + \Gamma'}$$

The specific volume of the solvated water, v_1, was taken to be one, and v_3 represents the extrapolated specific volume of CsDNA or LiDNA at $a_w = 0$. The value of $\frac{1}{v_3}$ used for CsDNA was 2.12, and for LiDNA was 1.783 gm/cc. The Γ' scale in figure 9 applies only to the CsDNA points. It appears from the LiDNA points that the lithium form of DNA binds water more readily than the cesium form. This could be real or just the result of an incorrect choice of v_1. The extension of this same plot to $\Gamma_n = 50$ for CsDNA assumes that the lithium

Figure 9 - Adsorption Isotherm

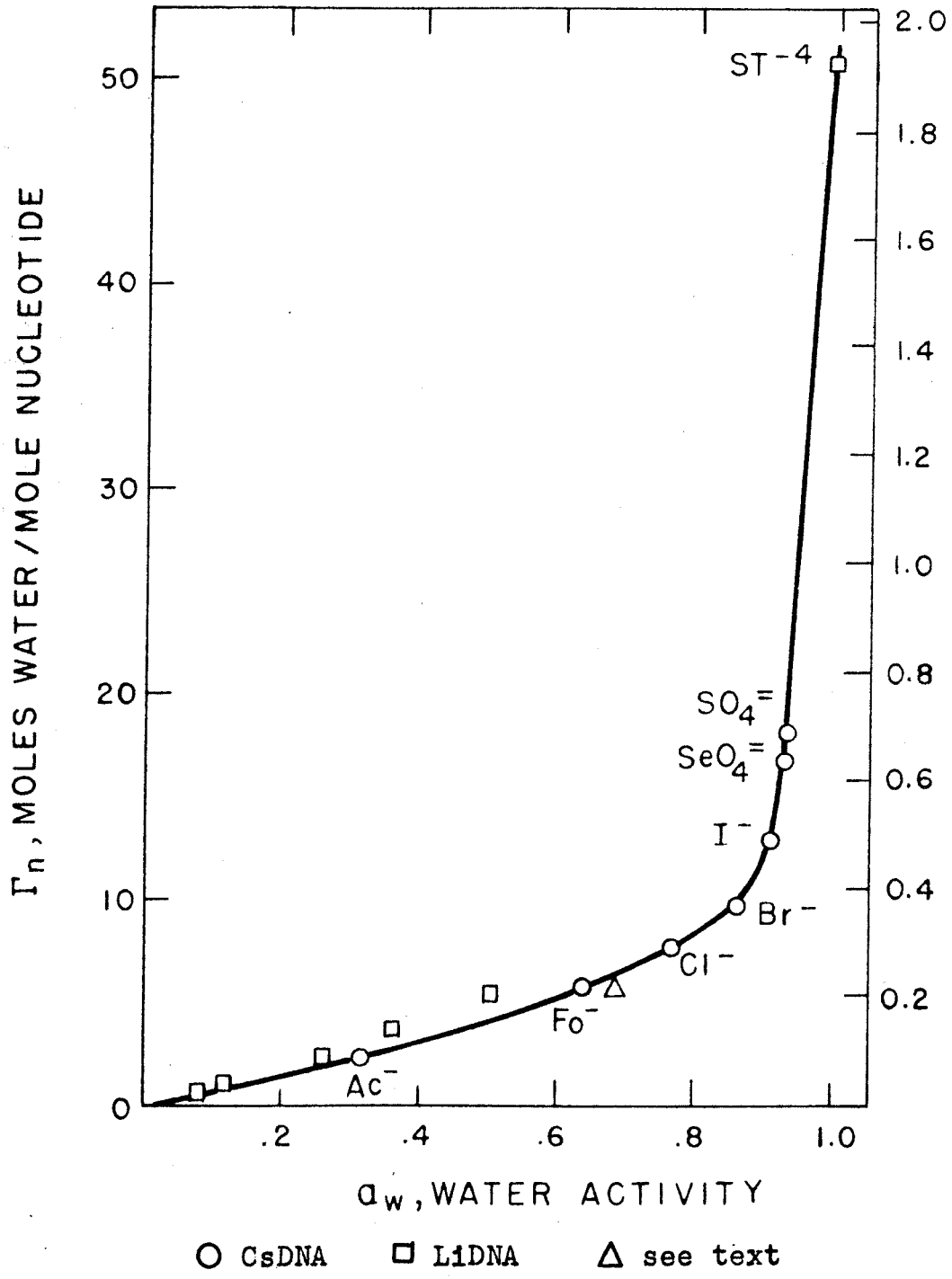

form and cesium form of DNA solvate equally. Although a difference is suggested, it is assumed to be small. The triangle on figure 9 refers to the first LiBr-CsBr point to be removed from the hyperbola, figure 6. It would be expected to be low in figure 9, as it is.

Figure 10 shows the results of the isopiestic measurements. The curves for cesium acetate, formate, selenate, and lithium silicotungstate were determined by the method previously described. The cesium chloride curve was calculated from osmotic coefficient data in Robinson and Stokes (13) using the relation

$$Wt\,\%\ CsCl = 137.48 - 138.11\left(\frac{1}{\rho_4^{25}}\right)$$

for CsCl solutions. The two circles on the CsCl plot represent activities evaluated by myself as a check on the system. These points were started much farther from equilibrium than any of the points evaluated on the unknown solutions. The two CsCl determinations, therefore, constitute a check that equilibrium was reached in all cases. The estimated accuracy of the activities determined is $\pm$ .002.

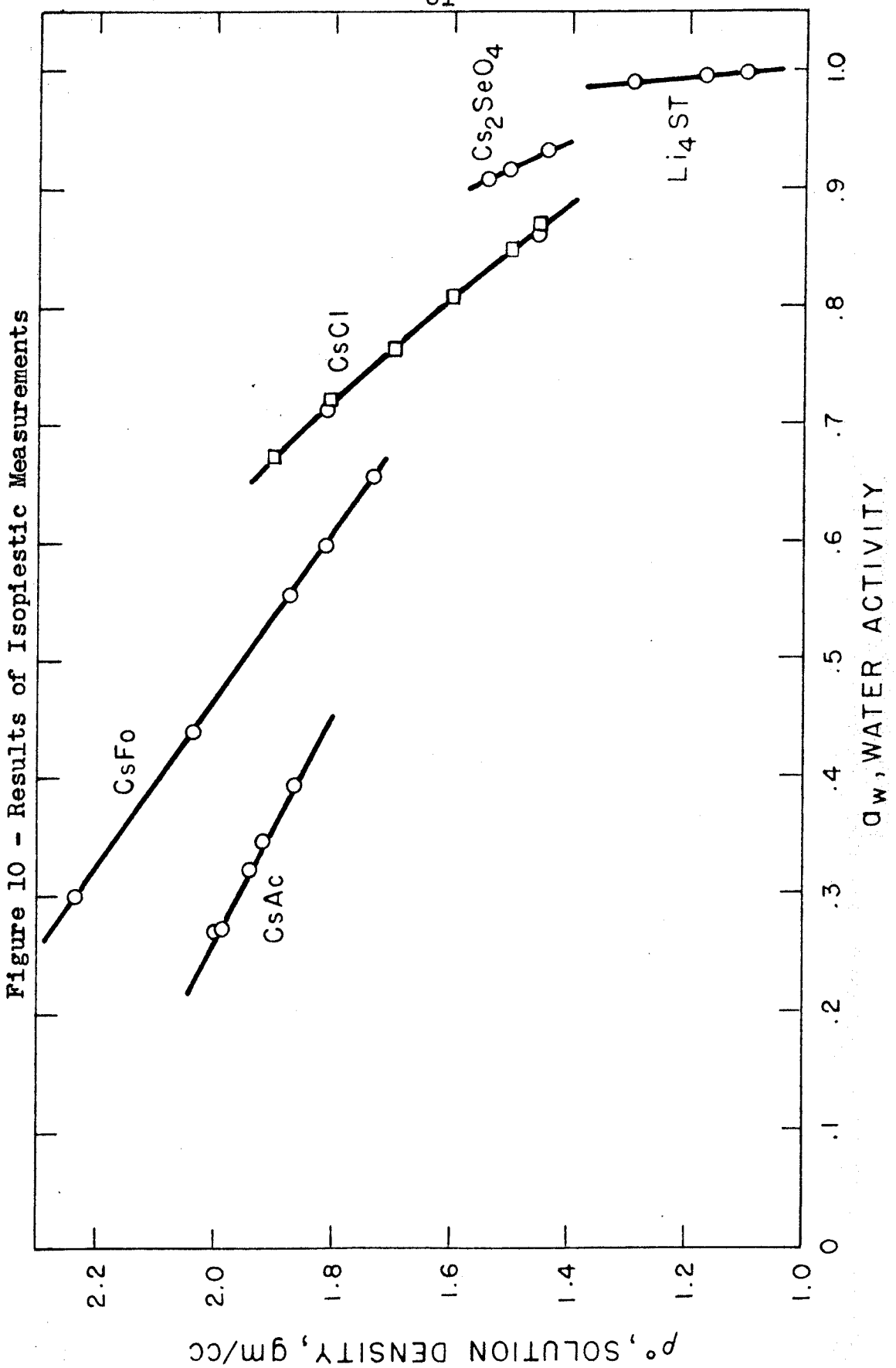

Figure 10 - Results of Isopiestic Measurements

Discussion

The results of the solvation studies indicate that sedimentation equilibrium in a density gradient becomes a powerful tool if properly interpreted. The three component systems which have been so elusive may now be thoroughly understood.

Three significant factors relating to this method with DNA should be emphasized. (a) The assumption that $\left(\partial \mu_3 / \partial m_3\right)_{\mu_1} = \frac{RT}{m_3}$ makes physical sense, for it says that the polymer molecules behave as independent particles when the composition of the bulk phase far from a single polymer molecule is unchanged. (b) The recognition that equation 13 has two solutions and the physical interpretation for these solutions leads to the decision that if an unsolvated molecular weight is desired, Γ should be defined so that it is a positive quantity. (c) The observation that Γ is a strong monotonic function of water activity adds complications to the evaluation of molecular weights, but simultaneously provides a means of determining an adsorption isotherm for DNA in solution.

The solvation parameter measured is a net solvation. It implies nothing about the structure of the water around the DNA. Very little can be said at this time

about this water structure, but the density gradient presents many possibilities. In order to calculate Γ' it was necessary to assume an effective density for the water in the hydrate layer, $\frac{1}{v_1}$, and use the equation $\frac{1}{\rho_o} = \frac{v_3 + \Gamma' v_1}{1+\Gamma'}$. The buoyancy condition is $\frac{1}{\rho_o} = \frac{\bar{v}_3 + \Gamma' \bar{v}_1}{1+\Gamma'}$. These two expressions are equal because $\bar{v}_3 = v_3 + \Gamma' \Delta v_1$ and $\bar{v}_1 = v_1 - \Delta v_1$ where Δv_1, is the change in the specific volume of water upon addition to the solvate layer. From the buoyancy condition it is possible to evaluate Γ', making no assumptions.

Although $\bar{v}_3$ in a concentrated salt solution is difficult to measure, Γ' can be evaluated unambiguously and without assumptions if the partial specific volume of the DNA and the solute are determined accurately at each of the banding condition. The specific volume of the water in the hydrate layer, v_1, can then be determined from the specific volume of the DNA at $a_w = 0$ by reversing the calculation used to determine Γ' in this thesis. In addition if $\bar{v}_3$ and $\bar{v}_1$ are evaluated at a temperature other than 25°C in the various salt solutions, and the buoyant densities are determined at

that temperature, a ΔH and therefore a ΔS for the hydration reaction can be determined as a function of Γ'. Such information would aid greatly in determining the structure of the hydrate layer.

The apparent compressibility, $K_s = -\frac{1}{\bar{v}_s}\left(\frac{\partial \bar{v}_s}{\partial P}\right)_{a_1^\circ}$ is evaluated at constant water activity at atmospheric pressure, which for a single salt solution implies constant molality. K_s may now be written

$$K_s = -\left(\frac{1+\Gamma'}{\bar{v}_3 + \Gamma'\bar{v}_1}\right)\left[\frac{\partial\left(\frac{\bar{v}_3 + \Gamma'\bar{v}_1}{1+\Gamma'}\right)}{\partial P}\right]_{m_1}$$

$$K_s = \frac{1}{\bar{v}_3 + \Gamma'\bar{v}_1}\left[\bar{v}_3\bar{K}_3 + \Gamma'\bar{v}_1\bar{K}_1\right] - \frac{\bar{v}_1 - \bar{v}_3}{(1+\Gamma')^2}\rho_0\left(\frac{d\Gamma'}{dP}\right) \quad (25)$$

where $\bar{K} = -\frac{1}{\bar{v}}\left(\frac{\partial \bar{v}}{\partial P}\right)_m$ *

---

* By substituting equation 25 into equation 24, keeping only the terms resulting from changes in solvation and neglecting small solution compressibility corrections the following expression is obtained for the term in the effective density gradient caused by solvation change at band center:
$\left[\frac{\bar{v}_1 - \bar{v}_3}{(1+\Gamma')^2}\left(\frac{d\Gamma'}{dP}\right)\rho_0^3 - \frac{1}{\beta_0^\circ}\left(\frac{\partial \rho_0^\circ}{\partial a_1^\circ}\right)\left(\frac{da_1^\circ}{dP^\circ}\right)\right]\omega^2 r$
The expression is equal to $-\left(\frac{\partial \rho_0}{\partial \Gamma'}\right)_{\bar{v}_1,\bar{v}_3}\left(\frac{d\Gamma'}{dr}\right)$ as would be expected. As $\left(\partial\rho_0/\partial\Gamma'\right)_{\bar{v}_1\bar{v}_3}$ equals $\left(\frac{1-\bar{v}_1\rho_0}{\bar{v}_3+\Gamma'\bar{v}_1}\right)$, this formulation is in agreement with that of Baldwin (7). The treatment in this thesis has distinct advantages over that of Baldwin because it is expressed in terms of experimentally attainable variables.

The conventional compressibility for the solvated species can be evaluated if $\frac{dr'}{dP}$ is known. This derivative is easily related to the difference in the average specific volume of water in the hydrate layer and the partial specific volume of water in the solution. In CsCl the density shift associated with this term has been calculated to be $\Delta\rho_0^\circ = (5\times10^{-4})(v_1 - \bar{v}_1)\,\Delta P$, where P is in atmospheres. If the partial specific volume measurements are available, the compressibility of the solvated species may then be determined.

The method of evaluating $\left(\partial\rho_0^\circ/\partial a_1^\circ\right)_p$ and $\left(da_1^\circ/d\rho^\circ\right)$ has been discussed earlier. For CsCl the value of their product is 0.24, Appendix, Table 4, page 103. Using the results of Part 5 the total effective density gradient, equation 24, for CsCl is $(.82)\left(\frac{1}{\beta^\circ}\right)\omega^2 r$.

Referring to the data of Meselson and Stahl (18), the solvation may be calculated from the observed shift in the density of DNA upon total N^{15} labelling. If this calculation is done using $\frac{d\rho}{dr} = \left(\frac{1}{\beta^\circ}\right)\omega^2 r$ or the density gradient due only to the salt distribution, the DNA appears to be unhydrated. The DNA, however, reacts to the entire effective gradient, equation 24. If this calculation is repeated using $\frac{d\rho}{dr} = (.82)\left(\frac{1}{\beta^\circ}\right)\omega^2 r$

the Γ' is found to be .22 $\pm$ .05. This number agrees well with the value of .28 on figure 9, considering the accuracy of the data in the Meselson, Stahl paper.

Part 5

The Effects of Pressure on the Buoyant Behavior of Deoxyribonucleic Acid and Tobacco Mosaic Virus in a Density Gradient at Equilibrium in the Ultracentrifuge

THE EFFECTS OF PRESSURE ON THE BUOYANT BEHAVIOR OF DEOXYRIBONUCLEIC ACID AND TOBACCO MOSAIC VIRUS IN A DENSITY GRADIENT AT EQUILIBRIUM IN THE ULTRACENTRIFUGE*

by John E. Hearst,† James B. Ifft,‡ and Jerome Vinograd

Gates and Crellin Laboratories of Chemistry§ and Norman W. Church Laboratory of Chemical Biology, California Institute of Technology, Pasadena, California

Communicated by

In the original analysis[1] of the behavior of macromolecules and viruses in a buoyant density gradient at equilibrium in the ultracentrifuge, all components were assumed to be incompressible. As a few hundred atmospheres are normally generated in the liquid it is to be expected that previous results based on the assumption of incompressibility require re-examination.

Several consequences arise on consideration of previously ignored pressure dependent terms. It is shown below that these may be separately considered.

(a) There is a redistribution of solute with respect to solvent in the binary medium.

(b) The solution is compressed with no change in molality in each of the thin layers perpendicular to the centrifugal field in the liquid column. This compression adds a compression density gradient to the composition density gradient.

(c) The banding macromolecular species is compressed and moves to a new neutrally buoyant solution. A change in band shape occurs.

It is shown in the analysis below that changes in salt molality in response to pressure are small and may be neglected. The combined effects

of compressing the solution and the macromolecular species are significant and affect the band shape, band position, and buoyant density.

THEORY

Although the effects of pressure in two and multicomponent sedimentation equilibrium experiments[2,3,4] have been considered by previous workers, the problem is examined here with special reference to the formation of the density gradient and the behavior of neutrally buoyant macromolecules. For a two-component system at equilibrium in a centrifugal field at constant temperature the thermodynamic relation,

$$M_2(1 - \bar{v}_{2,P}\rho)\ \omega^2\ r\ dr = \left(\frac{\partial \mu_2}{\partial m_2}\right)_P dm_2, \qquad (1)$$

is valid.[5] This expression remains valid for free solute[6] in the three-component system at low polymer concentration. In equation (1) M_2 is the molecular weight, $\bar{v}_{2,P}$ the anhydrous partial specific volume, $\mu_2(P,m_2)$ the chemical potential, and m_2 the molality of the solute. The density of the solution, the radial distance, and the angular velocity are $\rho\ (P,m_2)$, r, and ω respectively. In equation (1) $\bar{v}_2$, $(\partial\mu_2/\partial m_2)$, and ρ are pressure-dependent variables.

The first two variables are expressed in terms of first-order expansions in pressure about a pressure of 1 atm. by Taylor's theorem. Higher order terms in these expansions are small and therefore neglected. Throughout this paper P will refer to the pressure above atmospheric pressure.

$$\left(\frac{\partial \mu_2}{\partial m_2}\right)_P = \left(\frac{\partial \mu_2}{\partial m_2}\right)_{P=0} + \left(\frac{\partial^2 \mu_2}{\partial P\ \partial m_2}\right) P$$

Substituting the relation $(\partial \mu_2/\partial P)_{m_2} = M_2\bar{v}_2$ into the above equation gives a relation in terms of experimentally accessible variables,

$$\left(\frac{\partial \mu_2}{\partial m_2}\right)_P = \left(\frac{\partial \mu_2}{\partial m_2}\right)_{P=0} + M_2\left(\frac{\partial \bar{v}_2}{\partial m_2}\right)_{P=0} P. \qquad (2)$$

Similarly,

$$\bar{v}_{2,P} = \bar{v}_{2,P=0} + \left(\frac{\partial \bar{v}_2}{\partial P}\right)_{P=0} P .$$

Introducing the relation for the partial specific isothermal compressibility of the solute, $K_2 \equiv -\left[1/\bar{v}_2(d\bar{v}_2/dP)\right]_{P=0,m_2}$,

$$\bar{v}_{2,P} = \bar{v}_{2,P=0}\,(1 - K_2 P) . \qquad (3)$$

By a similar Taylor's expansion, the density of the solution may be expressed in terms of the isothermal compressibility coefficient of the solution, K , at P = 0, and the density, $\rho^{\circ}(m_2)$,[7] of the solution of molality, m_2, at atmospheric pressure.

$$\rho = \rho^{\circ}/(1 - K P) \qquad (4)$$

Upon substitution of the effects of pressure, equations (2), (3), and (4), the differential equation (1) becomes

$$\frac{dm_2}{dr} = \frac{M_2\left[1 - \dfrac{(1 - K_2 P)}{(1 - K P)}\,\bar{v}_2^{\circ}\,\rho^{\circ}\right]\omega^2 r}{\left(\dfrac{\partial \mu_2}{\partial m_2}\right)^{\circ} + M_2\left(\dfrac{\partial \bar{v}_2}{\partial m_2}\right)^{\circ} P} , \qquad (5)$$

Equation (5) provides a means of calculating the composition density gradient,

$$\left(\frac{d\rho}{dr}\right)^{\circ} = \frac{dm_2}{dr}\left(\frac{d\rho}{dm_2}\right)^{\circ} = \left(\frac{d\rho}{dm_2}\right)^{\circ} \frac{M_2\left[1 - \frac{(1 - K_2P)}{(1 - KP)}\,\bar{v}_2\,\rho^{\circ}\right]\omega^2 r}{\left(\frac{\partial \mu_2}{\partial m_2}\right)^{\circ} + M_2\left(\frac{\partial \bar{v}_2}{\partial m_2}\right)^{\circ} P}, \qquad (6)$$

and by comparison with the comparable equation at atmospheric pressure,

$$\left(\frac{d\rho}{dr}\right)^{\circ} = \left(\frac{d\rho}{dm_2}\right)^{\circ} \frac{M_2\left[1 - \bar{v}_2^{\circ}\,\rho^{\circ}\right]\omega^2 r}{\left(\partial \mu_2/\partial m_2\right)^{\circ}} \equiv \frac{\omega^2 r}{\beta^{\circ}}, \qquad (7)$$

we can estimate the effect of pressure on salt distribution. Equation (7) defines β°, a parameter previously calculated by Ifft, Voet, and Vinograd[8] and designated by them as β. Because the pressure correction terms are small, equation (6) may be simplified by expansion, retaining only first-order terms in the corrections. Incorporating the definition of β° expressed by equation (7),

$$\frac{d\rho}{dr}^{\circ} = \frac{\omega^2 r}{\beta^{\circ}}\left\{1 - \left[\frac{\bar{v}_2^{\circ}\,\rho^{\circ}\,(K - K_2)}{1 - \bar{v}_2^{\circ}\,\rho^{\circ}} + \frac{M_2\left(\frac{\partial \bar{v}_2}{\partial m_2}\right)^{\circ}}{\left(\frac{\partial \mu_2}{\partial m_2}\right)^{\circ}}\right] P\right\} \qquad (8)$$

$$\frac{d\rho}{dr}^{\circ} \equiv \frac{\omega^2 r}{\beta^{\circ}}\left\{1 - \phi P\right\}.$$

The quantity ϕ has been evaluated for CsCl solutions, Table 1. Pohl's compressibility data,[9] and data for ρ° and $\bar{v}_2^{\circ}$ used in reference 8 were employed in the calculations.[10]

Table 1. Pressure Correction Terms for the Composition Density Gradient, CsCl 25°C

ρ_o	κ atm.$^{-1}$	κ_2 atm.$^{-1}$	$\bar{v}_2^o \rho^o$	$M_2\left(\frac{\partial \bar{v}_2}{\partial m_2}\right)^o \Big/ \left(\frac{\partial \mu_2}{\partial m_2}\right)^o$	ϕ atm.$^{-1}$
1.3	34.2×10^{-6}	-33.4×10^{-6}	.342	42.4×10^{-6}	77.5×10^{-6}
1.5	29.5×10^{-6}	-15.9×10^{-6}	.405	26.8×10^{-6}	57.7×10^{-6}
1.7	25.8×10^{-6}	-5.9×10^{-6}	.464	21.8×10^{-6}	49.2×10^{-6}

As the pressure at the center of a 11 cm. CsCl column, $\rho^o = 1.7$ g. cm.$^{-3}$ at 44,770 rpm is approximately 130 atm.,[11] the ϕP correction terms will generally be less than 0.01 and are therefore neglected. The corrections become smaller if shorter CsCl columns are used. The advantage of neglecting the pressure correction term to the salt distribution is that ρ^o may then be calculated with the equation,

$$\rho^o = \rho_e^{\,o} + \int_{r_e}^{r} \left(\frac{d\rho}{dr}\right)^o dr = \rho_e^{\,o} + \int_{r_e}^{r} \frac{\omega^2 r}{\beta^o}\, dr , \qquad (9)$$

where r_e is the radius at which the molality of CsCl is that of the initial homogeneous solution, and $\rho_e^{\,o}$ is the initial density at atmospheric pressure. The isoconcentration distance, r_e, has been determined[8] for different salts as a function of $\rho_e^{\,o}$ and ω^2. Since the effect of pressure on salt redistribution is small, these data remain valid.

Having established that significant salt redistribution is not caused by the pressures encountered during density gradient analyses, we obtain the physical density gradient by differentiating equation (4) with respect to r,

$$\frac{d\rho}{dr} = \frac{1}{1 - \kappa P}\left(\frac{d\rho}{dr}\right)^o + \frac{\rho^o(m)}{(1 - \kappa P)^2}\,\frac{d(\kappa P)}{dr} \qquad (10)$$

Introducing $dP/dr = \rho \omega^2 r$, equation (10) for the case of constant compressibility coefficient becomes

$$\frac{d\rho}{dr} = \frac{1}{1 - K\rho}\left[\left(\frac{d\rho}{dr}\right)^{o} + \frac{K\rho^{o2}\omega^2 r}{(1 - K\rho)^2}\right] . \qquad (11)$$

Neglecting pressure correction terms of the order of 1% of $(\frac{d\rho}{dr})$, the above equation is

$$\frac{d\rho}{dr} = \left[\left(\frac{1}{\beta^{o}}\right) + K\rho^{o2}\right]\omega^2 r \equiv \frac{\omega^2 r}{\beta} . \qquad (12)$$

The second term in equation (12) is the significant compression term and is tabulated with $1/\beta^{o}$ in Table 2 for CsCl solutions. The values for the compressibility coefficient K are interpolated from the data of Pohl.[9] His data are extrapolated linearly from $\rho = 1.4$ to $\rho = 1.8$ g. cm.$^{-3}$

Table 2. The Effect of Compression on the Physical Density Gradient in CsCl Solutions at Equilibrium in the Ultracentrifuge at 25°C

ρ^{o}	$1/\beta^{o}$	$K\rho^{o2}$	$\frac{1/\beta^{o} + K\rho^{o2}}{1/\beta^{o}} = \frac{1/\beta}{1/\beta^{o}}$
1.2	5.042×10^{-10}	$.543 \times 10^{-10}$	1.108
1.3	6.468	.586	1.091
1.4	7.429	.629	1.085
1.5	8.034	.673	1.084
1.6	8.351	.714	1.085
1.7	8.400	.757	1.090
1.8	8.231	.797	1.097

With the aid of equation (12) it has been demonstrated[12] that the buoyancy condition in a density gradient experiment is[13]

$$\rho_o^{\circ} = \frac{1}{\bar{v}_{s,o}^{\circ}} \left\{ 1 - \frac{(K - K_s)P_o}{1 - \left(\frac{\partial \rho_o^{\circ}}{\partial a_1^{\circ}}\right)_P \left(\frac{da_1^{\circ}}{d\rho^{\circ}}\right)} \right\}. \qquad (13)$$

The slope of the ρ_o° vs. P_o relation is $-\psi/\bar{v}_{s,o}^{\circ}$, where ψ is $K - K_s \Big/ \left[1 - (\partial \rho_o^{\circ}/\partial a_1^{\circ})_P \, (da_1^{\circ}/d\rho_o^{\circ})\right]$. In the following experiments a study of the dependence of ρ_o° on pressure is made. This dependence is found to be linear.

The Determination of ψ. The value of ψ may be measured with adequate accuracy by noting the displacements of equilibrium bands upon changing the pressure. This was accomplished in two ways: An immiscible oil was layered in successive increments on a short column of CsCl solution containing a buoyant macromolecular species and rotated after each increment until equilibrium is attained. The cell containing a band was rotated to equilibrium at varying angular velocities.

EXPERIMENTAL

Materials. The CsCl was obtained from Maywood Chemical Co., Maywood, N. J., and recrystallized three times. Emission spectroscopic analyses performed in the Department of Geology showed less than 0.03% metallic impurities. The silicone oil was Dow Corning 550 fluid, Lot No. 88-161. According to the manufacturer, it is a methyl- and phenyl-substituted polysiloxane containing less than 10 parts per million of metal salt impurity. The FC-43 fluorochemical was obtained from the Minnesota Mining and Manufacturing Co. and is stated to be triperfluorobutylamine. The tobacco mosaic virus strain U 1 (TMV) was kindly supplied by

Professor S. Wildman, University of California at Los Angeles. The stock solution contained 5.47 mg./ml. TMV in 0.001 versene, pH 7.5. The preparation of the T-4 bacteriophage DNA has been described.[14] All other chemicals used were reagent grade materials.

Procedure. The Effect of Pressure on Band Position. The oil column experiments were performed with both TMV and DNA solutions. The speed variation experiments were performed only with DNA solutions. The solutions delivered into the standard 4°, 12-mm., Kel-F centerpiece cell assembly had densities, ρ°, of 1.325 and 1.704 g. cm.$^{-3}$ for TMV and DNA respectively. The first solution contained 46 μg. cm.$^{-3}$ of TMV and was buffered with .01 M tris at pH 7.0. The second solution was buffered with .02 M tris at pH 9. The DNA concentration in terms of $E^{260}_{1\ cm.}$ was 0.085. All experiments were begun by filling cells with .02 ml. of fluorocarbon, 0.18 ml. of CsCl solution, and 0.02 ml. of silicone oil. Both the fluorocarbon and the silicone oil were included to provide accurate means of recording the top and bottom menisci of the CsCl column. This column was about one-fourth the length attainable in the standard centerpiece.

The solutions were centrifuged at 25.0°C and photographed with the schlieren optical system after equilibrium had been established. The actual speeds were evaluated from odometer readings made at the beginning and end of the run. These agreed with the nominal values within ± .02%. In these short columns at 44,770 rpm the DNA runs required 14 hours and the TMV runs about 90 minutes to reach equilibrium. A typical pair of exposures is shown in Fig. 1. The top and bottom CsCl menisci and the silicone oil meniscus were taken to be the centers of the symmetrical

meniscus images. These, as well as the counter balance reference edges and the positive and negative peaks, associated with the inflections in the polymer concentration distributions, were measured with a coordinate plate and film Comparator Model M 2001-P, Gaertner Scientific Co., Chicago, Illinois. Reading accuracy was $\pm$ .01 mm,, which corresponds to $\pm$ 5 microns in the cell. The band position was taken to be the average of the distances associated with the positive and negative peaks.

In the oil column experiments the cells were reopened at the filling hole after the first equilibration and 0.16 ml. silicone oil added. The solutions were again run to equilibrium. The procedure was repeated twice again. Silicone oil was similarly removed with a 24-gauge needle in two or three stages.

In one of the DNA runs, after the cell was filled with silicone oil and centrifuged to equilibrium, the angular speed was dropped to 31,410 rpm, then raised to 39,460 rpm, and again raised to 44,770 rpm. Thirty-five hours were required for equilibrium at 39,460 rpm and 65 hours at 31,410 rpm. The slow step in these experiments was band motion. The band width became constant after 22 hours at both speeds. After 5 days continuous running the band returned to its original position at 44,770 rpm as indicated by the double point at 170 atm. Fig. 2.

The density of the silicone oil at 25°C was measured in a calibrated 0.3 ml. micropipet. The density was 1.067 $\pm$ .001 g. $cm.^{-3}$

The Effect of Pressure on the Composition Density Gradient. In the theoretical part of this paper it was noted that the composition density gradient is insensitive to pressure. To check this conclusion the effect of pressure on the refractive index gradient was measured. The 4° Kel-F,

12-mm. standard cell was filled with 0.02 ml. of fluorocarbon, 0.34 ml. of CsCl solution, ρ^{o} = 1.339 g. cm.$^{-3}$ and .02 ml. of silicone oil. The rotor was brought to 44,770 rpm as rapidly as possible, and schlieren images at a bar angle of 55° were photographed immediately upon reaching this speed and again after 10 hours, at equilibrium. The experiment was repeated after thorough homogenizing of the CsCl solution and the addition of 0.34 ml. of silicone oil. The composition density gradient was obtained at r_e from the difference in elevations between the early and equilibrium exposures.

For these experiments, tracings were made of 20-fold cell to vellum enlargements with an Omega D-2 enlarger. The CsCl meniscus was used for lateral orientation and the image of a horizontal wire mounted just in front of the schlieren camera for vertical orientation. Elevations proportional to the compression density gradient were measured with an accuracy of 0.4%.

CALCULATIONS

For evaluation of the results in accordance with equation (13), P_o, the pressure at band center, and ρ_o^{o}, the buoyant density at atmospheric pressure, must be derived from the experimental data. The pressure is the sum of the pressures generated by the action of the field in the silicone oil and in CsCl solution over the band.

The pressure at any point in a liquid volume is obtained by integration of the equation

$$\frac{dP}{dr} = \rho \omega^2 r \quad . \tag{14}$$

In order to integrate this expression, the r dependence of ρ is needed.

In a solution,

$$\rho = \rho_\alpha + \int_{r_\alpha}^{r} \frac{\omega^2 r}{\beta}\, dr , \tag{15}$$

where r_α is an arbitrary reference. It is sufficiently accurate to assume that β is a constant.

$$\rho = \rho_\alpha + \frac{\omega^2}{\beta}\left(\frac{r^2 - r_\alpha^2}{2}\right) \tag{16}$$

Substituting this expression into equation (1) and integrating from r_1 to r_2,

$$P_2 - P_1 = \rho_\alpha \omega^2 \left(\frac{r_2^2 - r_1^2}{2}\right) + \frac{\omega^4}{2\beta}\left[\frac{(r_2^4 - r_1^4)}{4} - r_\alpha^2 \frac{(r_2^2 - r_1^2)}{2}\right]. \tag{17}$$

To simplify computation, r_α is so selected that the term in the brackets in equation (17) vanishes. For this condition r_α is the root mean square between r_1 and r_2. In all cases the use of the arithmetic mean for r_α did not introduce a significant error.

$$r_\alpha = \sqrt{\frac{r_2^2 + r_1^2}{2}} = \frac{r_2 + r_1}{2} + \frac{1}{8}\frac{(r_2 - r_1)^2}{r_2} \cdots$$

The pressure at band center caused by the CsCl solution was evaluated as follows: The quantity r_α is the root mean square radius between band center, r_o, and the CsCl mensicus, r_{cm}. The density ρ_α is obtained with sufficient accuracy with equation (9) assuming β^o constant, the limits of integration being r_e and r_α. This neglects the effect of pressure on ρ_α. Substitution into equation (5) yields

$$P_{r_o, CsCl} = \frac{\rho_\alpha \omega^2}{1.103 \times 10^6}\frac{(r_o^2 - r_{cm}^2)}{2} . \tag{18}$$

The numerical coefficient is introduced in order to express pressure in atmospheres. ρ_α was found to vary only 0.12% in a given series over the entire range of oil column lengths and was therefore considered constant.

In the oil column treated as a one-component system, $1/\beta^\circ = 0$, and $1/\beta = \kappa' P^{\circ 2}$, equation (12), where κ' is the isothermal compressibility of the oil. The same arguments used for the CsCl column apply here. In this case, however, the compressibility and the pressure contribution of the oil are larger; the effect of pressure on ρ_α is therefore taken into account. For a good estimate of the pressure P_α, equation (1) is integrated between the oil meniscus, r_{om}, and r_α, under the assumption that the density is constant.

$$P_\alpha = \frac{\rho^\circ \omega^2}{1.013 \times 10^6} \frac{(r_\alpha^2 - r_{om}^2)}{2} = \frac{\rho^\circ \omega^2}{1.013 \times 10^6} \frac{(r_{cm}^2 - r_{om}^2)}{4} \qquad (19)$$

The r_α was eliminated with the definition of r_α. Upon substituting $\rho_\alpha = \rho^\circ(1 + \kappa' P_\alpha)$ and equation (19) into equation (17), and letting r_2 be the cesium chloride meniscus, r_{cm}, and r_1 be the oil meniscus r_{om},

$$P_{cm} = \rho^\circ \left\{ 1 + \kappa' \left[\frac{\rho^\circ \omega^2}{1.013 \times 10^6} \frac{(r_{cm}^2 - r_{om}^2)}{4} \right] \right\} \left(\frac{(r_{cm}^2 - r_{om}^2)}{2} \right). \qquad (20)$$

The pressure at band center is the sum of the pressures given by equations (18) and (20).

Now the shifts in band position must be expressed in density units. The buoyant density at atmospheric pressure, ρ_o°, is calculated with equation (9). In order to express the dependence of β° on r, β° is expanded:

$$\beta^\circ = \beta_\gamma{}^\circ + \left(\frac{d\beta^\circ}{dr} \right)_\gamma (r - r_\gamma)$$

where r_γ is again an arbitrary reference radius. Integrating and evaluating r_γ so that the $(d\beta^o/dr)_\gamma$ term equals zero as before, the following equations are obtained,

$$r_\gamma = \frac{r_2 + r_1}{2} + \frac{(r_2 - r_1)^2}{12\, r_2} \quad \cdots$$

and

$$\rho_2^{\,o} - \rho_1^{\,o} = \frac{\omega^2}{\beta_\gamma^{\,o}} \left(\frac{r_2^{\,2} - r_1^{\,2}}{2} \right).$$

As in the previous case, the selection of β^o at the arithmetic mean rather than at r_γ will not introduce a significant error.

Since the density shifts due to the pressure variation are very small, the quantity $\Delta\rho = \rho_o^{\,o} - \rho_e^{\,o}$ was evaluated and not $\rho_o^{\,o}$ itself. The desired expression is

$$\Delta\rho = \rho_o^{\,o} - \rho_e^{\,o} = \frac{\omega^2}{\beta_e^{\,o}} \left(\frac{r_o^{\,2} - r_e^{\,2}}{2} \right). \qquad (21)$$

The following relation utilizing the original comparator data (capital R's) and the magnification factor, MF, was used,

$$(r_o^{\,2} - r_e^{\,2}) = \frac{2 \times 5.725}{MF} \left(R_o - \frac{R_{cm} + R_{fm}}{2} \right) + \frac{1}{(MF)^2} \left(R_o^{\,2} - \frac{R_{cm}^2 + R_{fm}^2}{2} \right), \qquad (22)$$

where R_{fm} is the radius of the fluorocarbon meniscus.

According to theory a plot of $\Delta\rho$ vs. P_o should yield a straight line of slope $-\psi / \bar{v}_{s,o}^{\,o}$ and intercept $(1/\bar{v}_{s,o}^{\,o} - \rho_e^{\,o})$. Figures 2 and 3 present the data obtained for one series each of DNA and TMV. The value of $\bar{v}_{s,o}^{\,o}$ was determined from the intercept. From the intercept and the slope, values for ψ were obtained. Duplicate experiments in each case were performed.

In the measurements the radii were located with a precision of 0.01 mm. on the plate. The values of P_o were calculated with no significant error. The values of $\Delta\rho$ are very sensitive to the accuracy of measurement because these values are derived from the difference of the squares of two numbers of comparable magnitudes. The maximum error in each of the $\Delta\rho$ values was calculated to be $\pm$ 0.00012 g. cm.$^{-3}$ The two points obtained at lower speeds show an asymmetric maximum error interval. This is due to the difficulty in measuring the position of the broader bands at lower speeds. The flare at each maximum had to be used to find the peak. It was known from observations of the relation of the flare to the actual maxima on photographs at 44,770 rpm that the flare from both peaks is displaced approximately 0.02 mm. toward the center of rotation. This corresponds to an error of $-$ .00010 g. cm.$^{-3}$

The probable error of the function $\Delta\rho$ was computed using an expression given in Margenau and Murphy.[15] Assuming a probable error of 0.005 mm. in each comparator measurement, a probable error for the function, $\Delta\rho$, was found to be 0.00003 g. cm.$^{-3}$

The adherance of the points after the oil removal to the straight line showed that no detectable evaporation occurred. The points in general can be determined with an accuracy of 0.0001 g. cm.$^{-3}$ This corresponds to an evaporative loss of 0.026 mg. of H_2O and a meniscus shift of 0.5μ. Because the meniscus can be located with an accuracy of only 10 μ, it is clear that the band position is a much more sensitive test for evaporation than the change in meniscus height. A density shift of 0.004 g. cm.$^{-3}$ is required to cause an observable shift in CsCl column length.

RESULTS AND DISCUSSION

The examination of the effects of pressure-dependent terms in equilibrium sedimentation of macromolecules in a density gradient illuminates two important interrelated problems, solvation and compression. These effects are also encountered in conventional sedimentation equilibrium, but are smaller and frequently neglected.

The effects of compression on the physical density gradient in the CsCl solutions examined are capable of analysis. The result, Table 2, is to increase the physical density gradient by 8.5 to 10.8%. These effects are independent of speed. At a density of 1.7 g. $cm.^{-3}$, the compression gradient is 9% of the composition gradient.

That the compression gradient may be simply added to the composition gradient is shown in experiments in which the refractive index gradient at equilibrium was evaluated in a short CsCl column with and without a layer of silicone oil. The effect on the net refractive index gradient at the root mean square position in the cell due to this layer of oil, which corresponded to a pressure increment of 72.1 atmospheres, was -1.3%. This result is within the experimental measuring errors and the effect predicted by the theory, Table 1. It is consistent with the previously obtained agreement[8] between the composition density gradient obtained optically at the pressure in the cell and calculated from physical chemical data obtained at atmospheric pressure. Three approaches now show that the CsCl-water distribution is not significantly changed by compression, even though the solution is compressed and the physical density gradient increased.

In density gradient experiments the macromolecular species does not respond only to the physical density gradient. Of importance is the effective density gradient, which is shown in the preceding paper[12] to be

$$\left(\frac{d\rho}{dr}\right)_{eff} = \left[\frac{1}{\beta^o} + \psi \rho_o^{o2}\right](1-\alpha)\omega^2 r \qquad (23)$$

where $$\alpha = \left(\frac{\partial \rho_o^{\,o}}{\partial a_1^{\,o}}\right)_P \left(\frac{da_1^{\,o}}{d\rho^o}\right) .$$

The quantity ψ must therefore be known in order to evaluate correctly the effective density gradient and the molecular weight of either the anhydrous or the hydrated species.

The values of ψ and $\overline{v}^o_{s,o}$ obtained from the oil column experiments are given in Table 3. The numbers in the fifth column, $1/\overline{v}^o_{s,o}$ are the values of the composition variable $\rho_o^{\,o}$ when the band is at atmospheric pressure. The values listed as $\rho_o^{\,o}$ are values calculated for the pressure at the middle of a 1.1 cm. column of CsCl solution at 44,770 rpm. Thus significant deviations in $\rho_o^{\,o}$ will be encountered by workers banding the same material at different radii in the cell.

Table 3

Effect of Pressure on Buoyant Molecules in a Density Gradient

Material	Expt. No.	$\Psi \times 10^6$ atm.$^{-1}$	$\bar{v}^o_{s,o}$	$\frac{1}{\bar{v}^o_{s,o}}$	ρ_o^o
T-4 Bacteriophage DNA	1	23.1	0.587	1.704	1.699
	2	23.5	0.587	1.703	1.698
Tobacco mosaic virus, strain U 1	3	21.8	0.756	1.322	1.319
	4	21.5	0.757	1.321	1.318

If proper experimental data are available, Ψ can be used to calculate the apparent compressibility of the solvated polymer. A more complete discussion of this matter is presented in the preceding article.[12] If the effects of solvation are neglected, the value of κ_S for TMV obtained from Ψ and from Pohl's compressibility data is 12.9 x 10^{-6} atm. This value agrees favorably with the value 10 x 10^{-6} atm.$^{-1}$ which Jacobson[16] obtained for various proteins in dilute salt solutions. The agreement may be the result of coincidence, because the effects of solvation have been neglected.

For T-4 DNA Ψ was found to be 23.3 x 10^{-6} atm.$^{-1}$ The parameter α for DNA in CsCl is 0.24.[12] These numbers may now be used to calculate the difference in compressibility, $\kappa - \kappa_s$ = 17.7 x 10^{-6} atm.$^{-1}$ From this difference κ_s is found to equal 8.7 x 10^{-6} atm.$^{-1}$ It should be stressed that κ_s is an apparent compressibility. It not only includes the compression of the solvated species, but also a pressure dependence

of the amount of hydrated water.

The use of an insoluble marker material, such as a thin film of plastic, has been suggested by Szybalski.[17] Solvation effects for such a material should be negligible because surface areas are relatively small. Large pressure effects on marker positions are to be expected and have been observed.[17]

DNA samples, denatured, isotopically substituted, or of differing composition, can be used as density markers providing that the dependence of ψ and α on pressure for the marker is the same as the sample under investigation. The effective density gradient, equation (23), is used to calculate density differences in such experiments.

Cell Distortion. The CsCl column length was found to change in a characteristic manner with the level of the supernatant silicone oil, Fig. 4. The two sets of points correspond to two independent experiments. In these, the cell was disassembled and reassembled with a solution of slightly different density. The linear and elastic response reflects the behavior of a cell assembly with a Kel-F centerpiece and quartz windows. The observed decrease in CsCl column length of 2.1% is 10.8 times larger than that attributable to the compression of the solution.

Legends

Fig. 1. - The effect of pressure on band position of T-4 DNA in CsCl solution $\rho_e^\circ = 1.699$ g. cm.$^{-3}$ at 25°C at 44,770 rpm. The pressure at band center in the lower part of the photograph is 54.5 atm. and in the upper part is 170.7 atm.

Fig. 2. - Buoyant density increments for T-4 DNA in CsCl solution at various pressures, $\rho_e^\circ = 1.699$ g. cm.$^{-3}$ at 25°C at 44,770 rpm. Expt. no. 1 a, addition of oil; r, removal of oil; v, points obtained at 31,410 rpm., and 39,460 rpm. The coordinates at the top and right-hand side indicate the original data. Slope = -3.94×10^{-5} g. cm.$^{-3}$/atm. The maximum error intervals are indicated.

Fig. 3. - Buoyant density increments for TMV in CsCl solution at various pressures, $\rho_e^\circ = 1.324$ g. cm.$^{-3}$ at 25°C at 44,770 rpm. Expt. no. 3. a, addition of oil; r, removal of oil. The coordinates at the top and right-hand side indicate the original data. Slope = -2.88×10^{-5} g. cm.$^{-3}$/atm. The maximum error intervals are indicated.

Fig. 4. - The effect of pressure on CsCl solution column length. O, addition of oil; Δ, removal of oil. The lower line is from expt. no. 1 and the upper line is from expt. no. 2.

Figure 1

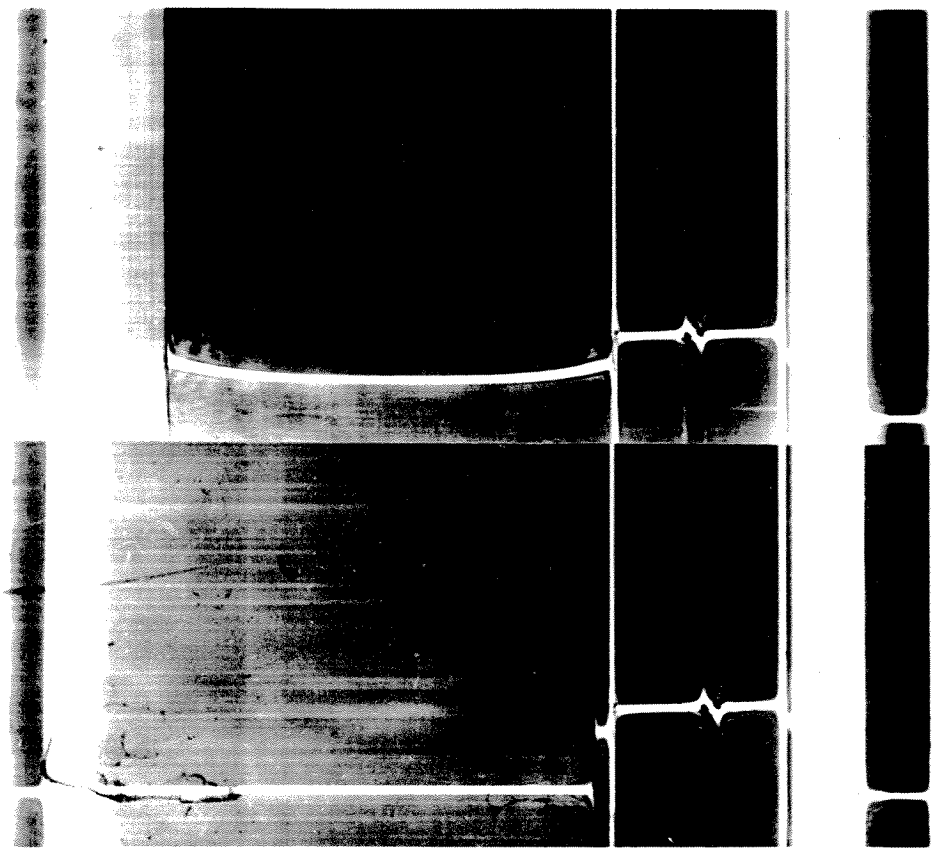

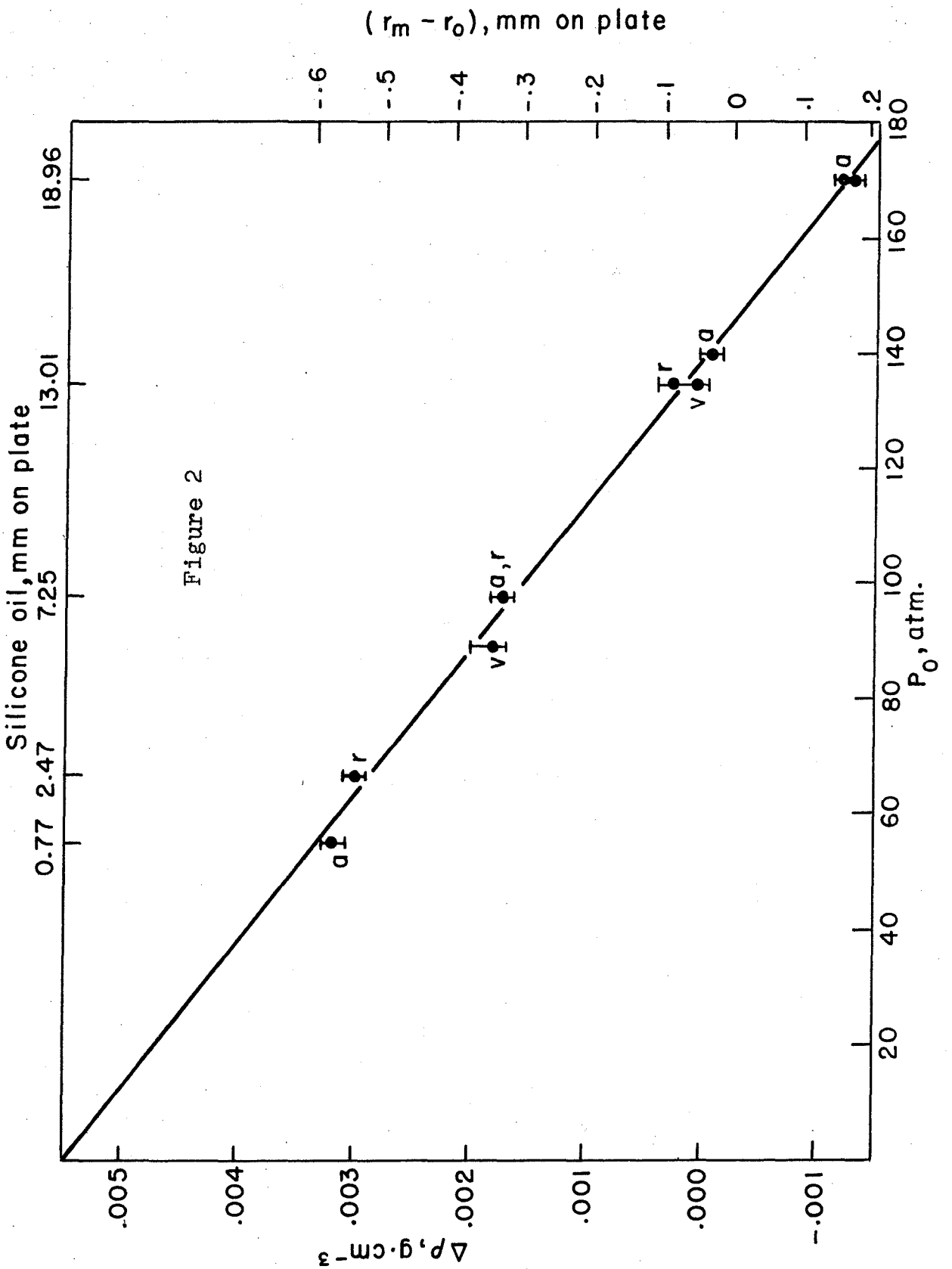
(r_m - r_o), mm on plate
-.6
-.5
-.4
-.3
-.2
-.1
0
.1
.2
Silicone oil, mm on plate
0.77
2.47
7.25
13.01
18.96
Δρ, g·cm⁻³
.005
.004
.003
.002
.001
.000
-.001
P_o, atm.
20
40
60
80
100
120
140
160
180
a
r
v
a,r
v
r
a
a

Figure 2

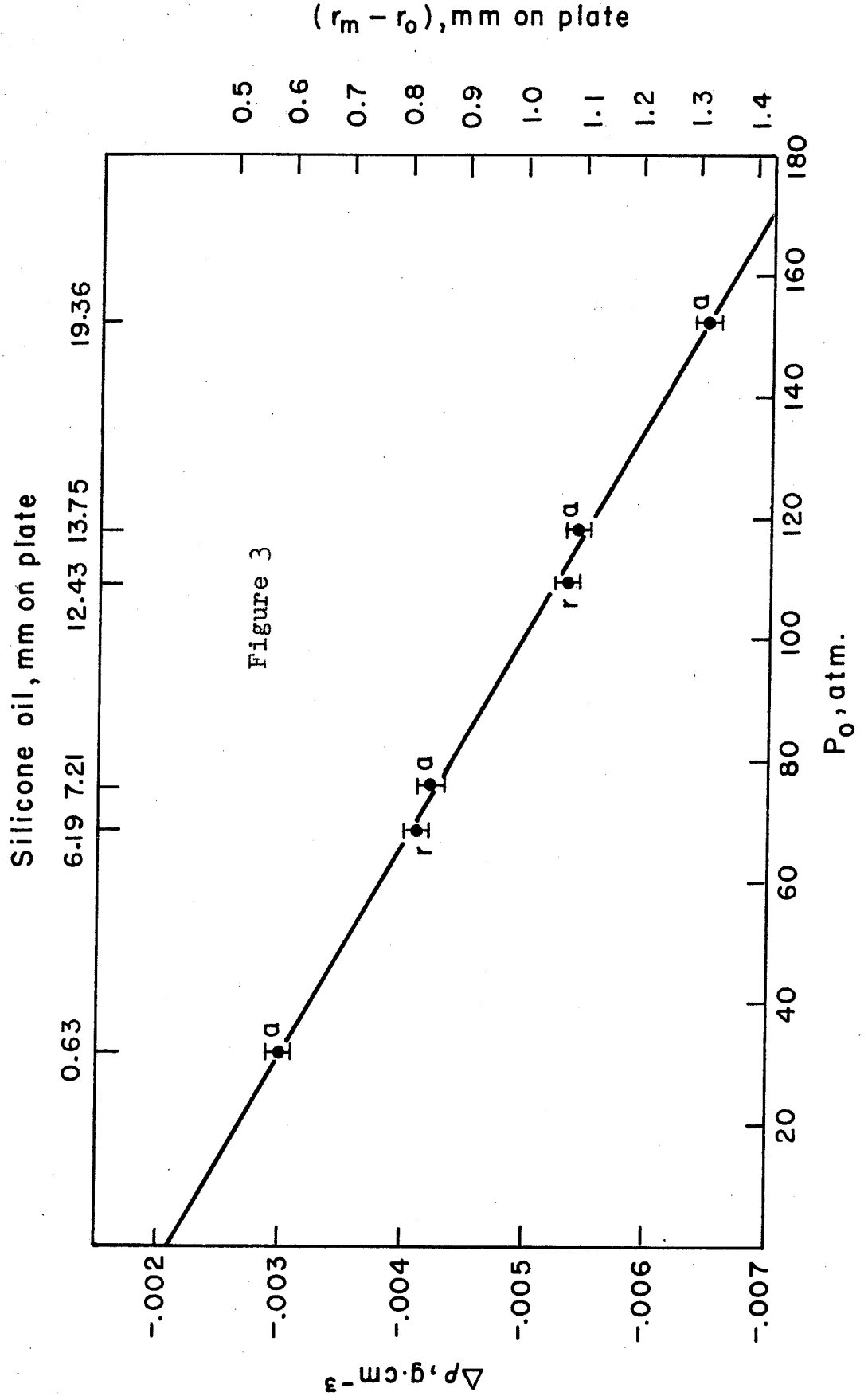
$(r_m - r_0)$, mm on plate
0.5
0.6
0.7
0.8
0.9
1.0
1.1
1.2
1.3
1.4
180
160
140
120
100
80
60
40
20
P_0, atm.
Silicone oil, mm on plate
0.63
6.19
7.21
12.43
13.75
19.36
a
r
-.002
-.003
-.004
-.005
-.006
-.007
$\Delta\rho$, g·cm^{-3}

Figure 3

Figure 4

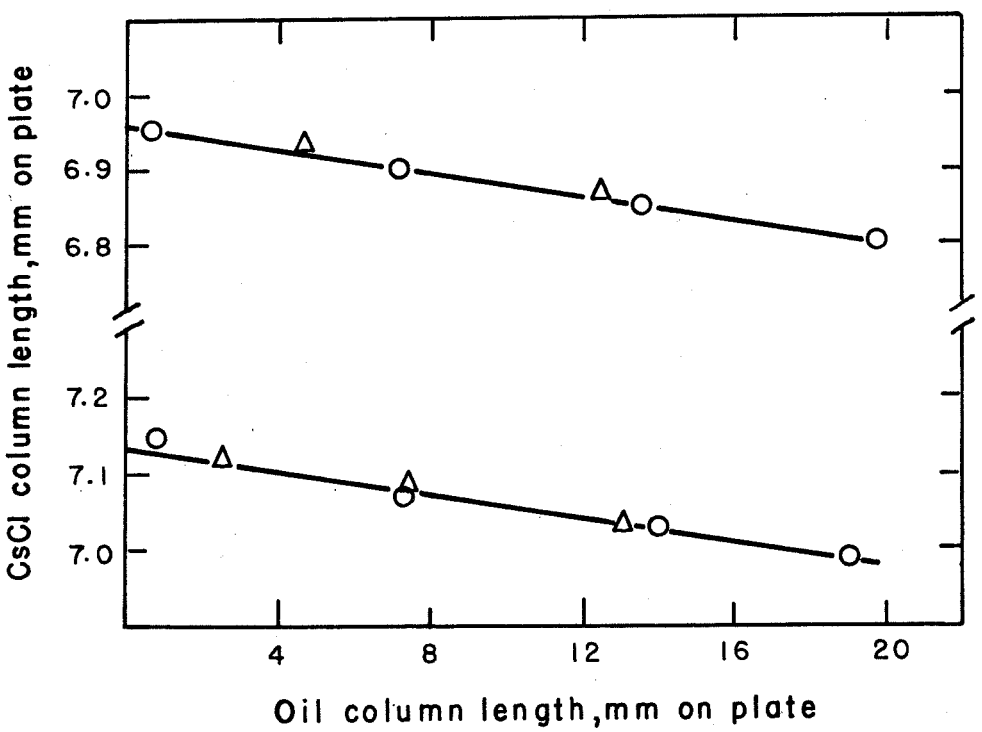
CsCl column length, mm on plate
7.0
6.9
6.8
7.2
7.1
7.0
4
8
12
16
20
Oil column length, mm on plate

Footnotes and References for Part 5

* This investigation was supported in part by Research Grant H-3394 from the National Institutes of Health, United States Public Health Service.

† Predoctoral Fellow of the National Science Foundation.

‡ U. S. Public Health Service Research Fellow of the Division of General Medical Sciences.

§ Contribution No. 2701

1. M. Meselson, F. W. Stahl, and J. Vinograd, these Proceedings, 43, 581 (1957). Their treatment also neglects the small pressure dependence of $(\partial \mu_2 / \partial m_2)_p$, equation (2).

2. T. F. Young, K. A. Kraus, and J. S. Johnson, J. Chem. Phys., 22, 878 (1954).

3. J. W. Williams, K. E. Van Holde, R. L. Baldwin, and H. Fujita, Chem. Revs., 58, 715 (1958).

4. R. L. Baldwin, these Proceedings, 45, 939 (1959).

5. R. J. Goldberg, J. Phys. Chem., 57, 194 (1953)

6. Refer to reference 12 for the definition of the term free solute.

7. The superscript zero is used throughout this paper to designate variables at atmospheric pressure. The density $\rho^0(m_2)$ is a function only of m_2 and should be thought of as a composition variable. The actual density ρ is a measure of physical density and is a function of m_2 and pressure.

8. J. B. Ifft, D. H. Voet, and J. Vinograd, J. Phys. Chem., in press.

9. F. Pohl, 1906. Dissertation, Rheinische Friedrich - Wilhelms - Universität, Bonn, Germany.

10. K_2 was evaluated with the aid of the following equation derived from equation (4) and with the aid of the intercept method for determining partial specific quantities:

$$K_2 = K + \frac{1}{\rho^\circ \bar{v}_2^\circ}\left(K_i - K\right)$$

The quantity K_i is the intercept at $Z_2 = 1$ of the tangent to the K versus weight fraction of CsCl, Z_2, curve.

11. All subsequent error approximations are based on a pressure of 130 atmospheres.

12. Part 4 of this thesis.

13. Equation 13 is equation 22 in Part 4 of this thesis.

14. J. E. Hearst and J. Vinograd, Arch. Biochem., Biophys., 92, 206 (1961).

15. H. Margenau and G. M. Murphy, "The Mathematics of Physics and Chemistry". D. Van Nostrand Co., Princeton, N. J., 1956, p. 515.

16. B. Jacobson, Arkiv för Kemi, 2, 177 (1951)

17. W. Szybalski, private communication.

Part 6

The Apparent Molecular Weight of T-4 Bacteriophage Deoxyribonucleic Acid

The preceding two parts of this thesis have indicated the corrections necessary for the accurate determination of molecular weight by the density gradient method. This part will deal with the accurate analysis of the apparent molecular weight of T-4 DNA.

The DNA was the same variety and was prepared by the method described in Part 1. The same care against DNA breakage was taken, including during cell filling. The CsCl used is described in Part 4. The CsCl-DNA solution was buffered with .004 M Tris at pH 9. The optical density at the maximum of the band was approximately $OD^{260} = 1$. The run was made at 25°C and at 25,980 RPM. The films were analyzed on the Joyce-Loebl densitometer.

After subtracting out the base line of the CsCl solution the resulting curve was plotted, figure 11. The units on this plot are graph paper units. The magnification along the x axis is a factor of 90. The arrow in figure 11 denotes the direction of the field. The natural logarithm of C was then plotted against the square of the distance from band center in figure 12.

There is an obvious skewing toward heavy densities in figure 11, indicating a density heterogeneity. The analysis will ignore this fact and two apparent molecular weights will be calculated from the two slopes in figure 12.

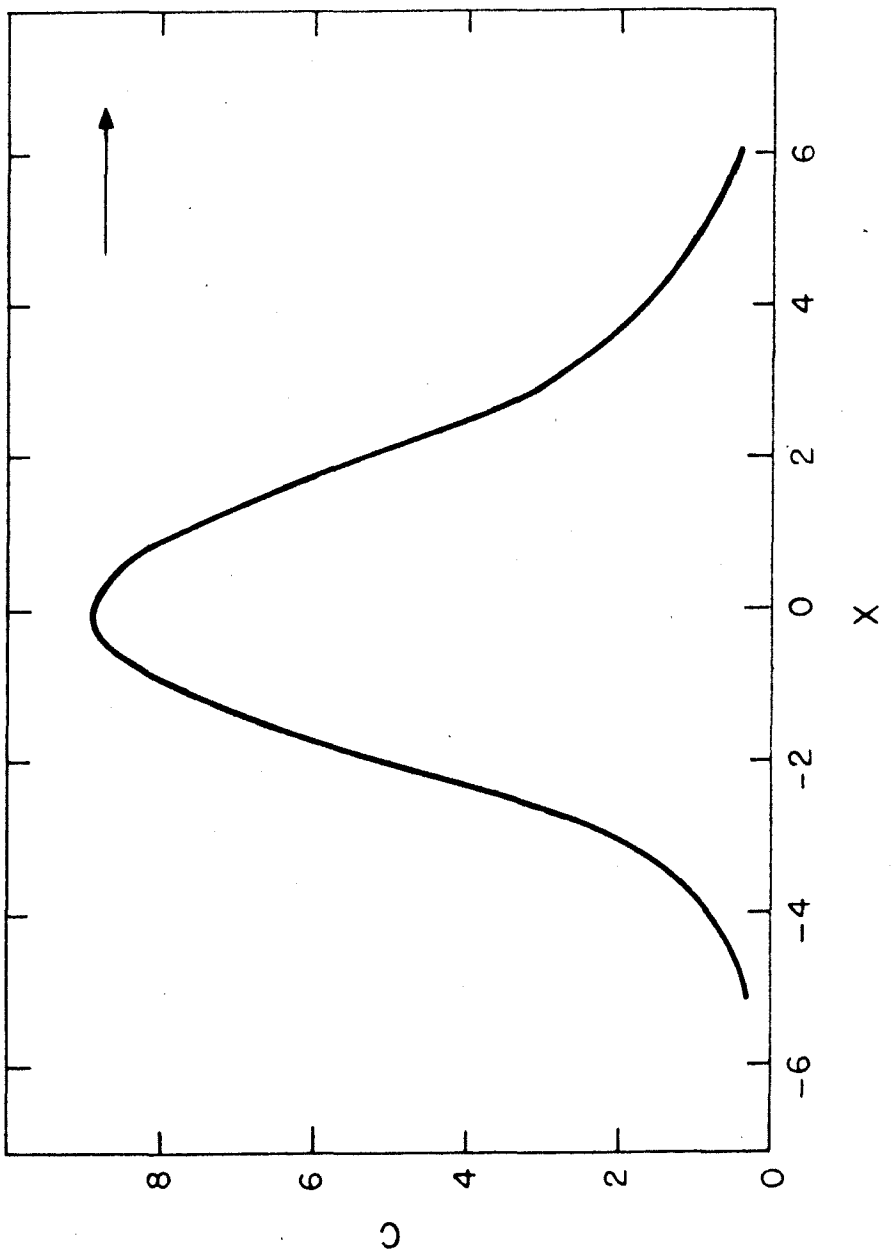

Figure 11 - DNA Concentration Distribution

Figure 12 - Determination of σ

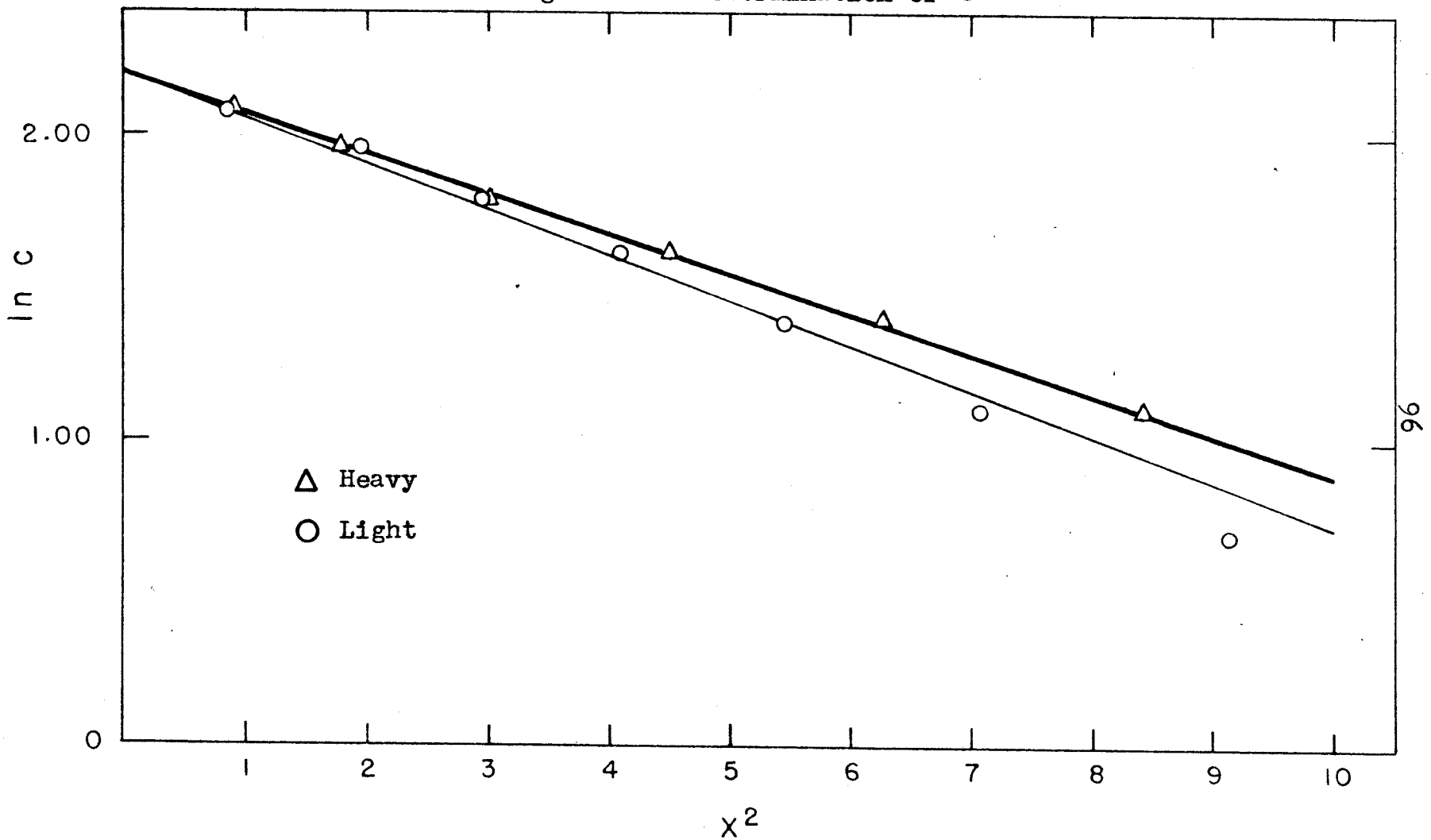

The value of Ψ determined in Part 5 was 23×10^{-12} (dyne/cm^2)$^{-1}$. From Table 2, Part 5 $\frac{1}{\beta^\circ}$ for a CsCl solution of density 1.7 equals 8.40×10^{-10}.

The quantity $\left(\partial \rho_o^\circ / \partial a_w^\circ\right)_p \left(da_w^\circ / d\rho^\circ\right)$ is tabulated in the Appendix, page 103, for various cesium salts at the buoyant density of DNA. For CsCl its value is 0.24. The effective gradient thus has a value of $(9.06 \times 10^{-10})(1-.24)\omega^2 r_o = 6.89 \times 10^{-10}\, \omega^2 r_o$

The two values of σ obtained from figure 11 are: on the heavy side, $\sigma_H = .0216$ cm, on the light side $\sigma_L = .0204$ cm.

The results of the molecular weight calculation using equation 17 are tabulated in Table 1. At these conditions $\Gamma' = .28$, figure 9. $M_{3,Na}$ is the anhydrous molecular weight corrected to the sodium salt of DNA.

Table 1

The Molecular Weight of T-4 Bacteriophage DNA

Side of Distribution	$M_{s,o}$	M_3	$M_{3,Na}$
Heavy	59×10^6	46×10^6	35×10^6
Light	66×10^6	51×10^6	39×10^6

In conclusion it should be stressed that these molecular weights are not believed to be correct. There is evidence for density heterogeneity which can have very large effects on the molecular weights determined in this manner. These effects can only lower the value of the molecular weight. A method for determining the molecular weight of a polymer sample with density heterogeneity is presented in Proposition 5.

Appendix

Figure 13

Renaturation of T-4 DNA in Formamide Solutions

DNA Concentration Series

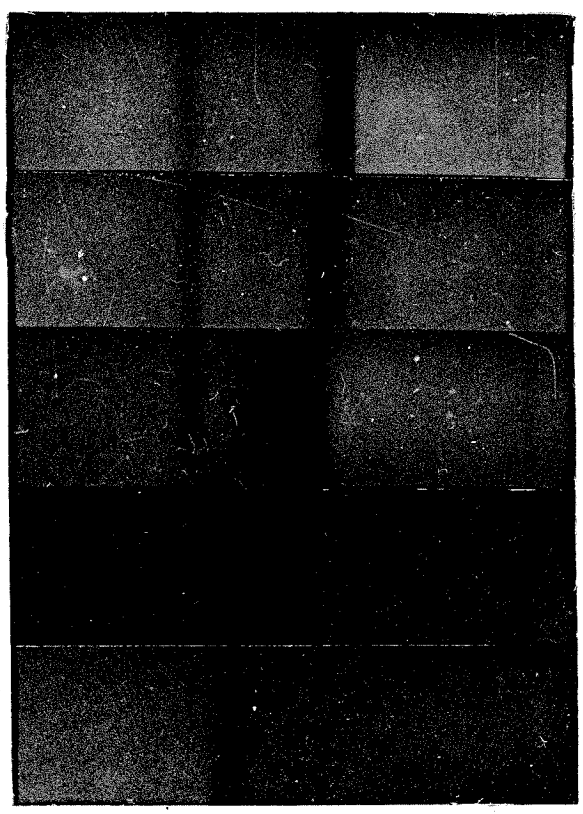

Native

.8 OD^{260}

.3 OD^{260}

.1 OD^{260}

Denatured

Table 2

Emission Spectrographic Analysis of Cesium Salts Used

	weight parts per million									weight percent			
	Ba	V	Ca	Mg	Ti	Zr	Al	Si	Fe	Na	K	Rb	Li
Cesium Chloride	t	20	30	--	10	2	50	30	--	.01	.005	--	--
Cesium Formate	15	80	60	--	60	6	150	80	t	.01	.2	.8	.002
Cesium Acetate	11	50	50	--	40	6	100	40	--				
Cesium Sulfate	2	30	70	t	20	4	80	15	t	.01	.2	.5	.002
Cesium Carbonate	6	20	25	--	--	2	60	50	t	.01	.3	1.0	.004
Cesium Bromide	t	30	50	--	15	2	80	10	--	.05	.03	.5	.005

t trace -- no detectable amount blank indicates no measurement made

Table 3
Refractive Index versus Density for Various Cesium Salts

Salt	Equation	Density Range
Cs_2SO_4	$n_D^{25} = .0730\,\rho_4^{25} + 1.2646$	1.40 - 1.70
Cs Formate	$n_D^{25} = .0728\,\rho_4^{25} + 1.2688$	1.72 - 1.82
Cs Acetate	$n_D^{25} = .0930\,\rho_4^{25} + 1.2485$	1.80 - 2.05
Cs_2SeO_4	$n_D^{25} = .0827\,\rho_4^{25} + 1.2547$	1.38 - 2.00

Table 4
Activity Dependent Correction Terms
for Various Cesium Salts at the Buoyant Density of DNA

Salt	$\left(\frac{d\rho^\circ}{da_w^\circ}\right)$	$\left(\frac{\partial \rho_o^\circ}{\partial a_w^\circ}\right)_p$	$\left(\frac{\partial \rho_o^\circ}{\partial a_w^\circ}\right)_p \left(\frac{da_w^\circ}{d\rho^\circ}\right)$
Cs Acetate	- 1.04	- .56	.54
Cs Formate	- 1.41	- .56	.40
CsCl	- 2.32	- .56	.24
CsBr	- 3.8	-1.0	.26
CsI	- 5.8	-3.2*	.55
Cs_2SO_4	- 7.0	-3.2*	.46
Cs_2SeO_4	- 3.8	-3.2*	.84

---

* Although the slope of the curve in figure 8 can be determined to an accuracy of at least ± 0.1, the drawing of the best curve through these points is in question. These numbers and the corresponding numbers in the last column should be considered accurate to only ± 20 percent.

References

1) Marmur, J. and Lane, D. (1960) Proc. Nat. Acad. Sci. U.S. 46, 453

2) Doty, P., Marmur, J., Eigner, J. and Schildkraut, C. (1960) Proc. Nat. Acad. Sci. U.S. 46, 461

3) Helmkamp, G. K. and T'so, P. (1961) J. Am. Chem. Soc. 83, 138

4) Ifft, J. B. , Voet, D. H., Vinograd, J. (1961) J. Phys. Chem. in press

5) Williams, J. W. (1960) Fortschr. D. Chem. org. Naturst. 18, 434

6) Baldwin, R. L. and Van Holde, K. E. (1960) Fortschr. Hochpolym. -Forsch. 1, 451

7) Baldwin, R. L. (1959) Proc. Nat. Acad. Sci. U.S. 45, 939

8) Jacobson, B., Anderson, W. A. and Arnold, J. T. (1954) Nature 173, 774

9) Wang, J. H. (1955) J. Am. Chem. Soc. 77, 258

10) Goldberg, R. J. (1953) J. Phys. Chem. 57, 194

11) Lenher, V. and Wechter, E. J. (1925) J. Am. Chem. Soc. 47, 1522

12) Veley, V. H. and Manley, J. J. (1905) Proc. Roy. Soc. 76 A, 469

13) Robinson, R. A. and Stokes, R. H. (1955) Electrolyte Solutions, Academic Press Inc., New York pp. 33, 426, 468-489

14) Harned, H. S. and Owen, B. B. (1950) Physical Chemistry of Electrolyte Solutions, Reinhold Publishing Corp., New York, p. 436

15) Adams, M. H. (1959) Bacteriophages, Interscience Publishers, Inc., New York, pp. 91-92

16) Davern, C. (1959) Doctoral Dissertation, California Institute of Technology p. 108

17) T'so, P. and Squires, R. (1959) Federation Proc. 18, 341

18) Meselson, M. and Stahl, F. W. (1958) Proc. Nat. Acad. Sci. U.S. 44, 671

Proposition 1

An experimental error exists in the use of absorption optics to evaluate concentration in a centrifuge cell in density gradient sedimentation studies (1), which is caused by the bending of the light in the refractive index gradient of the salt (2). As the light passes through the cell it is bent toward the high density end of the cell, and as a result a single light sheet does not pass through a region of constant macromolecule concentration.

In order to determine the magnitude of this effect and a method to minimize the resulting error, the photometric record of a Gaussian concentration distribution in the cell has been calculated.

The following assumptions have been made for the calculation:

1) The Beer-Lambert Laws apply to the absorbing macromolecule in the centrifuge cell.
2) The deflection of the light caused by the salt concentration gradient is small. Experimentally the maximum deflection is between 1^{o} and 2^{o} through a 1.2 centimeter cell.

3) $\frac{1}{n}\frac{dn}{dx}$ is constant over the width of the concentration band. This assumption is as good as the assumptions made in deriving the original expression for the Gaussian distribution in the cell (1).

4) The light passing through the cell is collimated.

5) Refraction by the polymer is negligible.

The equation for the path of light through a refractive index gradient for small deflections is (2)

$$x - x_0 = y\,\theta_0 + \frac{y^2}{2n}\left(\frac{dn}{dx}\right)$$

where y is the distance through which the light passes in the direction perpendicular to the direction of the gradient; θ_0 is the angle of incidence of the light (the angle being measured from the y axis), which in the case of the centrifuge is equal to zero; x_0 is the entrance position of the light into the gradient; and n is the refractive index of the solution.

If I is the light intensity, ϵ the extinction coefficient of the absorbing polymer, c the concentration of the polymer, and s the distance along the optical path, the Beer-Lambert Laws state that $\frac{dI}{I} = -\epsilon c\,ds$

Now $ds = \sqrt{1 + \left(\frac{dy}{dx}\right)^2}\,dx$, but since the deflection of the light is small, $\frac{dy}{dx} \gg 1$ so that ds

may be set equal to $\left(\frac{dy}{dx}\right) dx$. Evaluating $\left(\frac{dy}{dx}\right)$ from the equation for the parabolic path of light given above, the intensity of any sheet of light entering the cell at x_0 is determined by the following equation:

$$\ln \frac{I_0}{I} = \frac{\epsilon C_0}{\sqrt{2m}} \int_{x=x_0}^{x=\frac{ma^2}{2}+x_0} (x-x_0)^{-\frac{1}{2}} e^{-\frac{x^2}{2\sigma^2}} dx \qquad (1)$$

x is the distance from the center of the Gaussian concentration distribution, x_0 is the distance from the center of the concentration distribution to the point at which a single light sheet enters the cell, a is the height of the liquid column in the centrifuge cell, and m is $\frac{1}{n}\frac{dn}{dx}$. Expanding the exponential around x_0 and integrating, one obtains:

$$\ln \frac{I_0}{I} = \epsilon C_0 a e^{-\frac{x_0^2}{2\sigma^2}} \left\{ \left[1 - \frac{1}{40} N^2 + \frac{1}{1152} N^4 \cdots \right] - \left[\frac{1}{6} N - \frac{1}{112} N^3 \cdots \right] \frac{x_0}{\sigma} + \left[\frac{1}{40} N^2 - \frac{1}{576} N^4 \cdots \right] \left(\frac{x_0}{\sigma}\right)^2 \right.$$
$$\left. - \left[\frac{1}{336} N^3 \cdots \right] \left(\frac{x_0}{\sigma}\right)^3 + \left[\frac{1}{3456} N^4 \cdots \right] \left(\frac{x_0}{\sigma}\right)^4 - \cdots \right\} \qquad (2)$$

where $N = \frac{ma^2}{\sigma}$

On first observation the correction to the concentration distribution is large. For example, at $\chi_0 = \pm 2\sigma$ for $N = 0.5$, which is well within experimental conditions, the photometric record yields an apparent concentration from the sheet of light entering at χ_0 which is in error by $\mp$ 15% from the actual concentration at χ_0. This effect is primarily a shift of the optical band center to lighter densities with little skewing of the band. Analytically this can be explained by observing that the $-\frac{1}{6} N \frac{\chi_0}{\sigma}$ term of the correction factor is by far the most significant χ_0 dependent term. Considering this fact, one can rewrite equation 2 in a Gaussian form with a different center and an added correction series of terms of smaller magnitude than those of equation 2.

$$\ln \frac{I_0}{I} = \epsilon C_0 a \left\{ e^{-\frac{\left(\chi_0 + \frac{Na^2}{6}\right)^2}{2\sigma^2}} + e^{-\frac{\chi_0^2}{2\sigma^2}} \left[\left(-0.0110 N^2 + .000772 N^4 \cdots \right) \right. \right. \tag{3}$$

$$+ \left(.00662 N^3 \cdots \right) \frac{\chi_0}{\sigma} + \left(.0110 N^2 - .00155 N^4 \cdots \right) \left(\frac{\chi_0}{\sigma}\right)^2$$

$$\left. \left. - \left(.00221 N^3 \cdots \right) \left(\frac{\chi_0}{\sigma}\right)^3 + \left(.000257 N^4 \cdots \right) \left(\frac{\chi_0}{\sigma}\right)^4 \right] \right\}$$

If $N < 0.50$ all the terms in the above expansion are < 0.011 out to $x_0 = \pm 2\sigma$, and the optical error in concentration due to these terms is $< 1\%$ out to $\pm 2\sigma$. The major effect under these conditions is to shift the optical band center a distance $\frac{ma^2}{6}$ to the low density side of the concentration distribution center. This means that after superimposing the centers of the actual concentration distribution and the photometric record, the relative error of all points in the region $-2\sigma \leq x_0 \leq 2\sigma$ on the photometric record will be less than 1%.

The band center shift is a constant shift for all bands in the same gradient and cell. It is independent of the molecular weight of the polymer. The magnitude of the shift for a CsCl solution of density 1.700 and at a speed of 44,770 RPM is 0.002 cm. This corresponds to a density shift of 0.0002 gm./cc. For DNA of molecular weight 12×10^6, this shift amounts to about 15% of σ. N for these conditions is about 0.8.

The shift of band center does not affect the determination of molecular weight by this method. It is the expanded terms in equation 3 that will determine the magnitude of the optical error in molecular weight. This series must remain small or the Gaussian character of the distribution is lost. A practical maximum value

of N is about 0.5 for a maximum error of 1% in the region $-2\sigma \leq x_0 \leq 2\sigma$. Below this value the Gaussian character of the optical distribution is not affected significantly. Since N is proportional to the square of the length of the liquid column, the higher order corrections become significant if a 30 millimeter cell instead of a 12 millimeter cell is used. In this case, the assumption of small angular deflections becomes less justifiable.

Finally, the points beyond $x_0 = \pm 2\sigma$ must be used with care, for the fractional change in concentration that a single light sheet experiences becomes large. This is demonstrated by the expanded part of equation 3. Although the magnitude of the correction becomes small at large x_0, the relative correction becomes large.*

---

* This proposition has been accepted for publication in the Journal of Physical Chemistry, June, 1961.

Proposition 2

A great deal of work has been done on the electrophoresis of polymers in both artificial and natural pH gradients (3) in order to segregate polymers with different isoelectric points. Most of these systems have been stabilized against convection by the means of a density gradient in a binary solution containing an uncharged component such as sucrose. The polymer moves in the electric field until it reaches a region corresponding to its isoelectric pH and there it forms a sharp band.

Although these methods have been relatively successful, they are limited either by the buffer capacity of buffer in the solution, or by the formation of a region of very low conductivity. It is proposed that similar experiments could be done in a column of an ion exchange resin. A finely divided ion exchange resin would provide the density stability, eliminating the need for another density stabilizer. In addition, if the charged group on the resin is either a weak acid or base, the column provides a very large buffer capacity to hold the pH gradient column constant.

The resin column would have to be poured in small sections, each portion equilibrated with the same salt concentration, but at different values of pH. After

equilibration the resin acts as a buffer at the pH to which it is equilibrated. The salt concentration in the column should be the same as the salt concentration used in equilibrating the resin. The pH gradient can be made linear by passing a solution of this salt concentration through the column for a short period of time.

If the polymer is now introduced at the bottom of this column in a zone, and the polarity of the electric field picked so that the polymer moves upward, it should move until it reaches its isoelectric pH and stop. The resin should be picked to have the same sign of charge as the polymer in the lower region of the column. This will prevent the polymer from adsorbing to the resin.

After all the components in the polymer sample have reached their equilibrium positions, the separated bands could be recovered by passing salt solution through the column, thus moving the equilibrium bands out of the bottom of the column.

This procedure could provide a simple preparative method for separating polymers of different isoelectric points. Once the column is poured, it could be used several times before the pH gradient became too shallow for further use.

As an example of the application of the proposed method, it is suggested that sickle and normal hemoglobins be separated on a column of finely divided Amberlite IRC 50 which is polymethacrylic acid. The isoelectric pH values of normal and sickle hemoglobin are 7.0 and 7.2 respectively. The column should be set up so that it would be at pH 7.5 at the bottom and pH 6.7 at the top. Above pH 7.2 both hemoglobins have a net charge of the same sign as the resin. This decreases the likelihood of adsorption of the hemoglobins to the resin.

Proposition 3

Accurate determination of molecular weights of polymers larger than 10 million is a difficult problem. Light scattering can no longer be used because the dimensions of the polymer approach visible wave-lengths, and the theory becomes very complex (4). The ultracentrifuge is too unstable at the low speeds needed for two component sedimentation equilibrium of such large molecules. Although sedimentation equilibrium in a density gradient may develop into the most valuable method available, there is definite need for an independent method with which results may be compared.

It is proposed that in the case of charged polymers, electrophoretic equilibrium is an untried method which is available. It is relatively easy to keep an electric field stable for several days as would be necessary for such an experiment. The electric field would be vertical with a polarity such that the polymer would move downward, thus avoiding density instability. The electrolyte concentration must be small enough so that temperature gradients in the cell do not cause mixing, and yet large enough to make the effect of the polymer on the electric field negligible. The electrophoresis cell and buffer vessels must be immersed in a constant temperature bath.

The bottom and top of the electrophoresis cell would be bound by membranes impermeable to the polymer but able to pass water and electrolyte. The buffer vessels in contact with these membranes would hold large reservoirs of the same buffer contained in the cell. The solutions in the buffer vessels must not change their concentrations during an experiment. If reversible silver - silver chloride electrodes are used, the buffer solutions can be kept at constant concentration by continually circulating the buffer between the two buffer vessels without allowing electrical contact through the circulating system. This may be accomplished by introducing the circulating buffer to the buffer vessels drop-wise instead of in steady streams.

The condition for equilibrium in such a system is that the gradient in the electro-chemical potential be equal to zero.

$$\bar{\mu}_3 = \mu_3 + Z_3 F \phi$$

$\bar{\mu}_3$ is the electro-chemical potential, μ_3 is the chemical potential, Z_3 is the net charge on the polymer molecule, F is the Faraday constant and ϕ is the electric potential. Assuming the polymer is ideal and $\frac{d\phi}{dx}$ is a constant, the condition for equilibrium, $\frac{d\bar{\mu}_3}{dx} = 0$ leads to the following equilibrium distribution:

$$\frac{m_3}{m_{3,0}} = e^{-\frac{Z_3 F \left(\frac{d\phi}{dx}\right) x}{RT}}$$

where m_3 is the polymer molality, and $m_{3,0}$ is the molality of the polymer at $x = 0$. Thus Z_3 may be determined from the equilibrium distribution.

The polymer charge, Z_3, and the polymer molecular weight, M_3, may be connected in one of two ways. Donnan membrane potentials can be measured. The charge of the polymer is obtained by extrapolating the membrane potential divided by the polymer concentration to zero polymer concentration. The following equation for $0^{\circ}C$ is derived in Alexander and Johnson (5):

$$Z_3 = 0.00425\, M_3\, J \left(\frac{E}{c_3}\right)_{c_3 = 0}$$

where J is twice the ionic strength of the polymer free solution, E is the membrane potential in millivolts, and c_3 is the polymer concentration in gm/100 cc of solvent. Thus, if Z_3 is known from an electrophoretic equilibrium experiment, M_3 can be obtained.

By measuring the sedimentation coefficient and the electrophoretic mobility of the polymer, a second method for connecting Z_3 and M_3 is available. The electrophoretic mobility, u, equals $\frac{Z_3 F}{f}$ where f is the friction factor per mole of polymer. The sedimentation

coefficient, S, equals $M_3(1-\bar{v}_3\rho)/f$

It follows that $$\frac{M_3(1-\bar{v}_3\rho)}{S} = \frac{Z_3 F}{\mu}$$

Thus M_3 can again be calculated from Z_3 .

For an order of magnitude of variables involved, let us assume the polymer concentration in the equilibrium distribution decreases by 90% in 0.1 to 1.0 mm in the cell. For a polymer with $Z_3 = 1000$, $\frac{d\phi}{dx}$ would have to be about 1 millivolt/cm . Very small voltages are therefore needed if Z_3 is high, and very little current will be passed by the system.

Proposition 4

Emanuel (6) has recently reported the observation of salt hyperchromicity in DNA solutions. He plotted absorbancy at 260 mμ against salt molarity and observed that the effect was most pronounced in concentrated NaBr solutions. The effect was only slightly smaller for concentrated NaCl solutions, but was absent for LiCl solutions. The hyperchromicity was demonstrated to be reversible and clearly not caused by denaturation. It is accompanied by a drop in specific optical rotation at 589 mμ and a drop in intrinsic viscosity of 40 percent.

It is proposed that these observations are water activity effects resulting from the partial conversion of the DNA from form B to form A in solution (7). These two structures have been postulated from X-ray crystallographic studies on DNA fibers. Form B is the Watson-Crick (8) structure, in which the planes of the bases are perpendicular to the axis of the DNA molecule. In form A the bases make an angle of about 70° with the axis of the molecule (7).

The sodium, potassium, and rubidium salts of DNA are known to be in the B form at a relative humidity of 85 to 90 percent. They are transformed to the A form

as the relative humidity drops to 75 percent. The lithium salt of the DNA has not been converted to the A form, even at relative humidities as low as 66 percent.

If the NaBr and NaCl absorbancy points of Emanuel are replotted against water activity they lie on the same curve out to 4 M solutions. This, however, is not a very rigorous test because the graph is too small for an accurate analysis. If the change in form occurs, a change in the ultraviolet absorption would be expected because of the shift of the bases (9).

The viscosity decrease is expected because the Γ_n of the DNA would be estimated to change from 50 to less than 7 in the transition from a 0.1 M NaBr solution to a 7 M NaBr solution. This would decrease the solvated polymer excluded volume by about a factor of three assuming the hydrate layer is rigid. This drop in volume could easily account for the drop in viscosity. The A form might also be less rigid than the B form in solution.

The drop in specific optical rotation also substantiates the theory of a shift in the DNA structure, for loosening of the helix would be accompanied by a decrease in the specific optical rotation.

The fact that high concentrations of LiCl do not effect the absorbancy of the DNA is very strong evidence that the analogy between DNA fiber and DNA in solution, and between relative humidity and water activity is correct.

A complete study of the ultraviolet absorbancy, specific optical rotation, and intrinsic viscosity of DNA in a series of alkali salts would add interesting information regarding the structure of the solvated DNA as a function of water activity. It would also determine the differences in the stability of the B form for the alkali salts of DNA.

Proposition 5

The problem of density heterogeneity remains as a source of error in the density gradient method of molecular weight determination. Baldwin (10) has considered the restricted case of a sample of homogeneous molecular weight but with a Gaussian distribution of densities. Sueoka (11) has generalized this treatment by showing that the variance of the concentration distribution obtained in the centrifuge may be written as a sum of the variance due to diffusion and the variance due to the density distribution assuming no diffusion. The treatment is valid if the walls in the centrifuge cell are assumed to be parallel. For very narrow bands this is certainly a valid assumption. Sueoka (11) then showed by using an independent relation between the sedimentation coefficient and the molecular weight of DNA, the amount of density heterogeneity can be determined.

Using Sueoka's approach, I propose to show that density heterogeneity of a certain variety can be determined using only the density gradient technique.

The following quantities were defined by Sueoka:

$T(x)$ is the actual distribution by weight of the DNA in the cell. $\int_R T(x)dx = C$

C is the total weight of DNA in the band. R is the entire range of the function.

D(X) is the density distribution of DNA in the absence of diffusion. $\int_R D(X)dX = C$

B(X,x) is the distribution due solely to the diffusion of the molecules having a density corresponding to X. $\int_R B(X,x)dx = 1$

X is the mean of B(X,x) because the function is symmetrical about X. X and x are on the same scale.

Sueoka has shown that the variances related to these functions satisfy the following equation.

$$\sigma_T^2 = \sigma_B^2 + \sigma_D^2 \qquad (1)$$

σ_B^2 is the variance of the concentration distribution with all means X superimposed, and is therefore related to the number average molecular weight by equation 18 of Meselson, Stahl, and Vinograd (1).

$$\sigma_D^2 = \frac{1}{C}\iint_R (X - \bar{x})^2 D(X)\, dX \qquad (2)$$

where $\bar{x}$ is the mean of the actual distribution.

Under the assumption that all the density heterogeneity is caused by the heterogeneity of the unhydrated DNA, a new distribution function $\Phi(\rho_3)$ may be defined. ρ_3 refers to the density of the DNA at a water activity equal to zero.

$$\int_R \Phi(\rho_3)\, d\rho_3 = C \tag{3}$$

Assuming a constant density gradient the following equation may be written.

$$(\rho - \bar{\rho}) = \left(\frac{d\rho}{dr}\right)_{eff} (X - \bar{X}) \tag{4}$$

The banding density is given by $\frac{1}{\rho_0} = \frac{1/\rho_3 + \Gamma' v_1}{1+\Gamma'}$

where v_1 is the reciprocal of the density of the hydrated water and is assumed to be constant. Differentiating this equation yields $d\rho_0 = \left(\frac{\rho_0}{\rho_3}\right)^2 \frac{1}{1+\Gamma_0'}\, d\rho_3$.

Because the density differences in a band are small $(\rho - \bar{\rho})$ may be expressed in terms of ρ_3 by the equation

$$\rho - \bar{\rho} = \left(\frac{\rho_0}{\bar{\rho}_3}\right)^2 \frac{1}{1+\Gamma_0'} (\rho_3 - \bar{\rho}_3) \tag{5}$$

Equation 2 may now be rewritten

$$\sigma_D^2 = \frac{1}{C} \frac{1}{(d\rho/dr)^2_{eff}} \left(\frac{\rho_0}{\bar{\rho}_3}\right)^2 \left(\frac{1}{1+\Gamma_0'}\right) \iint_R (\rho_3 - \bar{\rho}_3)^2 \Phi\, d\rho_3 \tag{6}$$

$$\sigma_D^2 = \left(\frac{\rho_0}{\bar{\rho}_3}\right)^2 \frac{1}{(1+\Gamma_0')\left(\frac{d\rho}{dr}\right)^2_{eff}} \sigma_\Phi^2$$

Using the relation $\left(\frac{d\rho}{dr}\right)_{eff} = \frac{\omega^2 r}{\beta_{eff}}$ and equation 18 of Meselson, Stahl, and Vinograd (1) and remembering solvation,

$$\sigma_T^2 = \left[\frac{\beta_{eff} RT \rho_0}{M_N (1+\Pi_0')} + \left(\frac{\rho_0}{\bar{\rho}_3}\right)^2 \frac{\beta_{eff}^2 \sigma_\phi^2}{1+\Pi_0'} \right] \left(\frac{1}{\omega^2 r_0}\right)^2 \quad (7)$$

Clearly changing the speed of the centrifuge will not separate these terms, but studying a series of cesium salts with different β_{eff} will. Such a series provides a method of determining M_N using equation 7.

References for the Propositions

1) Meselson, M., Stahl, F. W. and Vinograd, J. (1957) Proc. Nat. Acad. Sci. U. S. 43, 581

2) Svedberg, T., Pedersen, K. O., (1940) The Ultracentrifuge, Clarendon Press, Oxford, p. 259

3) Svensson, H. private communication

4) Benoit, H. and Doty, P. (1953) J. Phys. Chem. 57, 958

5) Alexander, A. E. and Johnson, P. (1949) Colloid Science Clarendon Press, Oxford p. 82

6) Emanuel, C. F. (1960) Biochem. Biophys. Acta. 42, 91

7) Langridge, R., Seeds, W. E., Wilson, H. R., Hooker, C. W., Wilkins, M. H. F., and Hamilton, L. D. (1957) J. Biophys. Biochem. Cytol. 3, 767

8) Watson, J. D. and Crick, F. H. C. (1953) Nature 171 737

9) Tinoco, I. (1960) J. Am. Chem. Soc. 82, 4785

10) Baldwin, R. L. (1959) Proc. Nat. Acad. Sci. U.S. 45, 939

11) Sueoka, N. (1959) Proc. Nat. Acad. Sci. U.S. 45, 1480